SYNTHESIS OF ZEOLITE MEMBRANES IN FLOW SYSTEM

A THESIS SUBMITTED TO
THE GRADUATE SCHOOL OF NATURAL AND APPLIED SCIENCES
OF
MIDDLE EAST TECHNICAL UNIVERSITY

BY

AYLİN ÖNDER

IN PARTIAL FULFILLMENT OF THE REQUIREMENTS
FOR
THE DEGREE OF MASTER OF SCIENCE
IN
CHEMICAL ENGINEERING

SEPTEMBER 2012

Approval of the thesis:

SYNTHESIS OF ZEOLITE MEMBRANES IN FLOW SYSTEM

submitted by **AYLİN ÖNDER** in partial fulfillment of the requirements for the degree of **Master of Science in Chemical Engineering Department, Middle East Technical University** by,

Prof. Dr. Canan Özgen
Dean, Graduate School of **Natural and Applied Sciences** _____

Prof. Dr. Deniz Üner
Head of Department, **Chemical Engineering** _____

Assoc. Prof. Dr. Halil Kalıpçılar
Supervisor, **Chemical Engineering Dept., METU** _____

Examining Committee Members:

Prof. Dr. Levent Yılmaz
Chemical Engineering Dept., METU _____

Assoc. Prof. Dr. Halil Kalıpçılar
Chemical Engineering Dept., METU _____

Assoc. Prof. Dr. Yusuf Uludağ
Chemical Engineering Dept., METU _____

Assoc. Prof. Dr. Sena Yaşyerli
Chemical Engineering Dept., Gazi University _____

Asst. Prof. Dr. Pınar Zeynep Çulfaz Emecen
Chemical Engineering Dept., METU _____

Date: 07.09.2012

I hereby declare that all information in this document has been obtained and presented in accordance with academic rules and ethical conduct. I also declare that, as required by these rules and conduct, I have fully cited and referenced all material and results that are not original to this work.

Name, Last name : Aylin Önder

Signature :

ABSTRACT

SYNTHESIS OF ZEOLITE MEMBRANES IN FLOW SYSTEM

Önder, Aylin
M.S., Department of Chemical Engineering
Supervisor: Assoc. Prof. Dr. Halil Kalıpçılar
June 2012, 108 pages

Zeolite membranes are formed as a thin zeolitic layer on the supports. They are usually synthesized by hydrothermal methods in batch systems. In this study, MFI and SAPO-34 type zeolite membranes were produced on macroporous tubular alumina supports in a recirculating flow system at elevated temperatures for the first time in the literature. During the synthesis, the synthesis mixture is flown between the reservoir and the membrane module which includes the support material.

The synthesis temperatures were 180°C and 220°C, and the corresponding system pressures were approximately 20 and 30 bars for MFI and SAPO-34, respectively. The CH_4 and n-C_4H_{10} single gas permeances were measured through MFI membranes and the performance of membranes was investigated in the separation of equimolar CH_4/n-C_4H_{10} mixtures. The best MFI membrane had a CH_4 single gas permeance of $1.45x10^{-6}$ mol/m^2-s-Pa and CH_4/n-C_4H_{10} ideal selectivity of 35 at 25^{o}C. The membranes preferentially permeated n-C_4H_{10} in the separation of mixtures. The n-C_4H_{10}/CH_4 separation selectivity was 43.6 with a total permeance of approximately $0.8x10^{-6}$ mol/m^2-s-Pa at 25^{o}C.

The ideal selectivities of CO_2/CH_4 of SAPO-34 membrane synthesized in stagnant medium were 227, and >1000 at 220 and 200^oC, respectively. Formation of amorphous structure and the additional secondary phases (impurities) were observed on SAPO-34 membranes synthesized in recirculating flow system. The results showed that it is possible to produce SAPO-34 and high quality MFI membranes by a recirculating flow system operating at elevated temperature.

Key words: zeolite membrane, MFI membrane, SAPO-34 membrane, gas separation, synthesis in recirculating flow system

ÖZ

ZEOLİT MEMBRANLARIN AKIŞLI SİSTEMDE SENTEZLENMESİ

Önder, Aylin
Yüksek Lisans, Kimya Mühendisliği Bölümü
Tez Yöneticisi: Doç. Dr. Halil Kalıpçılar
Haziran 2012, 108 sayfa

Zeolit membranlar bir destek üzerindeki ince bir zeolit tabakadan oluşur. Genellikle hidrotermal yöntemlerle kesikli sistemlerde üretilirler. Bu çalışmada literatürde ilk kez MFI ve SAPO-34 tipi zeolite membranlar makro gözenekli alumina tüp destekler üzerinde yüksek sıcaklık ve basınç altında çalışan geri döngülü akış sisteminde üretilmiştir. Sentez süresince, sentez çözeltisi destek malzeme içinden akıtılarak bir rezervuara, oradan da tekrar destek malzemeye pompalanır.

Sırasıyla MFI ve SAPO-34 için sentez sıcaklığı 180°C ve 220°C, sistem basıncı ise yaklaşık 20 ve 30 bar'dır. Üretilen membranlar XRD ve SEM ile analiz edilmiştir. MFI membranların CH_4 ve n-C_4H_{10} tek gaz geçirgenlikleri ve %50-%50 CH_4/n-C_4H_{10} karışımlarının ayırımın performansları incelenmiştir. En iyi MFI membranın 25^oC'deki CH_4 geçirgenliği $1.45x10^{-6}$ mol/m^2-s-Pa ve CH_4/n-C_4H_{10} ideal seçiciliği de 35'dir. Gaz karışımlarının ayırımında membranlar n-C_4H_{10}'e seçici olup, 25^oC'deki n-C_4H_{10}/CH_4 ayırma seçiciliği 43.6 ve toplam geçirgenlik yaklaşık $0.8x10^{-6}$ mol/m^2-s-Pa'dır.

Durgun ortamda 220 ve 200^oC sentezlenen SAPO-34 membranların CO_2/CH_4 ideal seçicilikleri 227 ve >1000'tür. Akışlı ortamda sentezlenen SAPO-34 membranlarda amorf yapıların ve fazladan ikinci bir fazın (safsızlık) oluşumu gözlendi. Sonuçlar

SAPO-34 membranların ve yüksek kaliteye sahip MFI tipi membranların yüksek sıcaklıkta çalışan geri döngülü akış sistemlerinde üretilebileceğini göstermektedir.

Anahtar Sözcükler: zeolit membran, MFI membran, SAPO-34 membran, gaz ayırımı, akış sisteminde zeolit sentezi

To my family

ACKNOWLEDGEMENTS

I wish to express my gratitude to my supervisor Assoc. Prof. Dr. Halil Kalıpçılar for his guidance and interest throughout this study. His endless energy and enthusiasm about research made me to work eagerly and devotedly. I would like to thank Prof. Dr. Levent Yılmaz for his suggestions, criticism. I would also like to thank Dr. Berna Topuz for her help for any kind of problem, her guidance, suggestions and patience. Without her help it was impossible for me to do some experiments.

I would like to thank the financial supports from The Scientific and Technological Research Council of Turkey (TUBITAK) through the grant number 110M402 and Universal Oil Products (UOP).

I also thank to the technicians of Machine Shop of Chemical Engineering Department and Central Laboratory of Middle East Technical University.

I would like to thank my colleagues Nihan Uzunoğlu and Nilay Keser for their helps and suggestions. It was enjoyable to work with them during this study. Thanks also to all my lab mates. I would like to express my special thanks to Onur Can Saka for his endless support and affection.

Finally, I would like to express all my love to my family for their support, guidance, encouragement and patience.

TABLE OF CONTENTS

LIST OF TABLES

TABLES

LIST OF FIGURES

FIGURES

CHAPTER 1

INTRODUCTION

Zeolite membranes are typically synthesized by vapor-phase method or in batch systems enclosing the support material with the synthesis solution in an autoclave. In literature, MFI (Mobile Five) membranes were synthesized both at low temperature range (below 150°C) [1,2] and at high temperature range (150-200°C) [3-5]. Membrane synthesis at low temperatures results in thinner membranes, whereas increasing the synthesis temperature may cause an increase in the membrane thickness. Hedlund et al. obtained 0.5μm thick MFI membranes at 100°C with n-C_4H_{10}/ i-C_4H_{10} separation factor of 3 [1] and Çulfaz et al. synthesized 1-2 μm thick MFI membranes at 80 and 95°C with n-C_4H_{10}/ i-C_4H_{10} separation factor of 44 [2]. Xomeritakis et al. found that after one synthesis layer at 175°C, the membrane thickness was 12-15 μm and the thickness doubles after an additional synthesis [6].

MFI membranes with higher separation factors were generally synthesized in stagnant systems above 180°C. MFI membranes are used for the separation of methane and n-butane [7] and for the separation of higher hydrocarbons from methane [8]. For example, MFI membranes synthesized above 180°C have exhibited CH_4/n-C_4H_{10} ideal selectivities of 12.2 [3], 4.6 [4]) at the gas permeation temperature of 145°C and 105°C, respectively. Wohlrab et al. [5] and Vroon et al. [9] separated 50/50 CH_4/n-C_4H_{10} mixture with n-C_4H_{10}/CH_4 separation factor of 12.4 and 102 at 75°C and 25°C, respectively. Arruebo et al. separated hydrocarbons from natural gas with an n-C_4H_{10}/CH_4 separation factor of 14.2 [8]. Xomeritakis et al. found n-C_4H_{10}/CH_4 single gas permeation flux ratio as 0.58 whereas binary permeation flux ratio was 53 for the MFI membranes made by secondary growth [10]. Kwan et al. prepared ZSM-5 micromembranes on silicon with n-C_4H_{10}/ i-C_4H_{10} single gas permeance ratios between 30 and 65 [11].

Synthesis of SAPO-34(silicoaluminophosphates) membranes with high quality in the literature was achieved at synthesis temperatures between 200-220°C. SAPO-34 membranes were especially used for the separation of carbon dioxide and methane since CO_2 reduces the heating value of the natural gas and it may be corrosive in the presence of water vapor [12]. There are several works on SAPO-34 membranes for CO_2/CH_4 separation carried out by Falconer and Noble research group [13-19]. They usually used alumina supports with 5-cm long. Li et al. increased the support size from 5 to 25cm for SAPO-34 membranes by the synthesis at 220°C [13]. Average CO_2/CH_4 separation factor was 214 for 25cm long membranes and 234 for 5cm long membranes when 99.99% aluminum isopropoxide was used as the alumina source. Venna and Carreon synthesized SAPO-34 membranes at 220°C and functionalized them with organic amino cations [12]. CO_2/CH_4 separation factor for nonfunctionalized membranes was 159, whereas it was 245 for ethylenediamine functionalized ones at 22°C and 138kPa. CO_2/CH_4 separation performance was also studied by Chew et al. with cation exchanged SAPO-34 membranes, which were synthesized at 200°C by microwave heating [20]. CO_2/CH_4 separation factor was increased from 30 to 103 by the ion exchange of Ba^{2+} at 30°C and 100kPa.

On the other hand, some problems may arise in the synthesis of membranes in stagnant system, especially with longer support sizes. In stagnant systems, composition variations in the synthesis media and therefore along the support surface may take place with time [2, 21]. Variation in the composition throughout the support length may lead to some problems including nonhomogeneous membrane characteristics [21], variable membrane thickness [2], undesired crystalline phases on the membrane [2, 21, 22] or amorphous deposits [22]. Renewal or recirculation of synthesis solution is advantageous compared to stagnant counterpart by ease of the control of the composition of the reacting mixture [21, 23]. Synthesis of membranes where the synthesis solution is renewed periodically or recirculated in the reaction media is more flexible and increases the possibility of the implementation of the zeolite membranes in large scale [2, 21, 23]. Recirculation of the synthesis solution is also more economical compared to the non-recirculating flow synthesis system in terms of consumption of the chemicals needed for the synthesis solution [24].

In the literature, alternatives of the stagnant synthesis media have been introduced recent years. These are batch systems with recirculation of the synthesis solution; single-pass flow of the synthesis solution (by pressurized N_2 or by the action of gravity) through the membrane and periodic renewal of the synthesis solution through the synthesis media (a series of short synthesis durations with fresh synthesis solution). Çulfaz et al. synthesized MFI membranes in a recirculated flow system under atmospheric pressure with flow rates of 6, 24 and 48ml/min [2]. The components of the recirculated flow system; the reservoir, the membrane module and tubing were placed in a silicone oil bath in order to provide uniform synthesis temperatures which are 80°C and 95°C in this study. The membranes synthesized in recirculated flow system had N_2/SF_6 ideal selectivity between 9.1-14.9 and n-C_4H_{10}/ i-C_4H_{10} ideal and separation factors of 2.6-70.7 and 4-8.5, respectively at room temperature. Yamazaki and Tsutsumi synthesized A-type membranes by recirculation of the liquid phase of the hydrogel at around 80-130°C using a bellows pump [25]. Aguado et al. achieved the synthesis of NaA membranes by the recirculation of the solution by means of an HPLC pump at 80-90°C [23]. In a study performed by Pera-titus et al., NaA membranes were synthesized by continuous flow of the synthesis solution by the action of the gravity at 80-90°C [26]. Richter et al. synthesized ZSM-5 membranes by flowing the synthesis solution through the tubes or capillaries from one reservoir to another (single-pass) with a very low velocity of 0.25cm/min for 72h [27]. H_2/SF_6 permselectivity of the membranes was between 20 and 31 after one-step-crystallization. Pina et al. obtained NaA membranes at around 90°C by refreshing the synthesis solution for selected periods during synthesis [21]. Similar to Pina et al. [21], Pera-titus et al. also synthesized NaA membranes at 80-100°C by pulsed renewal of the synthesis solution in every 4-25min [22].

The alternatives of the stagnant synthesis media technique were applied only on MFI and zeolite A membranes in the lower synthesis temperature range. Synthesis with the recirculation of the synthesis solution at high temperature could be a good technique for the synthesis of MFI and SAPO-34 membranes since high quality MFI and SAPO-34 membranes were generally synthesized at high temperature range.

The aim of this study was to synthesize zeolite membranes in a synthesis system that operates at high temperature and pressure, and recirculates the synthesis mixture through the tubular support. For this purpose, MFI and SAPO-34 were selected as the model zeolites. MFI and SAPO-34 membranes were obtained by the recirculation of the synthesis solution at high synthesis temperatures (140-180°C, 140-220°C) for the first time in the literature. The syntheses were carried out under autogeneous pressure by single or multiple synthesis cycles. MFI membranes were characterized by X-ray diffraction (XRD), scanning electron microscopy (SEM), gas permeation of H_2, CO_2, N_2, CH_4, C_2H_6, C_3H_8, n-C_4H_{10} and i-C_4H_{10} and separation of CH_4/n-C_4H_{10} mixture. SAPO-34 membranes were also characterized by X-ray diffraction (XRD), scanning electron microscopy (SEM), gas permeation and separation of CO_2 and CH_4.

CHAPTER 2

LITERATURE SURVEY

2.1 Zeolites and zeolite membranes

Membrane is a selective barrier [28], which enriches one component on the permeate stream and the other on the retentate stream [29] (Figure 2.1). Permeate stream is the one where permeated components were collected and the retentate is where the nonpermeating components were collected. Permeation through the membrane occurs as a result of a driving force such as pressure, temperature and concentration [29]. Separation of gas mixtures is generally performed with a trans-membrane pressure difference of 1 and 100 bar where the size of the entities selectively rejected from the feed around 03.-0.5nm [29].

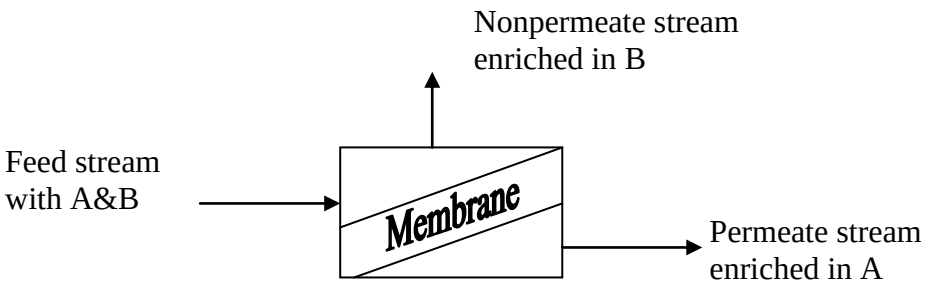

Figure 2.1: Idealized membrane process [29].

Selectivity and the permeance through the membrane are two important criteria defining the quality of the membranes. Permeance is defined as the ratio of molar flux and the driving force and given in Equation 2.1, by assuming the permeating gas to be ideal. Ideal selectivity was assigned as the ratio of single gas permeances and given by Equation 2.2.

$$P = \frac{\frac{p}{RT}\frac{\Delta V}{\Delta t}\frac{1}{A}}{\Delta p} \tag{2.1}$$

$$\alpha_{A/B} = \frac{P_A}{P_B} \tag{2.2}$$

P_A and P_B are single gas permeances of the two different gases.

Separation factor for a binary mixture, however, was defined in Equation 2.3, where y_i is the mole fraction of the gases in the permeate side and x_i is the mole fraction of the gases in the feed side. Separation factor was also defined as the ratio of molar fluxes of the components (Equation 2.4) in literature [30] and this definition is used in this study.

$$Separation\ Factor_{A/B} = \frac{\left(\frac{y_A}{y_B}\right)_{permeate}}{\left(\frac{x_A}{x_B}\right)_{feed}} \tag{2.3}$$

$$Separation\ Factor_{A/B} = \frac{Molar\ Flux\ of\ A\ /_{\Delta P_A}}{Molar\ Flux\ of\ B\ /_{\Delta P_B}} \tag{2.4}$$

ΔP_A (and ΔP_B)is the logarithmic mean of pressure difference:

$$\Delta P_A = \frac{\left(P_A^{feed} - P_A^{permeate}\right) - \left(P_A^{retentate} - P_A^{permeate}\right)}{ln\left(\frac{P_A^{feed} - P_A^{permeate}}{P_A^{retentate} - P_A^{permeate}}\right)} \tag{2.5}$$

Zeolites are crystalline materials which are aluminosilicates of group 1A and 2A elements. The structure of zeolites is based on the sticking out the framework of AlO_4 and SiO_4 by sharing the oxygen ions. This framework contains cations which can experience ion exchange and channels or interdependent voids which are filled with water. The framework has micropores which has uniform size of between 0.3 to

0.8 nm. Zeolites can selectively adsorb or reject the molecules according to their molecular size [31].

Zeolites are appropriate materials to make gas and liquid separation membranes [32]. Especially, they are used in the separation of small permanent gases like CH_4, CO, H_2 and N_2. Since it is hard to use zeolites in powder form directly as membranes; two methods have been proposed to use zeolites as membrane materials in the literature. First one is to put zeolite powders into polymeric membranes as filler which are called mixed matrix membranes [33-35]. Zeolites are expected to increase the selectivity and permeability of the membranes. Mixed matrix membranes are flexible and easy to scale-up, however, the permeabilities are generally low. Second approach is to grow zeolites on a porous surface to make membranes which are expected to show high selectivity and permeability [36-38]. It is generally difficult to prepare them in large areas but they have higher permeabilities than polymeric ones.

2.2 Description of MFI type zeolite membranes

Pore network of MFI crystals is composed of two types of channels which are cross-linked to each other [39]. First one is the straight channel in the crystallographic b-direction that is formed by 10-membered ring with a pore opening of 0.54×0.56nm [40, 41]. Sinusoidal channel has an elliptical pore opening (0.51×0.55nm) in the crystallographic a-direction [41]. (Figure 2.2)

MFI type membranes are used for the separation of different isomers such as butane [2,6, 43, 44], butane [45, 46], pentane [47], hexane [48] and xylene [43, 49] . Besides isomer separations, MFI membranes are generally used for separation of methane and n-butane [7] and separation of higher hydrocarbons from methane [8].

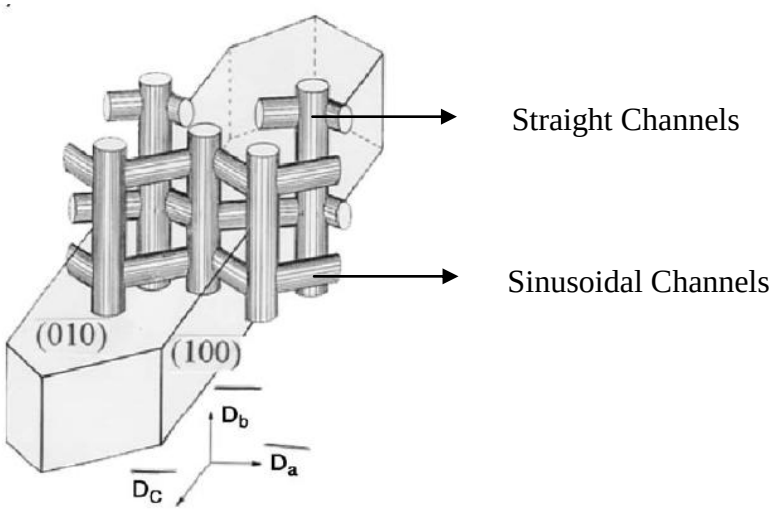

Figure 2.2: Pore network of MFI crystals [42].

Processing of natural gas is important and stands for the largest gas separation application in industry to meet the specifications of the pipelines. Raw natural gas contains mainly methane (75-90%), considerable amounts of ethane, propane and butane, and 1-3% higher hydrocarbons [50]. Generally separation of hydrocarbons from natural gas is performed with polymeric membranes such as POMS [poly(octyl-methyl-siloxane)] and PTMSP [poly(trimethyl-silyl-propyne)] [51]. Zeolite membranes can be used for hydrocarbon separations instead of polymeric ones since they are mechanically more stable (growing on a support material) [52-54].

2.3 Description of SAPO-34 type zeolite membranes

SAPO-34 which has a composition of $mR[Al_{17}P_{12}Si_7O_{12}]$ belongs to CHA framework type where R is an organic molecule acting as the template during the synthesis [55]. Quternary ammonium ions and amines are usually used as template. As it can be seen from the Figure 2.3, eight-membered ring forms the main pores which have a size of 0.38 nm. Moreover, SAPO-34 crystals have small size between 0,6 to 0.9μm [56].

SAPO-34 membranes has been mainly used for the removal of CO_2 from light-gas mixtures [19], to reduce the discharge of CO_2 to atmosphere [12, 20] and mainly to reduce the CO_2 concentration in purifying natural gas [12-16, 20, 30]. CO_2 is acidic and corrosive in the presence of water, and reduces the energy content of natural gas so its concentration in natural gas should be reduced before transporting the natural gas by pipelines.

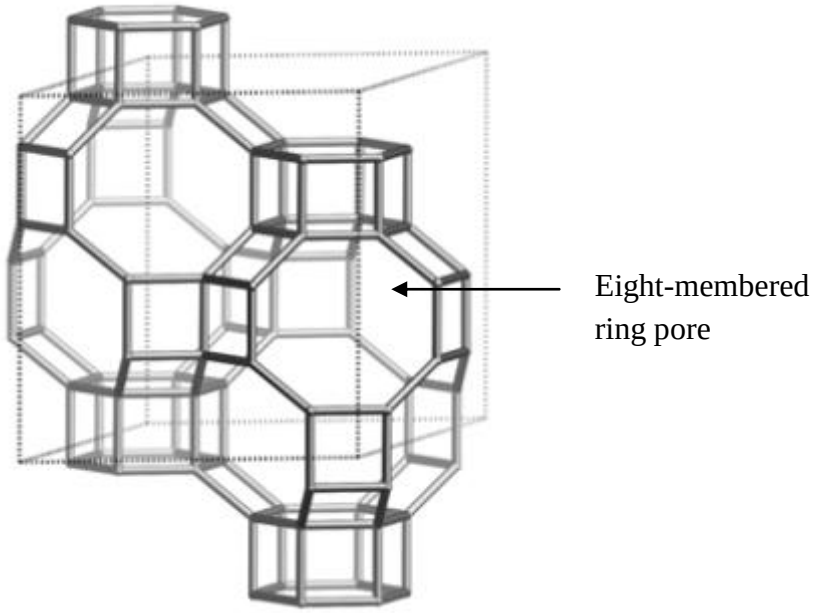

Figure 2.3: Structure of SAPO-34 [57]

SAPO-34 membranes were formed by intercrystalline cubic [18, 19], rectangular [16, 17] crystals. The thickness of the membranes with cubic crystals were 25µm [18] and 5-10µm [19], whereas it was around 5µm for the ones with rectangular crystals [16, 17]. Chew et al obtained 3-4µm thick SAPO-34 membranes with orthorhombic crystals by microwave heating at 200°C.

2.4 Synthesis of zeolite membranes by hydrothermal method

Zeolite membranes can be obtained either by self-supported or by growing it on porous supports. Self-supported membranes are not as common as the supported ones since they suffer from the mechanical strength. Lovallo and Tsapatsis obtained

composite silicalite/alumina unsupported films by film casting of aqueous silicalite/boehmite suspensions [58]. Supported material can be α-Al_2O_3 [43,60,70], γ-Al_2O_3 [63], stainless steel [8,15,44], silicon [11], mullite [62,64], PTFE [25] and titania [26] and support can be wafer [11], disc [3,9,47], tube [12,0,66], capillary [27] and hollow fiber [65] in shape and list of examples are given in Appendix A.

Syntheses of supported membranes were realized generally by hydrothermal synthesis. Support material is dipped into the synthesis solution before synthesis by hydrothermal method. Low temperature membrane syntheses (<100°C) such as LTA and FAU are carried out in polymer bottles, whereas syntheses are carried out in autoclaves for high temperature syntheses (>100°C) such as MFI [42]. Vroon et al obtained 2-7μm MFI membranes by one or more synthesis cycles with different particle sizes by changing the synthesis temperature [9].

In the secondary growth method, the surface of the support is seeded by rubbing [21], dip coating [65, 66] and vacuum [67, 68] prior to hydrothermal treatment. Advantages of secondary growth method are easy operation, high controllability in microstructure and thickness of the membrane which results in better reproducibility [39]. MFI membranes synthesized with secondary growth method by Noack et al have H_2/SF_6 permselectivity of 43 where the seed layer applied on the support surface after application of polycationic polymer [4].

SAPO-34 membranes are synthesized hydrothermally either on seeded [12-15, 73-75] or unseeded [18, 19, 71, 72] supports. Molar compositions synthesis solutions of SAPO-34 membranes contain one (e.g. $1Al_2O_3:1P_2O_5:0.6SiO_2:1.07TEAOH:56H_2O$ or $1Al_2O_3:1P_2O_5:xSiO_2:1.2TEAOH:55H_2O$) or two ($1Al_2O_3:1P_2O_5:0.3SiO_2:1.07TEAOH$: xDPA: yH_2O) type template molecules, details about synthesis compositions in the literature are given in Appendix B. The syntheses were carried out either by placing the support in the autoclave and filling it with synthesis solution [18, 19, 70, 71] or by filling just tubular support and plugging the both ends and placing it inside the autoclave [16, 17, 20]. Synthesis of SAPO-34 membranes with one structure directing agent molecule is carried out at 170-200°C

range [16-20, 30, 70-72, 74, 76, 77] and at 220°C [12-15, 73, 75, 78] for synthesis with two structure directing agents.

SAPO-34 membranes synthesized by filling the tubular support with synthesis solution whose both sides and the outer surface were wrapped with PTFE strip [18, 30]. These membranes showed CO_2/CH_4 separation factors of 52,7 [18], and 87 [30].

Synthesis of zeolite membranes by microwave heating both on unseeded and seeded supports is another method. The synthesis time is reduced by heating in microwave field where the synthesis solution is heated to the synthesis temperature rapidly [39]. Motuzas et al. synthesized from 200nm to a few μm thick silicalite-1 membranes by microwave heating at 120-180°C [40]. Chew et al. applied ion-exchange with alkaline earth cations to their H-SAPO-34 membranes which were synthesized at 200°C by microwave heating [20].

2.5 Synthesis of zeolite membranes in continuous systems

To the best of our knowledge, there are few articles on the synthesis of zeolite membranes by flow systems in the literature; two on MFI membranes and five on LTA membranes.

Richter et al. synthesized ZSM-5 membranes on tubes or capillaries in a 300ml autoclave which is connected to a storage tank [27]. During the synthesis (72 hours at 150°C), the synthesis solution was pumped through capillaries with a flow rate of 0.25cm/min from the storage tank. The membrane thickness after one-step crystallization on 25cm long supports was around 30μm. H_2 permeances of these membranes were between 4550 and 9540 l/m2.h.bar and H_2/SF_6 permselectivity was in the range of 20-31.

Second study on MFI membranes was carried out by Çulfaz et al. by circulation of the synthesis solution in our research group [2]. In that study, the syntheses were performed by placing the reservoir, the membrane module and the tubing in a

silicone bath where the synthesis temperatures were adjusted as 80°C or 95°C. MFI membranes were synthesized in a recirculated flow system under atmospheric pressure with flow rates of 6, 24 and 48ml/min. The membranes had N_2/SF_6 ideal selectivity between 9.1-14.9 after one synthesis step, while it was 141 after two consecutive synthesis steps. n-C_4H_{10}/i-C_4H_{10} ideal and separation selectivities of 10.6-71.4 and 6.1-7.6, respectively at room temperature with n-C_4H_{10} single gas permeances of 34-42.1x10^{-8} mol/m^2sPa.

Another study performed in our group belongs to Dede [79]. MFI membranes were obtained by the same synthesis setup with Çulfaz et al. at 95°C for 72 h with a flow rate of 6ml/min. Single gas permeation of N_2, H_2, CH_4, CO_2, n-C_4H_{10} and i-C_4H_{10} were done in the range of 25-200°C. The membranes were also used for the separation of 5wt% ethanol/water, 2-propanol/water and acetone/water by pervaporation with selectivities (fluxes) of 43 (0.2kg/m^2h), 36 (0.2kg/m^2h) and 1024 (0.1kg/m^2h), respectively.

In the third study done by our group, MFI membranes were synthesized in the same recirculated flow system at 95°C for 72 h [80]. The membranes synthesized in flow system were characterized by the separation of binary mixtures of (50/50) n-C_4H_{10}/ i-C_4H_{10}, n-C_4H_{10}/ CH_4, n-C_4H_{10}/ N_2 , n-C_4H_{10}/ CO_2 and ternary mixture of n-C_4H_{10}(10%)/ CH_4(70%)/ CO_2(20%). Soydaş et al. separated n-C_4H_{10}/ CH_4 (50/50) mixtures at 25, 50, 100, 150 and 200°C with separation factors of 38, 57, 67, 20, 18, respectively. When n-C_4H_{10} fraction decreased from 50% to 30% and 20%, separation factors exhibit similar trend for these n-butane amounts n-C_4H_{10}/ CH_4 separation factors were decreased to 36 and 16.5, respectively. For a ternary mixture of n-C_4H_{10}(10)/ CH_4(70)/ CO_2(20), n-C_4H_{10}/ CH_4 and n-C_4H_{10}/ CO_2 separation factors were 34.4 and 19.4 at 20°C.

There are two studies on zeolite A membrane synthesis in flow system performed in our group. Akbay synthesized zeolite A membranes both in batch and flow system at 60°C, 80°C and 95°C with starting molar composition of 49Na_2O:1Al_2O_3: 5SiO_2: 980H_2O [81]. The membrane synthesized in flow system with a flow rate of 6ml/min

at 80°C for 8h by two layers had pervaporation separation factor of 3700 for ethanol/water 92:8 (wt%) mixture at 45°C.

The other study of zeolite A membrane synthesis in flow system in our group was done by (Arıcan) Yüksel [82]. It was found that the membranes synthesized in flow system had higher pervaporation performances. The membranes had fluxes of 0.2-0.3 kg/m^2h and selectivities of 10-100 for batch ones, whereas it was 0.3-3.7 kg/m^2h and selectivities of 10^2-10^4 for the ones synthesized in flow system. A high quality membrane with a flux of 1.2 kg/m^2h and selectivity of >25000 at 50°C was synthesized at 95°C for 17h in flow system.

The first application of continuous synthesis systems on LTA membrane synthesis was done by Yamazaki and Tsutsumi [25]. They circulated the liquid phase of the hydrogel separated by centrifugation with a velocity of 50ml/min by means of a bellows pump in the range of 80-130°C synthesis temperature (by a plate heater). Formation mechanisms of the membranes were detected by the results of XRD and SEM analyses. Using a plate heater as the substrate guaranteed the formation of the membrane on top of the substrate not by the accumulation of the crystals formed in the liquid phase.

Pina et al. obtained NaA membranes in a semi-continuous system by periodical renewal of the synthesis solution (10 cm^3) [21]. The membranes were synthesized on the external surface of α-alumina tubular supports at around 90°C. The gel renewal rates of 1/13 min^{-1} -1/75 min^{-1} were investigated for synthesis duration of 5 hours. For the best renewal rate of 1/20 min^{-1}, pervaporation water flux was 3.8 $kg/h.m^2$ with a separation factor of 3603 for water/ethanol (10/90 wt%) mixture.

Pera-titus et al. used the same synthesis procedure with Pina et al. for synthesis of NaA membranes [22]. The renewal rate of the synthesis solution were investigated between 1/4 min^{-1} and 1/25 min^{-1} for the same synthesis duration at 90-100°C. Separation factor of a two-step synthesized membrane was 16000 with a flux of 0.5 $kg/h.m^2$ for water/ethanol (10/90 wt%) mixture.

The same group achieved the synthesis of NaA membranes on the inner side of a titania support in a continuous system [26]. The continuous flow was obtained by the action of gravity (flow of the synthesis gel from a 2L reservoir) with a flow rate of 1.5-4 ml/min. 10-20μm thick membranes were obtained at the end of a 6-7h synthesis period at 85°C. These membranes have the ability to dehydrate 92% ethanol- 8% water (w/w) mixture with a selectivity up to 8500 and flux of 1.2 kg/m^2h at 50°C by pervaporation.

Aguado et al. synthesized NaA membranes by the recirculation of the solution by means of an HPLC pump [23]. 5μm membranes, which were obtained at 80-90°C has N_2 permeance of $5.0x10^{-7}$- $1.0x10^{-6}$ mol/m^2sPa.

2.6 Gas permeation and separation through MFI membranes

The methods of determining the quality of zeolite membranes are characterization by single gas permeance and separation of gas mixtures through membranes. Although MFI membranes were characterized by different gas molecules such as H_2, CO_2, N_2, CH_4, n-C_4H_{10} and i-C_4H_{10}, frequently used quality criteria for MFI membranes are N_2/SF_6 [4, 63, 83] and n-C_4H_{10}/i-C_4H_{10} [9, 69, 84] ideal selectivity. N_2/SF_6 ideal selectivities of 80 [63, 83], is taken as quality criterion for MFI membranes in literature. Since kinetic diameter of N_2 is smaller than MFI pores and kinetic diameter of SF_6 is larger than MFI pores, it is expected to have high permeance of N_2 and low permeance of SF_6 through a good quality MFI membrane. H_2/SF_6 ideal selectivity is taken as quality parameter for MFI membranes instead of N_2/SF_6 [4]. A list of single gas permeances of H_2, CO_2, N_2, CH_4, n-C_4H_{10} and i-C_4H_{10} through MFI membranes in different studies in literature are given in Table 2.1.

Table 2.1:Permeances of several gas molecules through MFI membranes

		Permeance x10^8 (mol/m^2sPa)						
Perm. T(°C)	**ΔP (bar)**	**CO_2**	**N_2**	**H_2**	**CH_4**	**n-C_4H_{10}**	**i-C_4H_{10}**	**Reference**
105	1	79.3	73.2	134	97.6	14.4	24.4	[47]
200	1.38	7.7	4.8	9.5	-	6	1.1	[44]
50	1.13	-	148.5	503	173.4	35.4	72.8	[85]
25	-	-	960	400	1600	4	0.2	[11]
25	1.4	3.9	8.0	8.6	9.0	0.018	0.036	[67]
100	1.4	15.1	6.5	7.0	15.9	0.128	0.022	
150	1.4	4.4	4.3	5.3	9.5	0.147	0.0054	
200	1	3.8	2.5	6	4.6	4	1	[66]
145	1	1.1	0.07	4.88	0.06	0.005	0.006	[3]
105	1	0.15	0.015	0.24	0.024	0.015	0.015	[27]
21	1.38	340	220	310	-	110	5.7	[40]

MFI membranes were characterized by separating isomer mixtures in vapor phase such as n-butane/i-butane [2], 1-butene/i-butene [46], n-pentane/ i- pentane [47], n-hexane/2,2-dimethylbutane(DMB) [48] and p-xylene/o-xylene [43]. MFI membranes have also been used for separation of methane/n-butane mixtures [66]. In that study, for an equimolar mixture of methane/n-butane, n-butane permeance showed a maximum with increasing temperature where methane permeance decreased continuously [66]. When compared with single permeance, methane permeance in the mixture of methane/n-butane is smaller since n-butane is more strongly adsorbed on MFI crystals and hinders the interaction of methane. At room temperature, n-butane/methane separation factor was 38 with methane and n-butane permeances of $2.5x10^{-10}$ and $9.6x10^{-10}$mol/m^2sPa, respectively where n-butane/methane ideal selectivity was 0.0008 with methane and n-butane permeances of $6x10^{-7}$ and $4.7x10^{-10}$mol/m^2sPa, respectively.

2.7 Gas permeation and separation through SAPO-34 membranes

SAPO-34 membranes were generally characterized by both single gas permeation [16, 18-20, 71, 76] and mixture separation [12-20, 30, 71, 73-77] Single gas

permeances of CO_2 and CH_4 and ideal selectivities of CO_2/CH_4 reported in literature are tabulated in Table 2.2. The CO_2 permeance was $6.4x10^{-8}$mol/m^2sPa and CO_2/CH_4 ideal selectivity was 95 for a membrane with 0.15 Si/Al gel ratio [16]. The highest CO_2/CH_4 ideal selectivity for SAPO-34 membranes was reported by Hong et al., who ion-exchanged H-SAPO-34 membranes with Li^+, Na^+, K^+, NH_4^+ and Cu^{2+} cations and obtained highest CO_2/CH_4 ideal selectivity of 118 Li^+ exchanged membrane [77]. In another study, Chew et al., obtained the best selectivities with Ba-SAPO-34 membranes where the membrane was synthesized by microwave heating [20].

Table 2.2:Permeances and Ideal Selectivities of CO_2/CH_4 for SAPO-34 membranes in the literature

				Permeance (mol/m^2sPa*10^8)		**Ideal Selectivity**
Reference	**Feed P (kpa)**	**P drop (kpa)**	**T (°C)**	**CO_2**	**CH_4**	**CO_2/CH_4**
[71]	270	138	27	2.4	0.12	20
[19]	270	138	27	15	0.75	20
[18]	222	138	24	10.5	0.42	25
[76]	222	138	22	5.9	0.05	118
[16]	222	138	22	6.4	0.067	95
[20]	-	100	30	19.6	0.35	56

SAPO-34 membranes were characterized by CO_2/CH_4 (mainly) (Table 2.3), H_2/CH_4 [16, 19, 76], CO_2/N_2 [12, 16, 19], N_2/CH_4 [19], H_2/N_2 [19]) and H_2/CO_2 [19]. Li et al. obtained highest separation factor of CO_2/CH_4 with a value of 560 by performing the separation at 0°C by using an ethyl glycol/water (50/50) bath [16]. Tian et al. separated CO_2/CH_4 mixture with a separation factor of 9.3 and CO_2 and CH_4 permeances of $2.52x10^{-6}$ and $0.271x10^{-6}$, respectively by their a-oriented SAPO-34 membranes supported by stainless steel net [74]. Zhang et al. increased the separation factor by 20-150% by blocking the defects after immersing the membranes in 1-2% aqueous solution of β-cyclodextrin [73].

Table 2.3:Permeances and Separation factors of CO_2/CH_4 for SAPO-34 membranes in the literature (50% CO_2/50% CH_4)

				Permeance ($mol/m^2sPa*10^8$)		**Separation Factor**	**Thick. (μm)**
Reference	**Feed P (kPa)**	**P drop (kPa)**	**T (°C)**	**CO_2**	**CH_4**	**CO_2/CH_4**	
[71][a]	270	138	27	-	-	30	---
[19]	270	138	27	28 [b]	5.5 [b]	36	4-10
[18]	290	138	25	13.1	0.218	60	25
[17]	222	138		24	0.25	96	5
[30]	187	103	24	14	0.16	87	---
[77]	222	138	22	12	0.067	170	5
[16]	222	138	0	8.4	0.015	560	5
[13]	223	138	22	25	0.01	248	---
[15]	270	138	27	38	0.22	170	Not men.
[75]	224	138	22	180	1	171	7,50
[12]	-	138	22	49	20	245	6
[76]	222	138	22	6.3	0.044	144	---
[74]	120	-	-	252	27.1	9.3	10-20
[14]	4600	4516	22	36	1.67	60	---
[73]	222	138	22	24	0.085	283	---
[20]	-	100	30	37.61	0.37	103	3-4

[a] Mixture is 49% CO_2/51% CH_4

[b] Flux ($mol/m^2s \times 10^4$)

--- No SEM images of the membranes, no thickness data

CHAPTER 3

3. EXPERIMENTAL METHODS

3.1 Materials

The chemicals used for the synthesis of MFI seed crystals and membranes were tetrapropylammonium hydroxide (40 wt% in water, Merck) or tetrapropylammonium bromide (Merck) as template, tetraethyl orthosilicate (98%, Acros), Ludox HS-40 (40 wt% in water, Aldrich) or Ludox AS-30(30 wt% in water, Sigma Aldrich) as silica source, sodium aluminate as aluminum source, sodium hydroxide (Carlo Erba) and distilled water. For the synthesis of SAPO-34 seed crystals and membranes, tetraethyl ammonium hydroxide (20 wt% in water, Aldrich) and/or dipropylamine (DPA-98%) as templates, LUDOX HS-40(40 wt % in water, Aldrich) as the silica source, aluminum isopropoxide (98+%,ACROS) as the aluminum source and phosphoric acid (85 wt % solution in water, ACROS) and distilled water were used.

α-Al_2O_3 tubular supports which had an inner diameter of 0.7 cm with 0.15 cm wall thickness (Fraunhofer-IKTS) were used for the membrane synthesis. Tubular membrane supports have asymmetric pore structure with top inner layer of 200 nm pore size on a macroporous outer structure. 4.5 cm in length tubes were washed in boiled water for two hours and then dried at 120°C overnight. Then both ends of the tubes are glazed with Duncan IN1001 Envision Glaze in order to avoid bypass throughout gas permeance/separation experiments. The membranes had an effective permeation area of 5.5cm^2. The glazed membrane supports were heat treated at 900^oC for 1h with 1.5^oC/min heating and cooling rates.

3.2 Membrane preparation

3.2.1 High temperature flow system

The schematic drawing of the system used for membrane synthesis is given in Figure 3.1. The difficulty throughout this study is the necessity of constructing flow system that is able to withstand the relatively high temperatures and pressures required for the synthesis of SAPO-34 and MFI membranes with high quality. This system has been extremely robust and enabled the synthesis of membranes at 220^{o}C. The setup was located in an oven to keep the temperature constant and uniform. Flow system setup consists of a stainless steel autoclave with inlet and outlet, magnetically coupled centrifugal pump, PTFE hose covered by stainless steel braid (Swagelok), a flow indicator and a pressure gauge. The autoclave and pump has a volume of 39.92 cm^3 and 17.10 (empty volume) cm^3, respectively with an autoclave inside diameter of 16.53mm. The tubings between the pump and autoclave, and the autoclave and pressure gauge have a diameter of ¼ inches. α-Al_2O_3 tubular support outside wrapped with PTFE strip (to isolate the outer surface) was placed inside the autoclave with a membrane holder between the inlet and outlet. The aim of the use of the holder is to fill the space between the support and autoclave and to ensure the flow through the support. The autoclave was also magnetically stirred in order to prevent any precipitation and stagnation. The synthesis solution is flown inside the support from bottom to top of the autoclave with a flow rate of 55ml/min, which was measured at room temperature. During the synthesis, pressure of the system was recorded. Flow indicator is made of three different sizes of PTFE tubings that can fit nested on each other, making gradually increasing crosssection area for the indicator with a stainless steel ball inside. Flow indicator was only used at the 140°C and lower temperatures. It is assumed that flow was achieved at higher temperatures since the flow was observed before and after the synthesis when the autoclave was opened. For membrane synthesis, the autoclave is filled with the synthesis solution till 1cm higher than the outlet of the autoclave, which is approximately 60grams of synthesis solution. The autoclave is also used in classical stagnant synthesis by using blind flange on inlet and outlet of the autoclave.

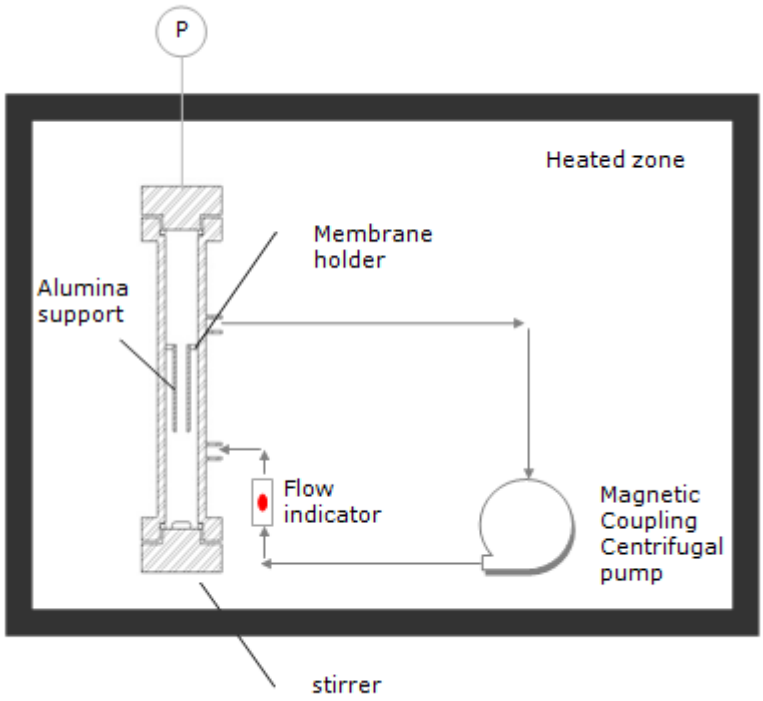

Figure 3.1:Schematic drawing of recirculated flow system for membrane synthesis

3.2.2 Membrane Synthesis

Synthesis of MFI membranes was carried out on the inner surfaces of the seeded support by secondary growth method. Four different synthesis solution compositions were used for membrane synthesis and they were given in Table 3.1. Hydrothermal treatment was carried out both in the recirculated flow synthesis system and stagnant synthesis in autoclaves between 130 and 220°C under autogeneous pressure. After the synthesis, the crystal products were obtained by centrifugation of product solution at 6000rpm for 15minutes. The precipitate washed with distilled water three times and centrifuged. Then the products were dried at 80°C overnight. Membranes were also washed with distilled water and dried at 80°C overnight and N_2-tight membranes subsequently heat treated at 450^{o}C for 6 h with 0.5^{o}C/min heating and cooling rates.

Table 3.1:Synthesis compositions of MFI

Code	Composition	Silica Source
A1	$1SiO_2$:0.2TPAOH:19.2H_2O	Ludox HS-40
A2	$1SiO_2$:0.2TPAOH:19.2H_2O:4C_2H_5OH	TEOS
B	$1SiO_2$: 0.04Na_2O:0.276 TPABr:45.44H_2O	Ludox AS-30
C	$1SiO_2$:0.102TPAOH:0.0026Na_2O:0.0019Al_2O_3:61.46H_2O: 4C_2H_5OH	TEOS

Batch system with stagnant mixture and stirred-recirculated flow mixtures were used to synthesize SAPO-34 membranes in the temperature range of 140-220^oC for 5 to 48h. Low temperature (140-180^oC) and high temperature (180-220^oC) synthesis were performed by using two different gel compositions. The low temperature membrane/seed synthesis gel molar Al_2O_3:P_2O_5:SiO_2:TEAOH:H_2O ratio was 1.1.5:0.3:3:103 (composition D) while gel molar composition of Al_2O_3:P_2O_5:0.3SiO_2:TEAOH:1.6DPA:150H_2O (compositon E) was utilized for high temperature membrane synthesis (Table 3.2).

Table 3.2:Synthesis compositions of SAPO-34

Code	Composition	Synthesis T Range
D	1Al_2O_3:1.5P_2O_5:0.3SiO_2:3TEAOH:103H_2O	140-180^oC
E	Al_2O_3:P_2O_5:0.3SiO_2:TEAOH:1.6DPA:150H_2O	180-220^oC

Hydrothermal treatment in stagnant mixture was performed for the SAPO-34 seed crystals synthesis at 160^oC for 24 h with composition D. Before calcination of the membranes, overnight drying at 80^oC was applied and N_2 impermeable SAPO-34 membranes were heat treated at 400^oC for 10 h with 0.5^oC/min heating and cooling rates. Both MFI and SAPO-34 membrane codes and synthesis conditions were given in Table C.1 and Table C.2, respectively. (Appendix C)

3.2.3 Preparation of the synthesis solutions

Four different synthesis compositions of MFI were used in this study. Composition A1 and A2 were basically the same composition and obtained using two different silica sources: LUDOX HS-40 and TEOS. Synthesis with TEOS results in 4 moles of C_2H_5OH for each SiO_2 [24]. Composition B results in (h0h)/c-axis oriented membranes containing Na_2O [67] and composition C contains Na_2O and Al_2O_3 [68] distinctively from A1 and A2. Sample calculation of the materials used for composition A1 is given in Appendix D.

33.63 g Ludox HS-40, 22.77 g TPAOH and 43.6 g distilled water is necessary for 100g synthesis solution of Composition A1. Firstly, the silica source and the template are weighed in a beaker and this mixture is mixed by a magnetic stirrer. Then, distilled water is added to this mixture and the resulting mixture is mixed for an hour.

For a synthesis solution of Composition A2, TEOS as silica source, TPAOH as template and distilled water were required. For a 100g synthesis solution, 17.15g TPAOH and 47.89g distilled water are poured in a beaker. This mixture is heated up to 50°C and mixed magnetically at the same time for 15 minutes. Then, 34.96g TEOS is added to the mixture dropwise. The resulting mixture can be used after mixing it for three hours at the same temperature.

Synthesis solution of the oriented membranes is prepared by 20.97g Ludox AS-30, 0.34g sodium hydroxide pellets, 7.69g TPABr and 71g distilled water for 100g solution. TPABr and sodium hydroxide pellets are dissolved in one fifth of the water by mixing. In another beaker, the remaining water is added to silica source, which is being mixed, slowly. The first mixture is added to the second and it is mixed for an hour before using.

100g synthesis solution of Composition C is prepared by using 15.9g TEOS, 3.88g TPAOH, 0.027g sodium aluminate and 80.19g distilled water. Sodium aluminate and one quarter of the water is mixed and dissolved in a beaker. In another beaker,

template and the remaining water is stirred magnetically for 15 minutes. TEOS is added drop by drop to the second beaker. Finally, the mixture in the first beaker is added to the second one. This mixture is used for synthesis after aging the mixture by mixing it for 24 hours.

Synthesis solution of SAPO-34 membranes synthesized at low temperature range was prepared by using aluminum isopropoxide, phosphoric acid, Ludox HS-40 and tetraethyl ammonium hydroxide (TEAOH). For a 100g batch, 13.45g aluminum isopropoxide and 71.375g TEAOH were mixed and stirred on magnetic stirrer at 50°C for 2 hours. Then, 1.45g Ludox HS-40 is added and carried on mixing for 2 hours. Finally, 11.16g H_3PO_4 is added dropwise and mixed for 3 hours before synthesis.

High temperature synthesis solution of SAPO-34 membranes was prepared by 11.465g aluminum isopropoxide, 6.342g phosphoric acid, 1.239g Ludox HS-40, 20.2518g TEAOH, 4.498g dipropylamine (DPA) and 56.204g distilled water. Aluminum isopropoxide, phosphoric acid and water were added in a polypropylene bottle and stirred for 2 hours. Then, Ludox HS-40 is added and mixed for 3 hours; TEAOH added and mixed for 1 hour. Finally, DPA is added and mixed for 72h at 50°C prior to synthesis [14]. All experimental results other than with composition A2, D and E were given in Appendix.

3.3 Seed Synthesis and Deposition

In this study, all membranes were seeded prior to hydrothermal synthesis either by dip coating or by rubbing. Molar compositions of the MFI seed synthesis solutions used in dip coating and rubbing were $1SiO_2$:0.375TPAOH:$19.2H_2O$ and $1SiO_2$:0.2TPAOH:$19.2H_2O$:$4C_2H_5OH$, which is the same as composition A2, respectively. MFI seed crystals were synthesized in an autoclave at 90°C for 72 h(1^{st} composition) 140°C for 16 h(2^{nd} composition). SAPO-34 seeds were obtained by composition D; $1Al_2O_3$:$1.5P_2O_5$:$0.3SiO_2$:3TEAOH:$103H_2O$, at 160°C for 24h.

In dip coating method, firstly, the outside of the tubular supports were wrapped with PTFE strip. Tubular support is located on top side of the dip coating setup as seen in Figure 3.2. The tubular support is dipped into 0.25%(wt) MFI seed suspension by ascent of the seed suspension on plastic syringe with a dipping speed of 1.5cm/h. After dipping, the support is waited in seed suspension for 10 minutes and seed suspension is lowered with the same speed. After this treatment, the support is turned upside down and the procedure is applied again. The average particle size of MFI crystals in seed suspension was 300nm.

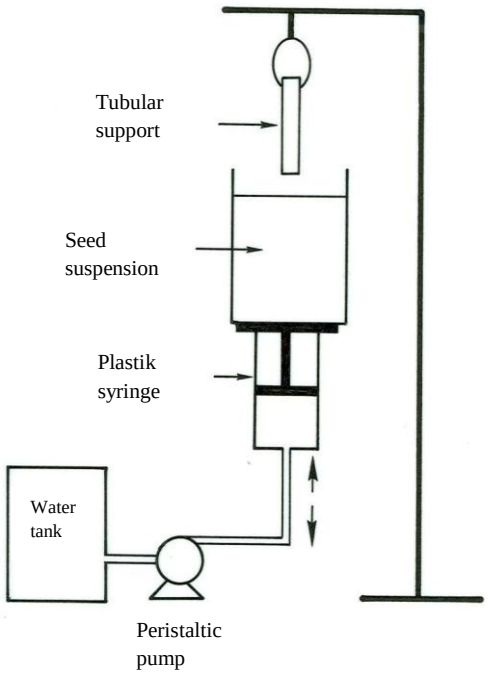

Figure 3.2:Dip coating setup

Seed layer was also applied on the inner surface of the tubular support by using wet rubbing technique. In wet rubbing method, tubular support has been wetted by ethanol-ethylene glycol mixture (50-vol%) and then inner surface rubbed gently with a calcined MFI seed crystals about 5 min or SAPO-34 seed crystals about 5 min. The use of ethylene glycol was expected to increase the ordering of monodispersed particles on support surface by preventing the formation of agglomerate. Drying of the seeded supports was performed at 140^{o}C for 3h before the membrane synthesis.

3.4 Membrane/Powder characterization

Phase identification of the seeds, membranes and the residual powders from the membrane syntheses was performed by Philips PW 1840 X-ray diffractometer having Cu-Kα radiation from Ni filter. Voltage and current values for powder and membrane analyses were 30kV- 24mA and 40kV-30mA, respectively. Phase identification was based on the three characteristic peaks at Bragg angles of 23^o, 24^o and 24.5^o for MFI and 9^o, 16^o and 21^o for SAPO-34.

Dynamic light scattering (DLS) was used to determine the particle size distribution of the seed crystals (Malvern Mastersizer 2000). DLS measurements determine the velocity at which particles within a solvent diffuse due to Brownian motion. This random motion causes the intensity of light scattered from the particles to form a moving pattern and it is possible to convert size distributions into volume and number based distributions by using Mie theory. In general, measured particle sizes are in the order of intensity>volume>number [86]. Morphology and size of the seed particles, and morphology and thickness of the membranes were figured out by JEOL JSM-6400 scanning electron microscope (SEM) after coating the samples with gold and palladium mixture to have a conductive layer on the samples. Specific surface area measurements of the residual powders were performed by N_2 adsorption/desorption in accordance with BET method (Micromeritics).

3.5 Gas permeation measurements

Single gas permeation experiments were conducted in dead-end mode permeation setup at room temperature (Figure 3.3). One end of the feed side is connected to the gas cylinders with polyurethane tubing and the other side is tied to a T-connector; one side is tied to the pressure gauge and the other side is tied to the membrane module. Membrane is inserted to the membrane module and both ends are sealed with viton o-rings. The module is made of brass and the length is 45mm. Permeate

side is connected to the soap film bubble flow meter with silicon tubing, which is open to the atmosphere.

The first test of the as–synthesized membranes is the N_2 permeation through the uncalcined membranes. If the membrane is impermeable to N_2 (permeance< 10^{-11}mol/m^{2}sPa), it is thought to be defect free since pores of the zeolite crystals are filled with template molecules [87]. Then, the membrane is calcined to open the pores at 450^{o}C for 6 h with 0.5^{o}C/min heating and cooling rates for MFI(at 400^{o}C for 10 h with 0.5^{o}C/min heating and cooling rates for SAPO-34) and gas permeation with different gases was performed. In these experiments, transmembrane pressure difference was 1 bar and permeate side flow rate was measured by a soap film flow meter for H_2, CO_2, N_2, CH_4, C_2H_6, C_3H_8, n-C_4H_{10} and i-C_4H_{10} for MFI and CO_2 and CH_4 for SAPO-34 in every 15 minutes till steady state conditions are reached. Permeances of the membrane for these gases were calculated by Equation 2.1 (page 1). Sample calculations of permeance and ideal selectivity are given in Appendix E.

Where P is the permeance (mol/m^{2}sPa), p is the atmospheric pressure (Pa), R is the ideal gas constant (Pa.m^3/mol.K), T is the room temperature (K), $\Delta V/\Delta t$ is the volumetric flow rate of the permeate (m^3/s), A is the effective permeation area, which is 5.5x10^{-4} m^2 (the area between the glazed parts) and Δp is the transmembrane pressure difference (Pa).

Binary gas separation setup is shown in Figure 3.4. CH_4 and n-C_4H_{10} or CO_2 cylinders were connected to the feed side of the separation setup with polyurethane tubings. Feed side is composed of firstly gas filters to remove impurities if any and then the mass flow controllers. The two feed parts are united with a tee-union and send to the membrane module. There exist a by-pass line connecting to the permeate side before the membrane module. The gas mixture is prepared using that line and releasing the gas mixture also discharges the air in the permeate side. The membrane module is similar to the one for single gas permeation; however, retentate side is not in the dead-end mode. Retentate is open to the atmosphere and a back pressure valve on that line is used to adjust the transmembrane pressure difference.

Binary mixture of 50% CH_4 and 50% n-C_4H_{10} were separated in the room temperature-100°C temperature range for MFI membranes, whereas mixture of 50% CH_4 and 50% CO_2 separated by SAPO-34 membranes . Separation experiments above room temperature were performed by heating the membrane module with a temperature controller. Gas mixture was prepared by adjusting the flow rates of the gases with mass flow controllers. Calibration of the mass flow controllers are given in Appendix F. Transmembrane pressure difference of 1 bar was obtained by a back pressure valve on the retentate side. Both permeate and retentate sides were analyzed online by Varian CP-3800 gas chromatograph with a TCD detector and Propak T packed column in separations with MFI membranes. Gas chromatograph calibrations for CH_4 and n-C_4H_{10} and CO_2 are given in Appendix G. The chromatograms of feed, permeate or retentate and the GC calibrations of the gases were used for the calculation of molar fluxes (Appendix H) Separation factor calculations were done by Equation 2.4 and a sample calculation of Separation factor is given in Appendix I.

3.6 Measurement of the Pressure of the System

In this study, pressure measurements were done by using a batch autoclave having a connection to a pressure gauge. About 70% of the autoclave was filled with synthesis solution and the system was heated to the selected temperature. When the oven reached to the selected temperature, the solution was waited at that temperature approximately 3 hours. During this process, pressure of the system was recorded in every 20 minutes. When the system reached the steady state, temperature of the system increased to the other selected temperature and steady state was waited by recording the pressure.

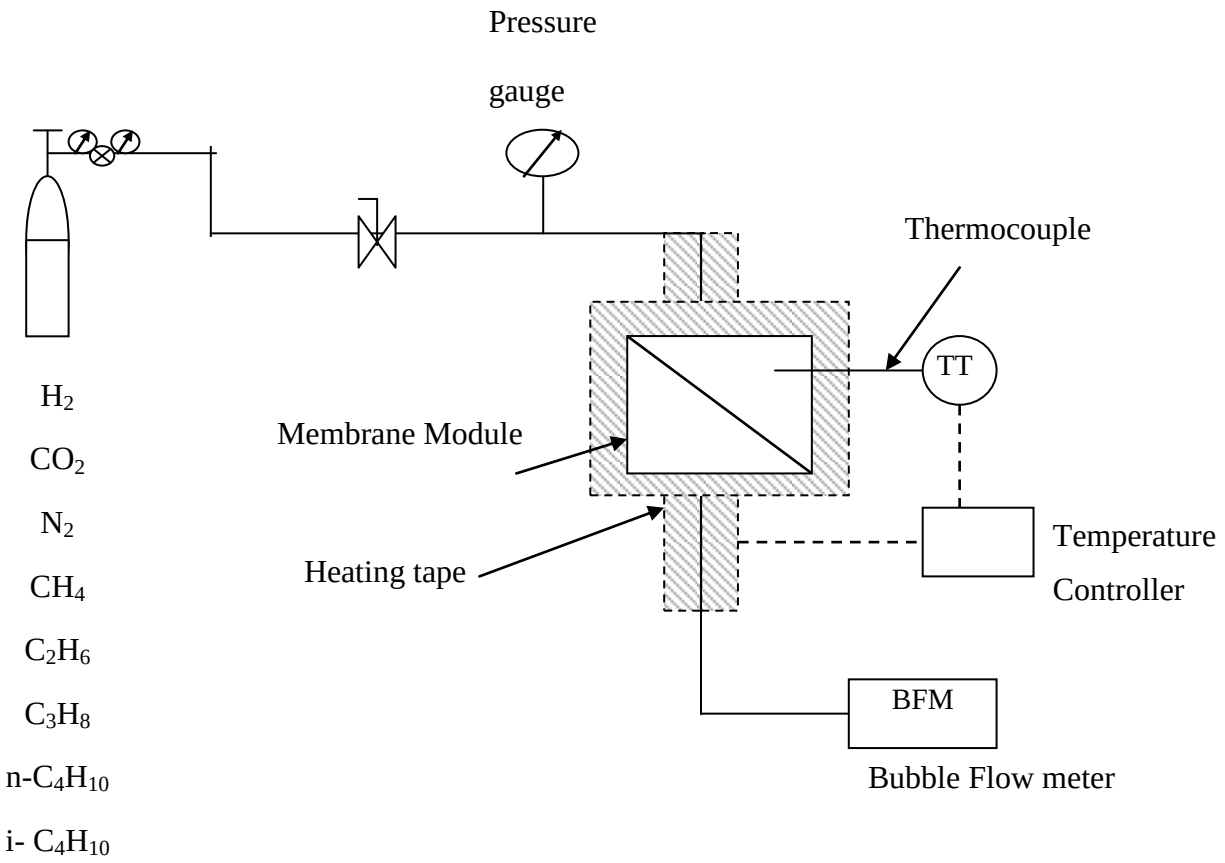

Figure 3.3:Single gas permeation setup

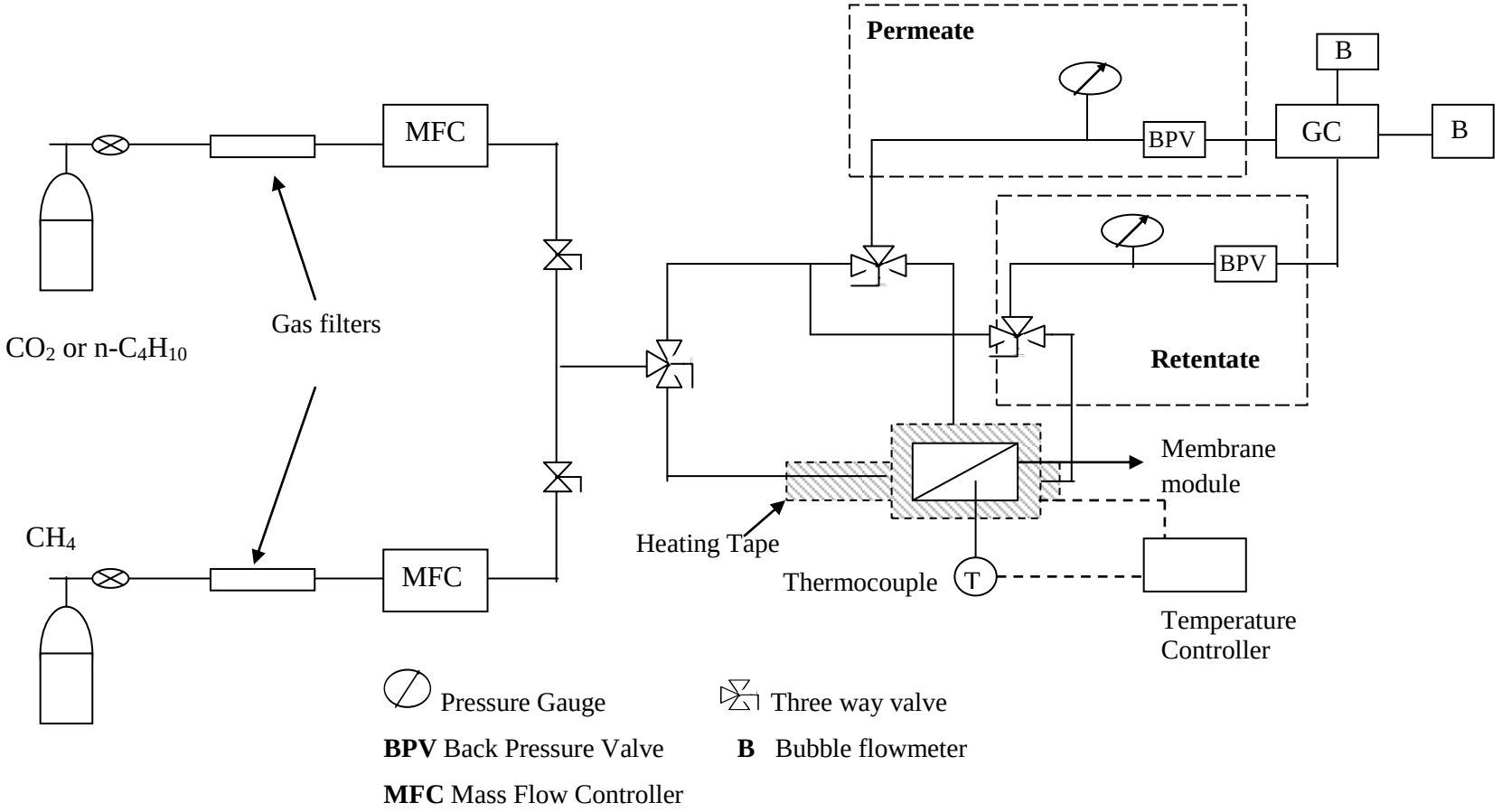

Figure 3.4:Binary gas separation setup

CHAPTER 4

RESULTS AND DISCUSSION

4.1 Characteristics of MFI and SAPO-34 Seed Crystals used in Dip-coating and Wet-rubbing

The inner surface of tubular alumina supports were coated with MFI and SAPO-34 seed crystals before hydrothermal treatment to obtain membranes. The seed crystals were characterized by XRD, SEM and DLS. MFI seed crystals used in dip coating were synthesized at 90°C for 72 h in a stagnant batch synthesis media with a molar composition of $1SiO_2$:0.375TPAOH:$19.2H_2O$. The seed crystals used for dip coating were characterized by XRD (Figure 4.1) and SEM (Figure 4.2). Figure 4.3 shows the particle size distribution of the seed particles used in dip coating (two analyses). The XRD pattern of the seed crystals was the sign of highly crystalline material. According to SEM image of the seed crystals, the size of the particles is mostly 250nm and size of the crystals changes in the range of 100-300nm. Particle size distribution results are also compatible with SEM results having volume average particle size of 295nm for two batches of seeds.

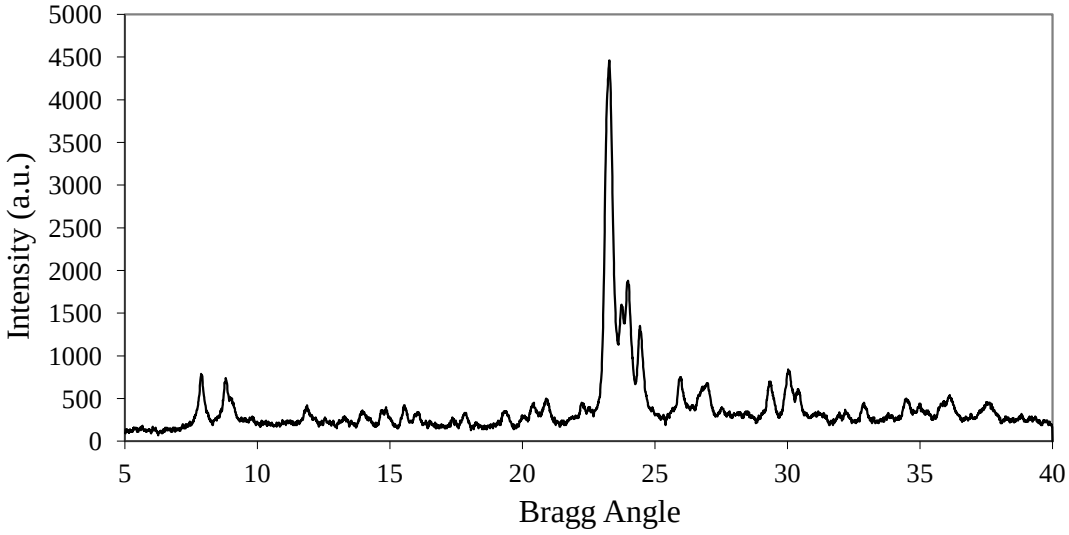

Figure 4.1:XRD pattern of seed crystals used in dip coating (MFI, at 90°C for 72 h)

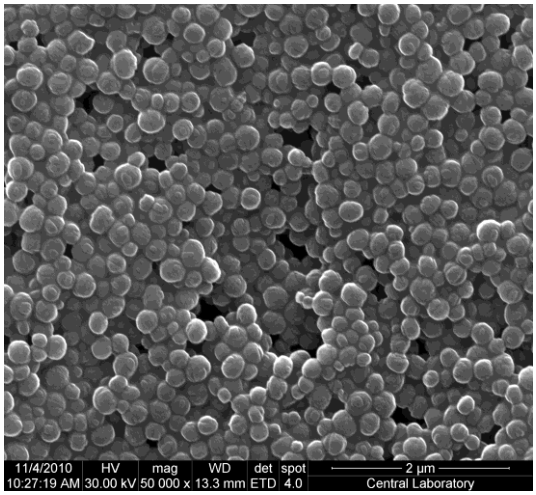

Figure 4.2:SEM image of seed crystals used in dip coating (MFI, at 90°C for 72 h)

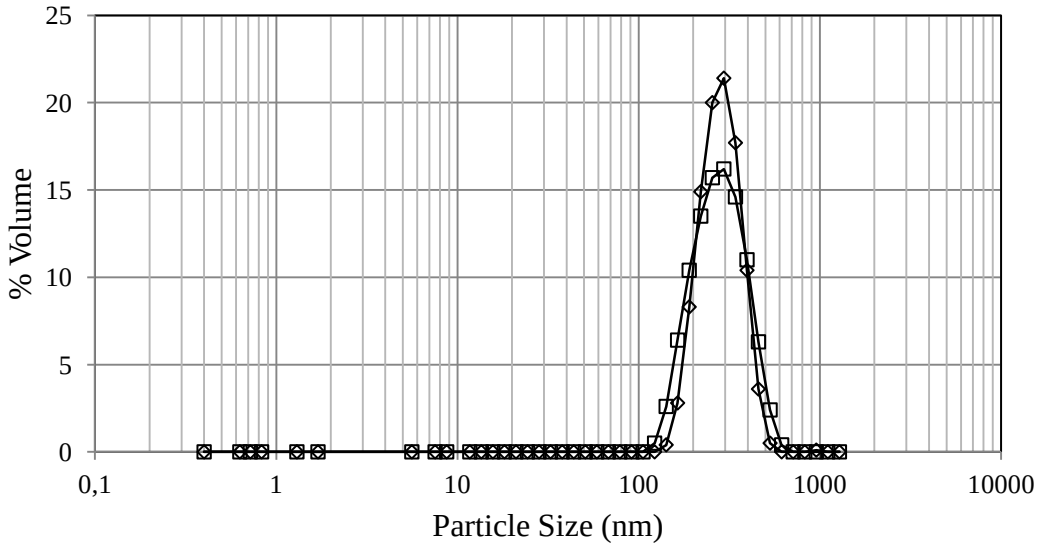

Figure 4.3: PSD of seed crystals used in dip coating (obtained by DLS, MFI, at 90°C for 72 h)

The SAPO-34 and MFI seed crystals used for wet rubbing were synthesized from $1Al_2O_3:1.5P_2O_5:0.3SiO_2:3TEAOH:103H_2O$ at 160°C for 24h for SAPO-34 and $1SiO_2:0.2TPAOH:19.2H_2O:4C_2H_5OH$ at 140°C for 16 h for MFI. The characteristics of SAPO-34 and MFI crystals used for seeding by wet rubbing are described below. XRD patterns of the seed crystals are shown in Figure 4.4. No reflections other than characteristic SAPO-34 and MFI peaks were identified on the patterns, implying that the seed crystals are pure. Particle size distributions of both MFI and SAPO-34 seed

crystals are shown in Figure 4.5. The volume average particle sizes of MFI and SAPO-34 crystals are 140 nm and 350 nm with distributions between 90 nm-350 nm and 190 nm-720 nm, respectively. The use of nano-size seed crystals with narrow particle size distribution has been shown to increase membrane performance by improving the seed layer uniformity and reducing the layer thickness [15]. In Table 4.1, some properties describing the MFI and SAPO-34 seed crystals are given such as average particle size, BET surface area and pore volume which are all comparable with those reported in the literature. The size of MFI seeds was between 50 nm and 3 μm [1, 2, 40, 66-68], mostly around 100 nm [8, 10, 11, 85] while SAPO-34 membranes were seeded with seed crystals having a size of 0.7-4μm [13], 0.5-3μm [15] and ~0.6μm [12]. MFI seed crystals used in this study had BET surface area of $392 m^2/g$ with total pore volume of $0.288 cm^3/g$. In literature, BET surface area of MFI crystals were found as $302 m^2/g$ [88] with total pore volume of $0.29 cm^3/g$, 469-$711 m^2/g$ [89] and $520 m^2/g$ [90]. BET surface area of SAPO-34 seed crystals was $457 m^2/g$ with total pore volume of $0.265 cm^3/g$, whereas it was between 420 and $700 m^2/g$ [20, 91-93], in which the use of crystal growth inhibitor increased BET surface area from 496 m^2/g to 700 m^2/g [91].

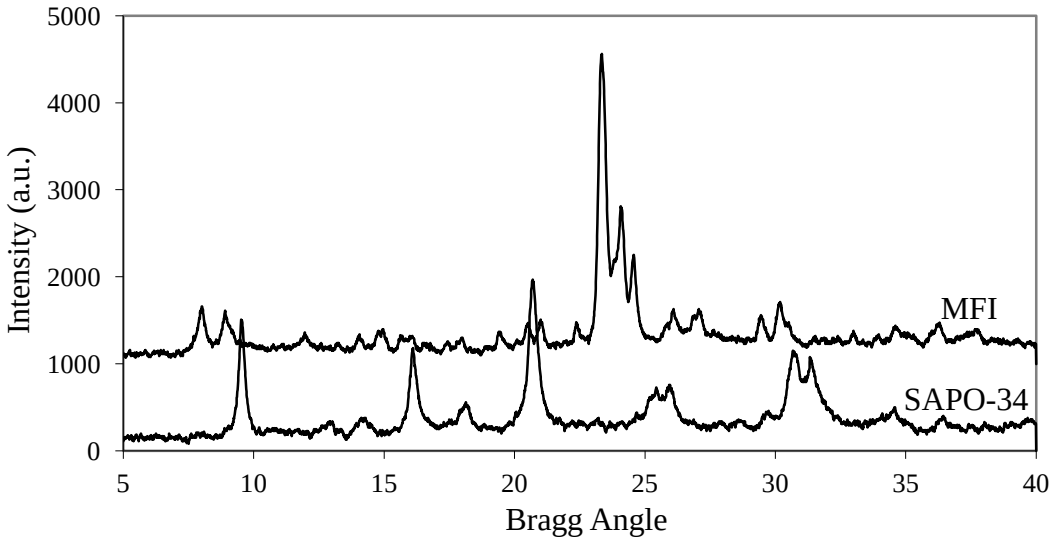

Figure 4.4:Uncalcined XRD patterns of MFI and SAPO-34 seeds (calcination at 450^{o}C for 6 h for MFI and 400^{o}C for 10 h for SAPO-34)

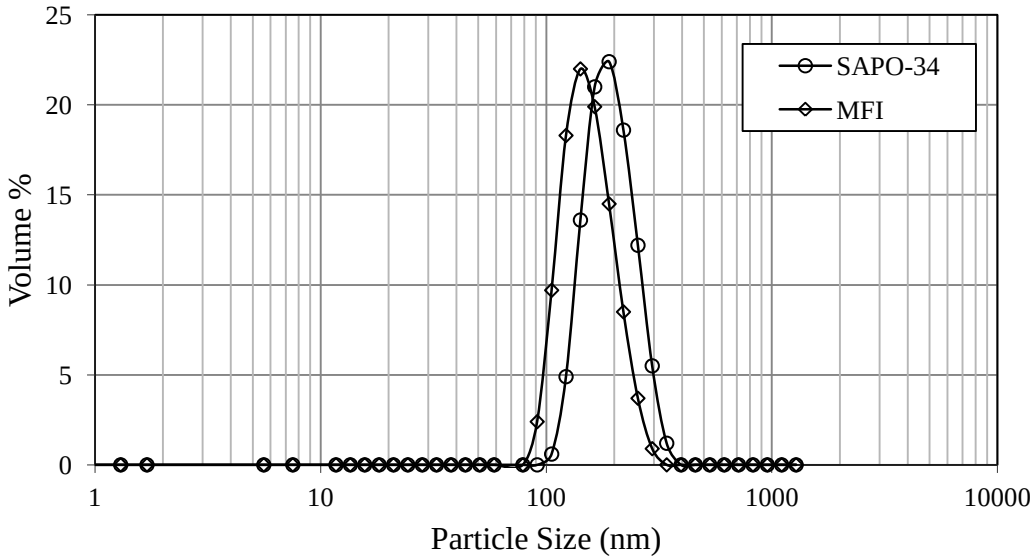

Figure 4.5:Particle size distribution of MFI and SAPO-34 seeds

Table 4.1:Properties of the seed crystals used in wet rubbing. MFI was synthesized from composition A2 at 140°C for 16 h. SAPO-34 was synthesized from composition D at 160°C for 24 h.

Seed Crystal Type	**Av.Size (vol-%) (nm)***	**BET (m^2/gr)**	**Pore Volume (cm^3/gr)**
MFI	163	392	0.288
SAPO-34	190	457	0.265

*DLS results

4.2 Characterization of Support Surface coated with MFI and SAPO-34 seed crystals

Application of seed onto the support surface before membrane synthesis affects the quality of the membrane directly. Seed layer has an effect on the crystal growth and final microstructure [6] such as thickness and crystal orientation of the membrane [58]. Rubbing [12, 13, 15, 24], dip-coating [2, 8, 27, 58, 65, 66] and vacuum seeding [67, 68] are most widely used seeding techniques for secondary growth of membranes. Rubbing is an easy method to apply, but packing of the seed crystals on

the support surface may not be enough to obtain a uniform seed layer. Dip coating method results in thin crystal deposits on the support surface which is generally a slow process in order to get a thinner membrane layer. Vacuum seeding give rise to non-homogeneous seed layer especially if accumulation occurs at certain places. Among these methods, dip-coating and wet-rubbing were tried in this study because these methods were applicable for tubular supports. Wet rubbing is the special application of rubbing the seed crystals on the support where the support is wetted by ethylene glycol-ethanol mixture prior to rubbing. The main advantage of wet rubbing over dry rubbing is to increase in the ordering and closely packing of the seed crystals, thus wet rubbing is preferred over dry-rubbing as the second seeding technique in this thesis. Seeding of SAPO-34 membranes was only performed by wet rubbing method since it was discovered in MFI seeding that wet rubbing is more efficient compared to dip coating.

Although dry rubbing is conventional technique for zeolite membrane seeding in the literature [12-15, 75, 77] in this study, seed crystals were rubbed on the support after wetting the inner support surface with ethanol-ethylene glycol mixture (50-vol%). In Figure 4.6, surface SEM images of dry rubbing and wet rubbing of the seed on the support can be compared. As all the other SEM images in this study, the given images are representatives of the entire sample. While there are some discontinuities on the seed layer of conventionally dry rubbed supports, a more closely packed seed layer on alumina support was obtained by using wet-rubbing method. Dispersive effect of wetting the support with ethylene-glycol solution decreases the intercrystalline regions by slow vaporization due to the presence of ethylene-glycol. The size distribution and shape of the crystals may affect the packing seeds on alumina surface. Since spherical MFI crystals are almost monodisperse, their packing is more closed and uniform than those for SAPO-34 crystals. Mean and maximum sizes of seed crystals are 260 nm and 550 nm for MFI, whereas 700 nm and 1.6 μm for SAPO-34 according to SEM images. The difference in sizes of seed crystals, especially for SAPO-34, based on the DLS and SEM results might be due to the plate like crystals of SAPO-34. The particle size that is obtained by DLS technique is the

diameter of sphere, and the diffusion speed is strongly affected by the change of particle shape.

During the membrane synthesis in a stirred-recirculated flow system, the volumetric flow rate of the synthesis solution was 55ml/min and linear velocity of the synthesis solution inside the tubular support was calculated as 2.38cm/s. Thus, synthesis solution flowed through the support in one second since the effective permeation length of the tubular support was approximately 2.5 cm. The synthesis solutions were flown over the supports for 1.5h after applying the seed layer to ensure that the seed layer was not swept off the support. SEM micrographs of seeded both MFI and SAPO-34 supports after flow of synthesis solutions through the supports for 1.5h are shown in Figure 4.7. Both SAPO-34 and MFI seed crystals were adhered on the support surface and sustained their existence after flow of the solution. This signified that the adhesion between each SAPO-34 or MFI crystal and the alumina support is strong enough to endure the recirculated-flow.

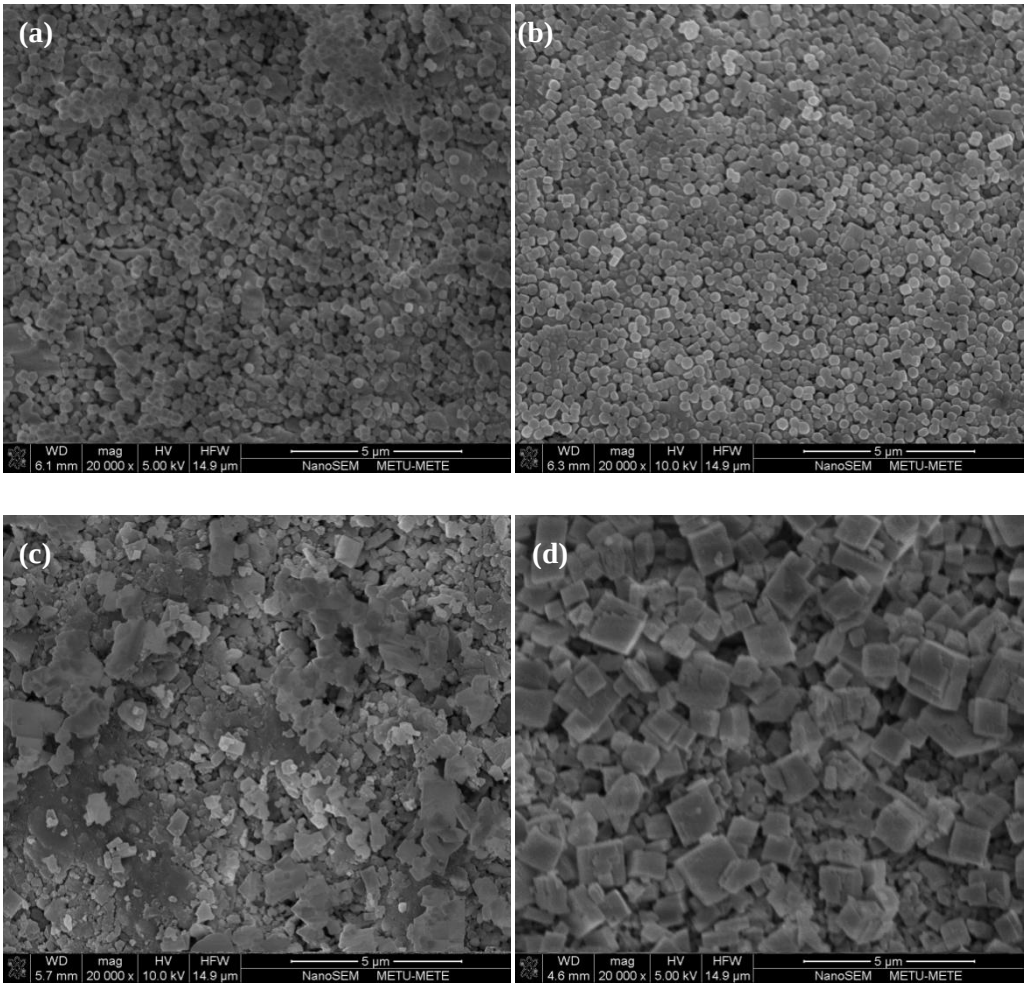

Figure 4.6: SEM images of seed crystals on supports deposited by a)dry-rubbing b) wet-rubbing of MFI and c) dry-rubbing d) wet-rubbing of SAPO-34.

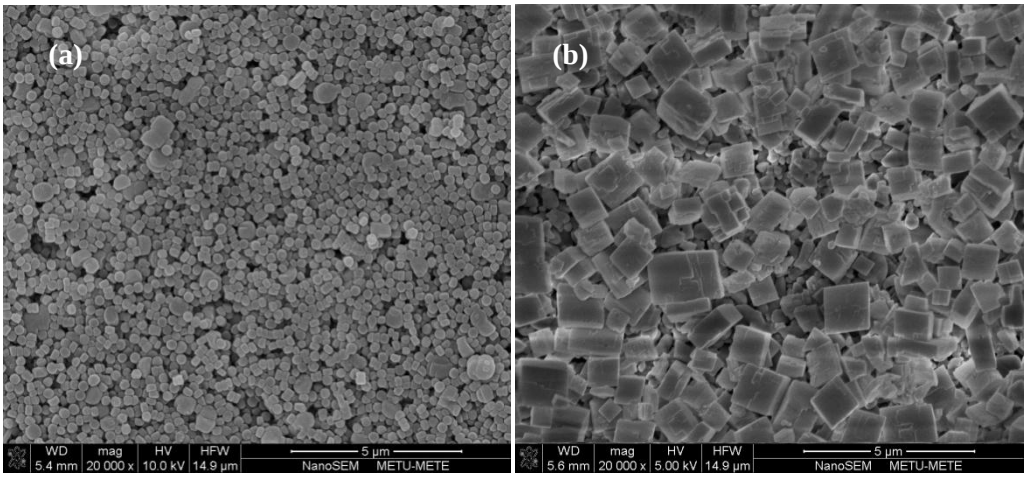

Figure 4.7: SEM images of wet rubbed seed crystals after the flow a) MFI and b) SAPO-34.

4.3 Pressure of the synthesis system

The most challenging part of synthesis of zeolite membranes in recirculated flow system is the elevated autogenous pressure which increases exponentially with temperature. It is generally found that the microporous materials with low level of intercrystalline void spaces can be prepared at high temperature [94]. The pressure of the system is dependent on both the composition of the synthesis mixture and the synthesis temperature [95]. Because the system is closed to the atmosphere during the synthesis and high synthesis temperatures were applied, the internal pressure of the system is higher than atmospheric pressure.

Figure 4.8 shows the change in the measured and predicted vapor pressure values with temperature for the SAPO-34 and MFI crystallization. Bubble point pressure values of pure water are taken from Steam Tables whereas bubble point pressure values of pure ethanol and isopropanol were estimated by Antoine Equation. Antoine Equation is defined as the following where A, B and C are special parameters for the material P^{vap} is the vapor pressure of the material in bars at a defined temperature and T is the temperature in Kelvin [96]. The parameters for ethanol and isopropanol are given in Table 4.2.

$$lnP^{vap} = A - \frac{B}{T + C} \tag{4.1}$$

Table 4.2: Parameters for ethanol and isopropanol used in Antoine Equation

Name	A	B	C	T_{max}	T_{min}
Ethanol	122.917	3803.98	-41.68	369	270
Isopropanol	120.727	3640.20	-53.54	374	273

SAPO-34 and MFI synthesis gel composition led to the formation of isopropyl alcohol and ethanol, respectively as a hydrolysis product and bubble point pressure is

affected by the fraction of isopropyl alcohol or ethanol and the solid particles in the synthesis composition. Bubble point pressure of synthesis compositions were estimated by Modified Raoult's law and Unifac activity coefficient model by assuming that the synthesis mixture is only isopropyl alcohol-water or ethanol-water solution. According to Unifac model, the subgroups forming the molecule are determined and then the activity coefficients of the molecules are calculated [97]. The subgroups forming isopropyl alcohol-water solution are; H_2O, CH_3, CH_2 and OH while H_2O, CH_3, CH_3 CH_2 and OH are the subgroups of ethanol-water solution. The activity coefficients at selected temperatures for isopropyl alcohol-water and ethanol-water solutions are given in Table 4.3. The boiling point elevation due to the formed solid particles was neglected for the model calculations. Isopropyl alcohol and ethanol mole fraction of the synthesis gels were 0.05 and 0.18, respectively. However, the synthesis mixtures were not just two components and were not ideal. The dissociation of the solute may result in free ions in the solution and may cause ion-association, which ends up with the lowering of the vapor pressure.

Table 4.3: Activity coefficients for isopropyl alcohol-water and ethanol-water solutions

	Activity Coefficients		**Activity Coefficients**	
T(°C)	**Water**	**Ethanol**	**Water**	**Isopropyl Alcohol**
100	10.822	23.617	10.145	71.090
120	10.848	22.752	10.152	66.873
140	10.865	21.544	10.158	61.565
160	10.872	20.023	10.164	55.359
180	10.864	18.231	10.170	48.412
200	10.838	16.244	10.176	41.004
220	10.788	14.153	10.181	33.460

a)

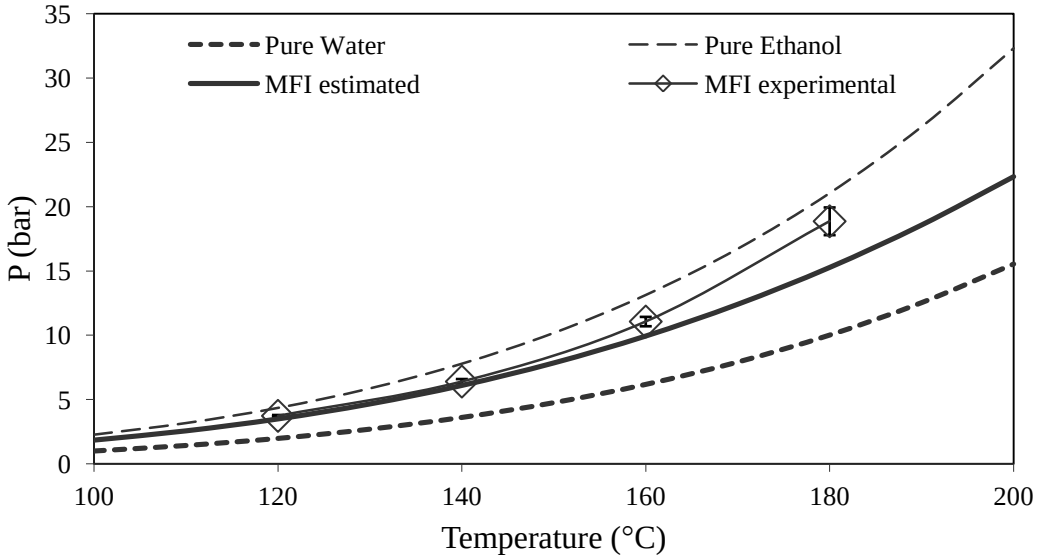

b)

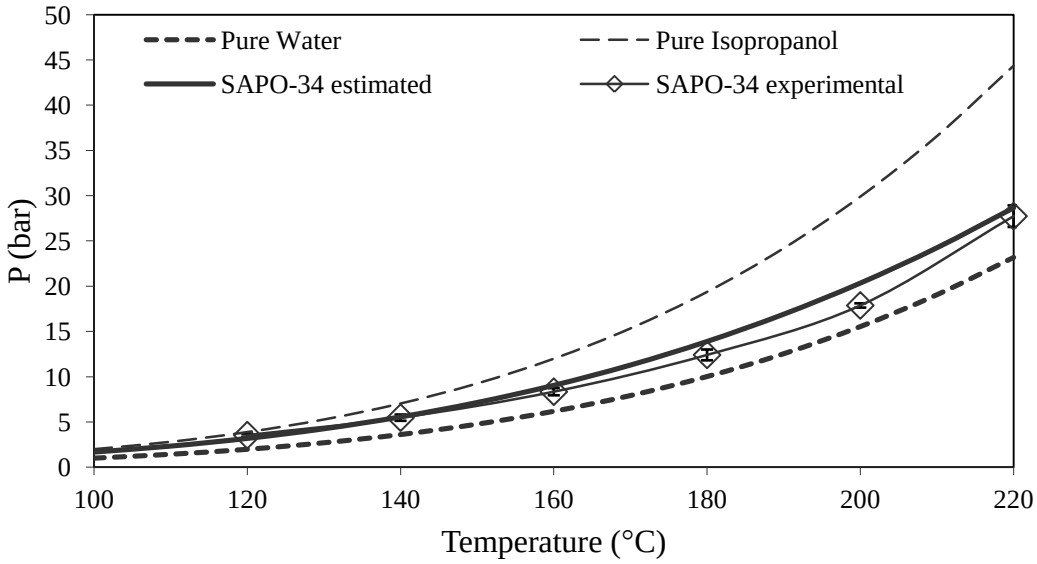

Figure 4.8: Measured and estimated pressures as a function of temperature for a) MFI, b) SAPO-34 synthesis compositions.

Experimental bubble point pressure values were found as very comparable with the estimated pressure values for both MFI and SAPO-34 systems. Experimental bubble point pressure values are greater than the estimation values with a pressure difference range of 0.3 to 3.6 bars. Pressure difference between the estimation and measurement increases with increasing temperature. Bubble point pressure of MFI synthesis gel at

180°C, which was the highest synthesis temperature, was measured as 18.9 bars absolute. Experimental bubble point pressure values of SAPO-34 were both greater and less than the predicted ones. The differences between the predicted and experimental values are in the range of 0.2 to 2.5 bars. The largest difference in the experimental and prediction values were at 200°C, where prediction was 20.3bars and experimental was 17.8 bars. Bubble point pressure of SAPO-34 gel at 220°C reaches 27.7 experimentally.

The effects of high syntheses temperatures are not limited with high autogeneous syntheses pressures. It is also resulted in expansion of the liquid synthesis mixture. As mentioned in the experimental part 60g of synthesis mixture is used in flow synthesis setup. As a rough estimate; 11.23cm^3 volume increase will occur for a 60g water (for estimation) from increasing its temperature from 25°C to 220°C (the highest synthesis temperature); approximately 20% volume increase. Therefore, the empty volume of the system should be larger than the expected increase in volume and it should be durable for vapor pressure as well. The use of robust recirculated flow system without any safety concern and leakage is necessitated due to the increase in vapor pressure and liquid volume during the crystallization of MFI and SAPO-34 at high temperature.

4.4 Characterization of MFI membranes

4.4.1 Phase Identification of MFI membranes synthesized in stagnant system

Synthesis of membranes in stagnant system was carried out with composition A2 at 140°C and 180°C for checking the composition and comparison with the ones synthesized in the recirculating flow system. The XRD pattern (Figure 4.11) and the particle size distribution (Figure 4.12) of the residual powder of the membrane synthesized at 140°C showed that the powder was highly crystalline with a relative crystallinity of 96% and average particle size of 295nm.

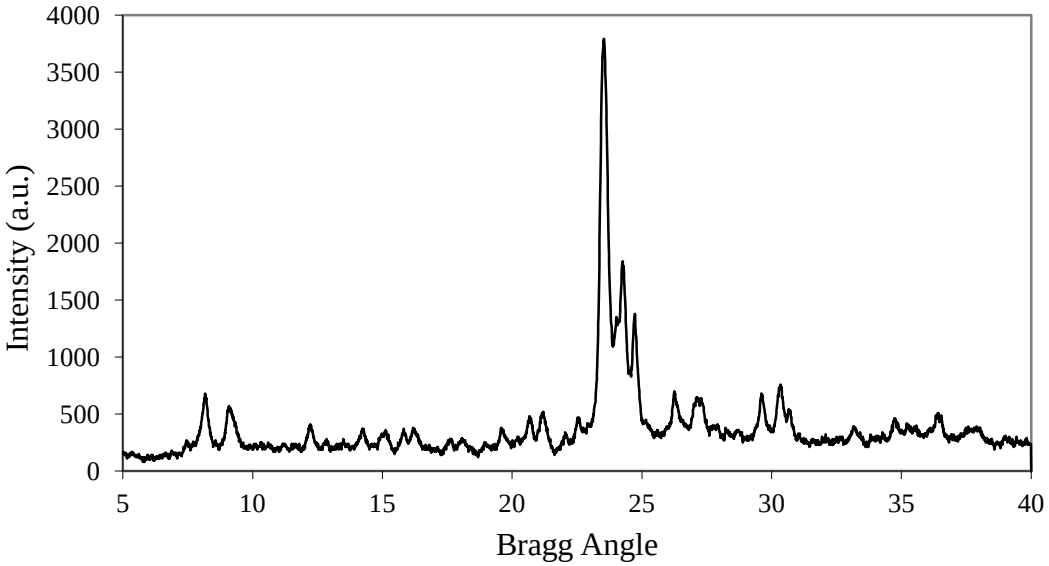

Figure 4.9: XRD pattern of the residual powder of AON-28(AON-30) synthesized at 140°C

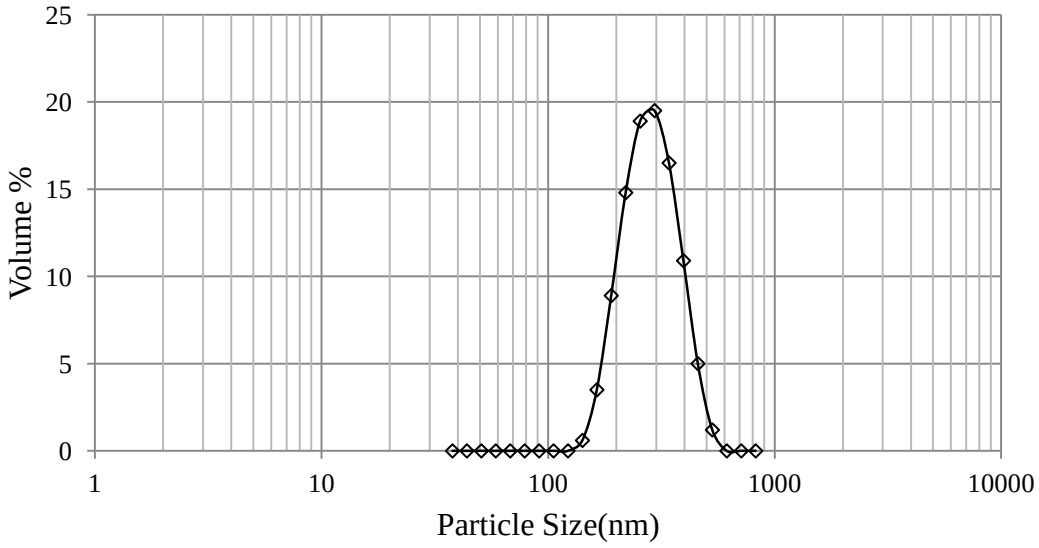

Figure 4.10: PSD distribution of the residual powder of AON-28 (obtained by DLS) synthesized at 140°C

4.4.2 Morphology of MFI membranes synthesized in recirculating flow system

The effect of synthesis temperature in the recirculating flow system was investigated for MFI membranes. Synthesis parameters of the membranes investigated in this section are given in Table 4.4.

Table 4.4: Synthesis parameters of MFI membranes

Membrane Code	Synthesis T(°C)	Synthesis Time(h)	Number of Layers	N_2 permeance before calc.
AON-51	140	24	4	$1.22x10^{-10}$
AON-184	160	16	2	$4.85x10^{-11}$
AON-180	180	13	2	$<10^{-12}$

XRD patterns of the membranes synthesized at 140°C, 160°C and 180°C were given in Figure 4.11. The XRD patterns of the membranes synthesized at 140°C, 160°C and 180°C were shown from bottom to the top of the figure. Characteristic MFI peaks and alumina peaks were observed on the XRD patterns of the membranes. These three α-Al_2O_3 peaks were mainly due to the curved surface geometry of XRD samples. Characteristic peaks of the membranes synthesized at 140°C can be determined hardly. When the characteristic peaks of the membranes could not be observed on the XRD pattern or when it is inappropriate to break the membrane, the analysis of the residual powder from the membrane synthesis is common. Many researchers agree that crystal phase of the residual powder is the sign of the phase of the membrane [63, 98]. The XRD patterns of residual powders of the membrane synthesized at 140°C, 160°C and 180°C with composition A2 were given in Figure 4.12. The relative crystallinities of these powders were 95, 92, 90 % for the powders synthesis at 140°C, 160°C and 180°C, respectively.

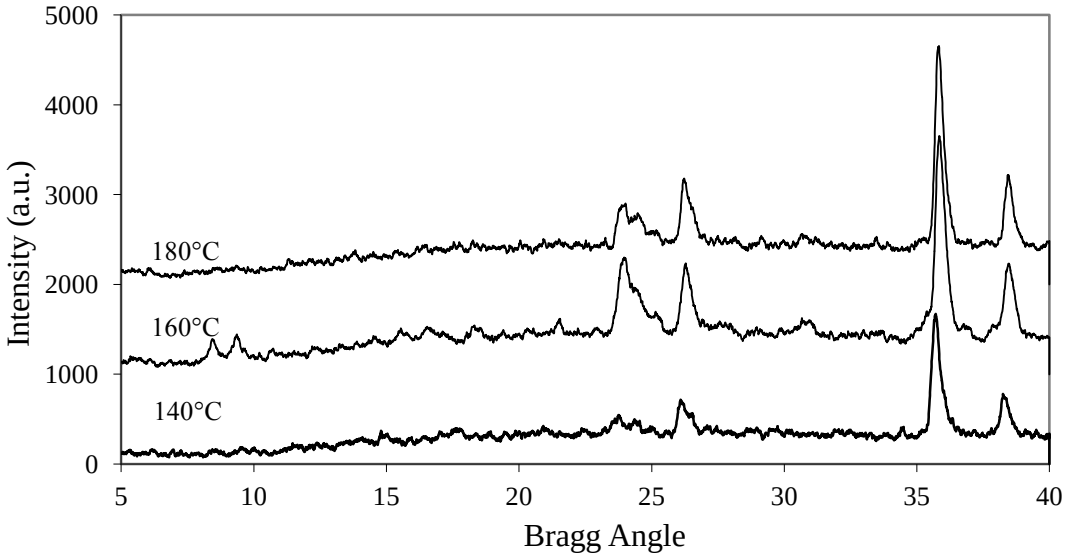

Figure 4.11: XRD patterns of the membranes synthesized at 140°C, 160°C and 180°C in the recirculating flow system

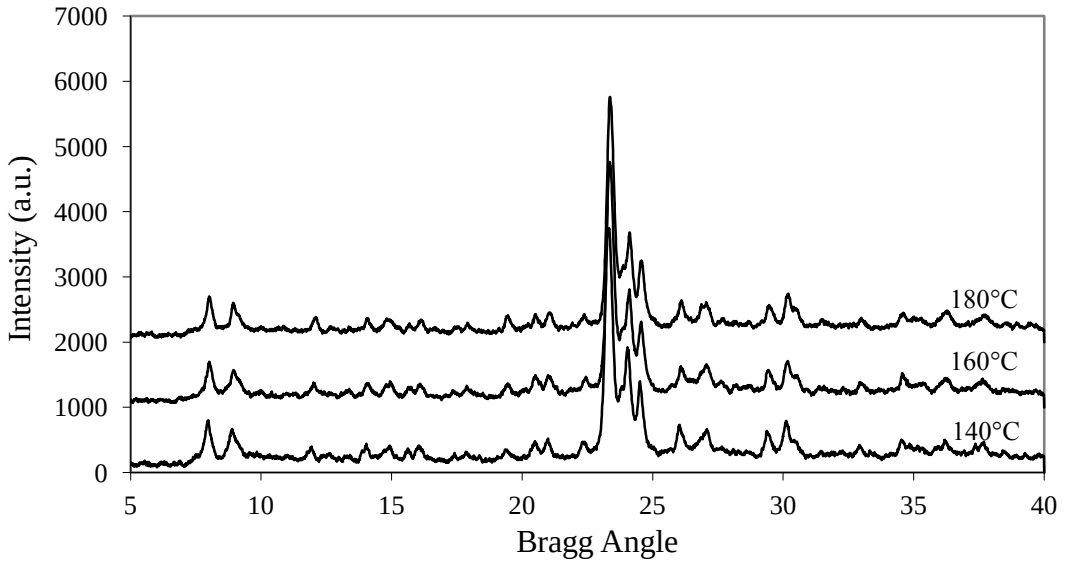

Figure 4.12: XRD patterns of the residual powders synthesized at different temperatures with Composition A2

Cross-section and surface views of the MFI membranes synthesized at 140°C, 160°C and 180°C are shown in Figure 4.13. The thicknesses of AON-51 (4-layered), AON-184 (2-layered) were around 3-4μm, and the thickness of AON-180 (2-layered) was around 5 μm. Richter et al. obtained c-oriented MFI membranes inside capillaries by

flowing the synthesis solution with a flow rate of 0.25cm/min [27] . The thickness of the membranes was around 30μm and the number of layers increased by decreasing the support diameter from 7mm/4mm to 3.9mm/1.9mm (OD/ID). Surface images of AON-51, AON-184 and AON-180, especially AON-184 and AON-180, are very similar. Globular MFI particles are present on the the intergrown MFI layers for the membrane synthesized at 140°C. Çulfaz et al.,who used recirculated flow system, obtained 1-2μm thick MFI membranes by synthesis at 80°C or 90°C with smoother surface compared to that for batch ones[2]. A similar study, where the membranes were synthesized in a recirculated flow system at 95°C, showed that recirculation of the synthesis solution sweeps away MFI crystals formed in the bulk and results in a smoother membrane surface [66]. Contrary to the results obtained by refrences [2] and [66], the surfaces of the membranes synthesized in recirculated flow system at 160°C and 180°C are nearly-cubic and not very smooth. Yan et al. were also obtained MFI membranes with nearly-cubic crystals at 165°C by synthesis in autoclave [99]. Cubic MFI crystals were observed for MFI membranes where the synthesis solution contains high SiO_2 and TPAOH [100,101].

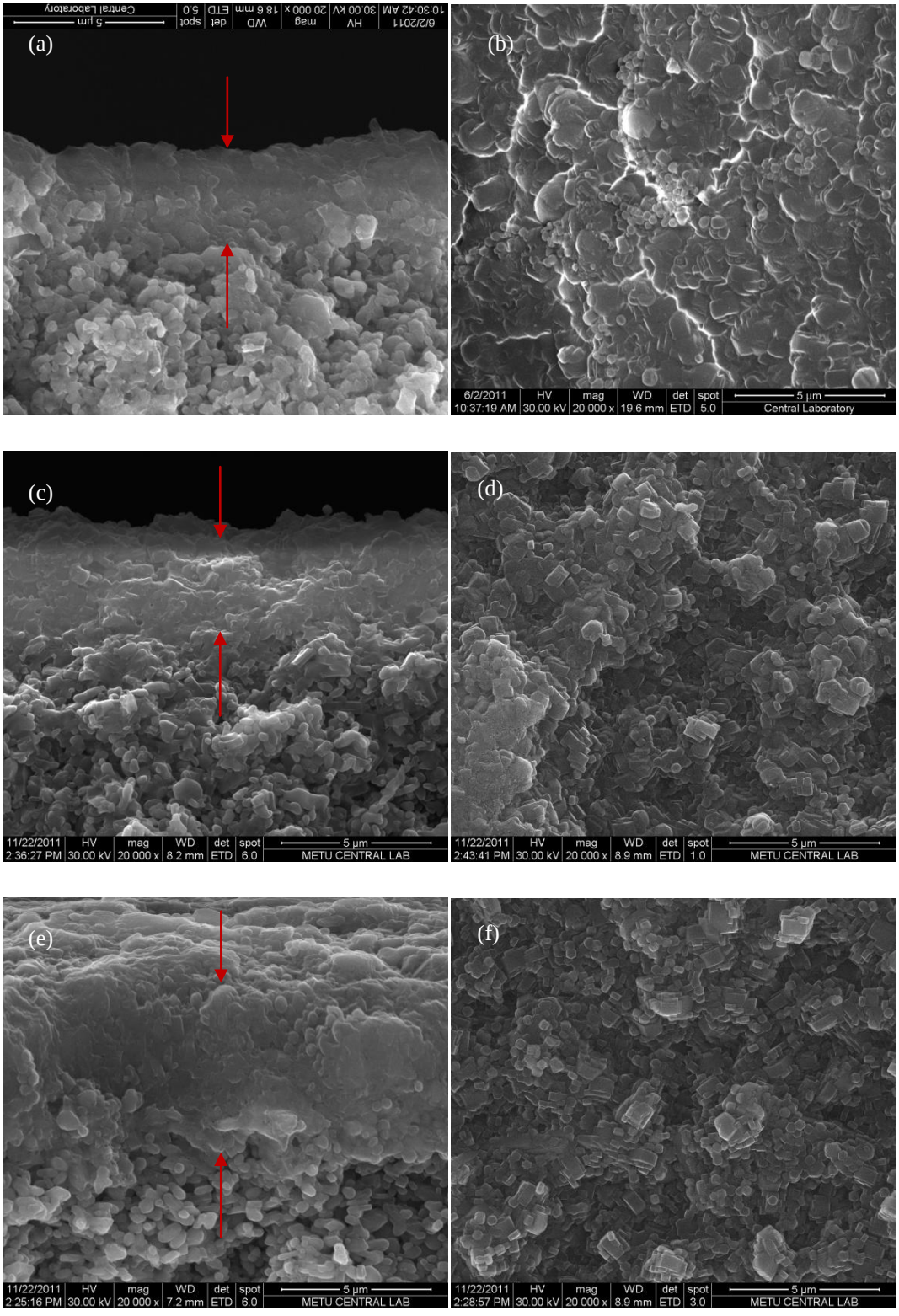

Figure 4.13:Cross section views of a)AON-51 c)AON-184 e)AON-180 and surface views of b)AON-51 d)AON-184 f)AON-180

4.4.3 Gas permeation through MFI membranes synthesized in the recirculating flow system

The multiple synthesis steps were carried out until the membrane become impermeable to N_2 before the calcination. Although impermeable membrane layer was obtained after one layer synthesis in the recirculation of the synthesis solution at 160°C and 180°C, the non zeolitic pores were eliminated with the consecutive synthesis up to 4-layers (4 synthesis steps) at 140°C. Therefore, the increase in synthesis temperature in flow system may contribute the formation of thin membrane layer by preventing the application of consecutive layers.

Single gas permeances of H_2, CO_2, N_2, CH_4, C_2H_6, C_3H_8, n-C_4H_{10}, i-C_4H_{10} were performed through membranes AON-28(B-140), AON-226(B-180), AON-52(F-140), AON-147(F-160), AON-173(F-180) at 25°C. The codes in the brackets, near the membrane codes represent the synthesis mode; B: batch and F: flow and the number indicate the synthesis temperature in °C. Single gas permeances of these membranes were represented in Figure 4.14 with increasing kinetic diameter. CO_2 permeance is the highest permeance for these five membranes; however, the data in references [11, 27, 47, 67] showed the highest permeance values for CH_4 among H_2, CO_2, N_2, CH_4, n-C_4H_{10}, i-C_4H_{10}. However, both batch and flow membranes synthesized at 140°C had lower permeance values compared to those synthesized at higher temperatures. Decrease in the permeance with increasing kinetic diameter was also observed in the literature [9, 69, 80]. An increase in permeance with increasing kinetic diameter is due to strong adsorption of those molecules on zeolites [84]. Such an increase in CO_2 permeance was also observed for MFI membranes synthesized in this study. Permeances and ideal selectivities of the membranes synthesized in this study are given in Appendix J.

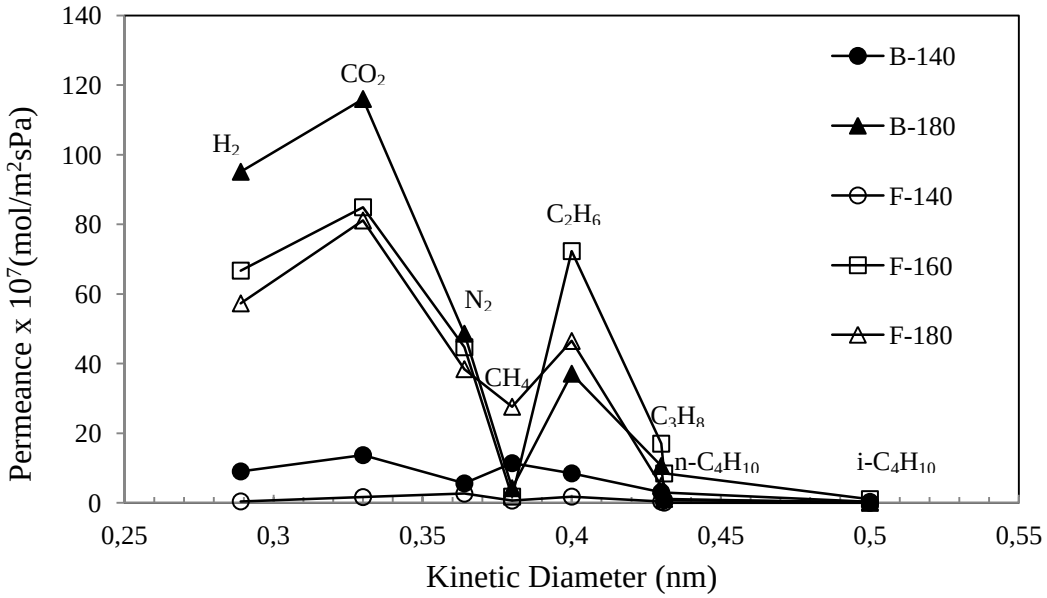

Figure 4.14:Single gas permeances of the MFI membranes for different gases

Figure 4.15 shows the comparison of all membranes with the literature in terms of CH_4/ n-C_4H_{10} ideal selectivity and CH_4 permeance. Literature values were measured at 25-200°C range, while the values obtained in this work were at 25°C. The data, belonged to this study, used in Figure 4.15 are given in Appendix J. The literature values are grouped into four; diamond shapes belonged to a study done by our research group in which membranes were synthesized in a recirculated flow system open to the atmosphere [79], the values shown by squares belonged to oriented membranes [67], empty circles belongs to a micromembrane study [11] and the triangles represent the other studies in the literature [9, 11, 47, 67, 69, 79, 85]. Highest CH_4/n-C_4H_{10} ideal selectivities were obtained in three studies in literature [11, 67, 79]; low temperature recirculated flow synthesis, h0h/c-oriented membrane synthesis and micromembrane synthesis. In this study, highest CH_4/ n-C_4H_{10} ideal selectivity was around 10 with $8x10^{-6}$ mol/m^2sPa. The ideal selectivities and permeances obtained in this study were mostly comparable with those values found in the literature except those three ones with highest selectivities. Therefore, the synthesis method; synthesis of membranes at high temperature and pressure with recirculation of the synthesis solution provided the synthesis of the membranes having comparable quality values with the one in literature.

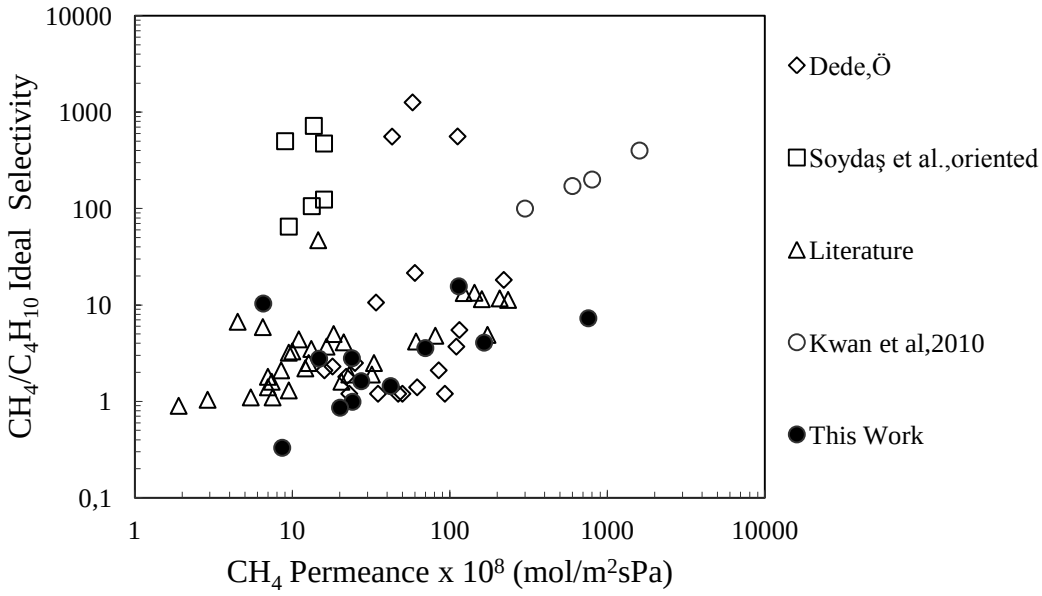

Figure 4.15:Comparison of the ideal selectivities with literature

4.4.4 Separation of CH_4/n-C_4H_{10} Mixtures with MFI Membranes

Separation performances of the membranes were tested by using equimolar mixture of CH_4/n-C_4H_{10} assuming an ideal gas mixture. Total feed molar flow rate was 40ml/min at 25°C and it was increased to 140ml/min for higher separation temperatures since permeate flux increases drastically at higher temperatures. Separation factors were defined as the ratio of molar fluxes of the components in this study [30]. Figure 4.16 compares the separation performance of the membranes synthesized in a recirculated flow system with those reported in the literature. Experimental data of Figure 4.16 was given in Appendix J. Separation performances of the membranes in literature can be investigated in two separation temperatures ranges: (25-75°C) and (100-200°C) since temperature affects the selectivity and permeance considerably. n-C_4H_{10}/CH_4 separation factor is in the range of 10-100 and n-C_4H_{10} permeance is between $3x10^{-11}$ and $5x10^{-8}$ mol/m^2sPa at lower separation temperature range. In this study, n-C_4H_{10} permeance is higher and between $2x10^{-8}$ and $9x10^{-7}$mol/m^2sPa at lower separation temperature range. For higher separation

temperature range n-C_4H_{10} permeance gets higher and is in the range of 2-6x10^{-6} mol/m^2sPa and n-C_4H_{10}/CH_4 separation factor is between 2 and 15.

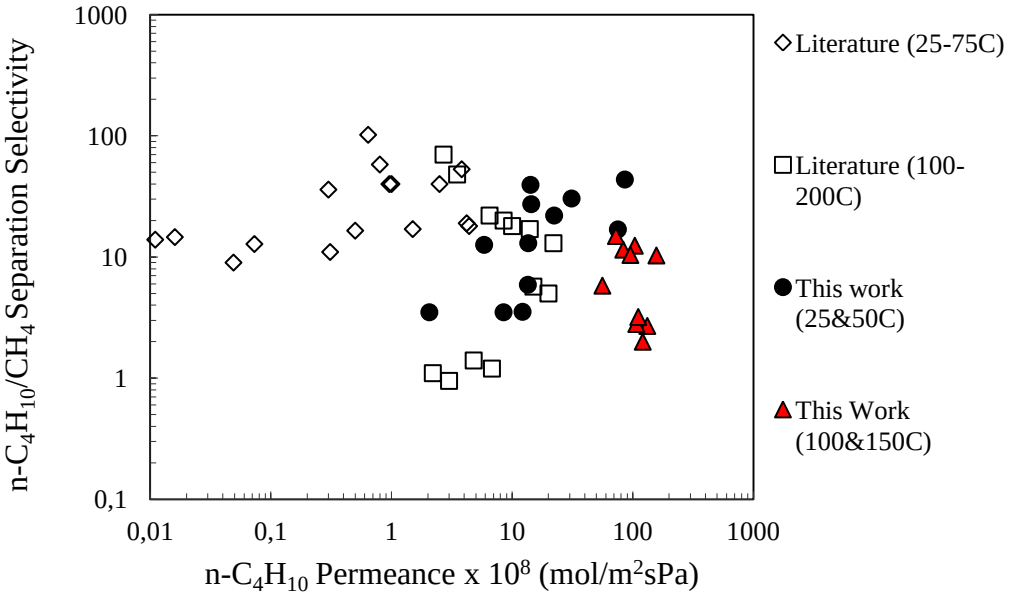

Figure 4.16:Comparison of the flow membranes with the ones in the literature

In a previous work done by our group, MFI membranes were synthesized at 95°C in a recirculating flow system [66]. Separation of n-C_4H_{10}/ CH_4 mixture was studied in the temperature range of 25-200°C and n-C_4H_{10}/ CH_4 separation factor had a maximum at 100°C with a value of 67 for 50/50 n-C_4H_{10}/ CH_4 mixture. Arruebo et al. investigated the separation of hydrocarbons from natural gas. n-C_4H_{10}/ CH_4 separation factor was 14.2 at room temperature for a feed of 0.4% n-C_4H_{10} in natural gas [8]. When they pre-treated the supports with iron oxide before seeding, n-C_4H_{10}/ CH_4 separation factor was increased up to 31.5. Vroon et al studied the effect of synthesis temperature on separation performance of MFI membranes [9]. n-C_4H_{10}/ CH_4 separation factor at 25°C was in the range of 4.5-19 for the membranes synthesized at 120°C, while 102 for the membranes synthesized at 185°C for a feed of 50/50 n-C_4H_{10}/ CH_4 mixture. Xomeritakis et al. found n-C_4H_{10}/CH_4 single gas permeation flux ratio as 0.58 whereas binary permeation flux ratio is 53 for the MFI membranes obtained by secondary growth at 175°C [10]. Wohlrab et al. reported the effect of support, synthesis duration, ratio of template, Si/Al ratio and water fraction

in the synthesis composition on the separation performance of the membranes and n-C_4H_{10}/ CH_4 separation factors were between 9 and 14.8 at 25 and 75°C [5].

The C_4H_{10} permeances through the membranes synthesized in a flow system were higher than those through reported in the literature. On the other hand, the n-C_4H_{10}/CH_4 separation factors were comparable at temperatures in the range of 25-150^{o}C. Unlike in the case of single permeation, MFI membranes are selective to n-C_4H_{10} in binary permeation of CH_4 and n-C_4H_{10} mixture. n-C_4H_{10} blocks the pores of the membrane due to preferential adsorption on MFI membranes [8, 66].

4.5 Characterization of SAPO-34 membranes

4.5.1 Morphology of SAPO-34 membranes

Synthesis composition of E was used to prepare SAPO-34 membranes at high temperature ranging from 180 to 220°C in both stagnant and recirculated flow media. XRD patterns of SAPO-34 membrane synthesized in a recirculated flow mixture at 200°C and 220°C and corresponding residual powders are given in Figure 4.17. Although the residual powder obtained during the membrane synthesis were highly crystalline SAPO-34, the XRD pattern as well as top-view SEM micrograph (Figure 4.18.a) of the membrane indicated that hydrothermal treatment at 200^{o}C resulted in a continuous membrane layer which is composed of amorphous structure. This is not usual for zeolite membranes and SAPO-34, especially during the synthesis at such an elevated temperature. Although increase in synthesis temperature to 220^{o}C caused a small increase in characteristics SAPO-34 peak intensities, recirculated flow induced secondary growth at 220°C led to the formation of rod-like impurities which have not been observed for stagnant counterpart (Figure 4.18.d).

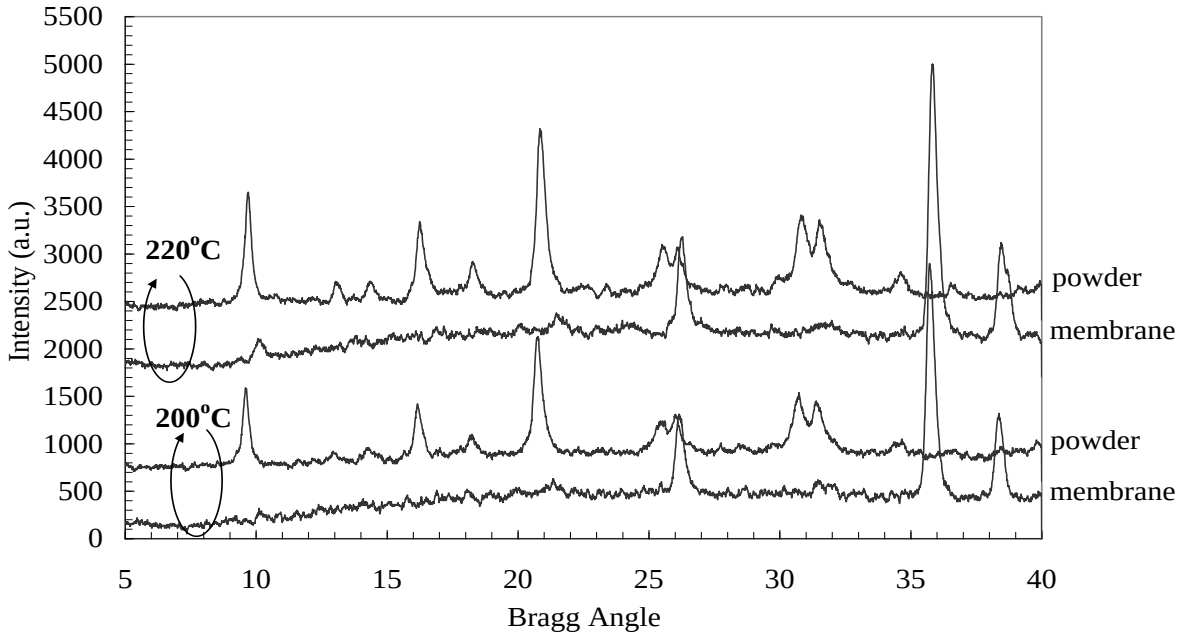

Figure 4.17:XRD patterns of SAPO-34 membrane synthesized in a recirculated flow mixture at 200°C and 220°C with corresponding residual powders.

However, the synthesis of highly crystalline pure SAPO-34 membrane on alumina support unlike the recirculated flow system could be possible for the stagnant system. XRD patterns of SAPO-34 membrane synthesized in a stagnant mixture at 200°C and corresponding residual powder are given in Figure 4.19. Both XRD patterns had characteristic SAPO-34 peaks and alumina peaks were also observed on the XRD pattern of the membrane. Alumina support was responsible from these three α-Al_2O_3 peaks. The considerable decrease and the small shift in the intensity values for the membrane might be related to the curved surface geometry of XRD sample. SEM micrographs of SAPO-34 membranes synthesized in a stagnant mixture at 200°C and 220°C are shown in Figure 4.20. SEM micrographs indicated that both membranes with about 5-7 μm in thickness had well intergrown and highly crystalline SAPO-34. Almost the same layer thicknesses for SAPO-34 membrane with same composition have been reported by Funke et al. who performed synthesis at 210°C [63].

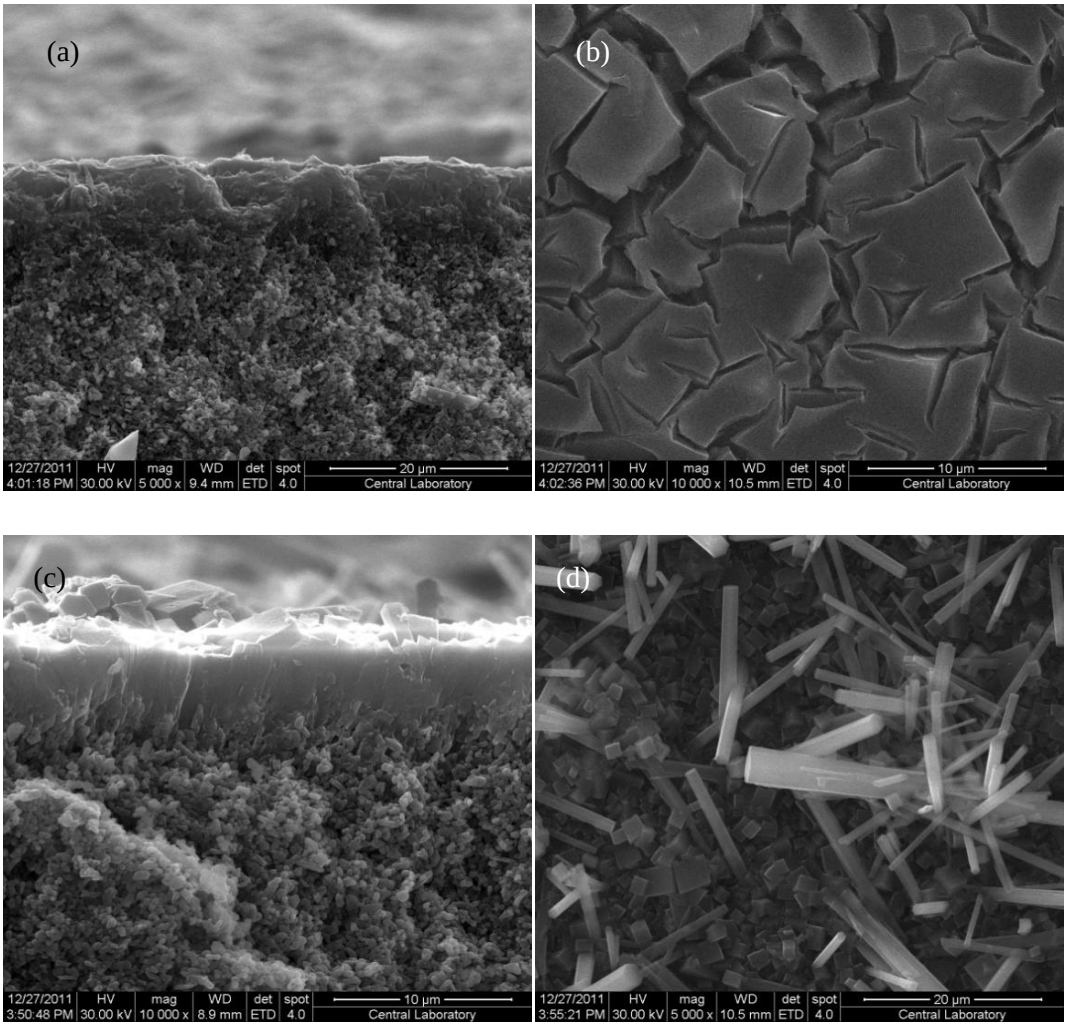

Figure 4.18:SEM micrographs of SAPO-34 membranes synthesized with in recirculated flow mixture at 200°C (AON-240) (a) cross section (b) surface views and at 220°C (AON-245) (c) cross section (d) surface views.

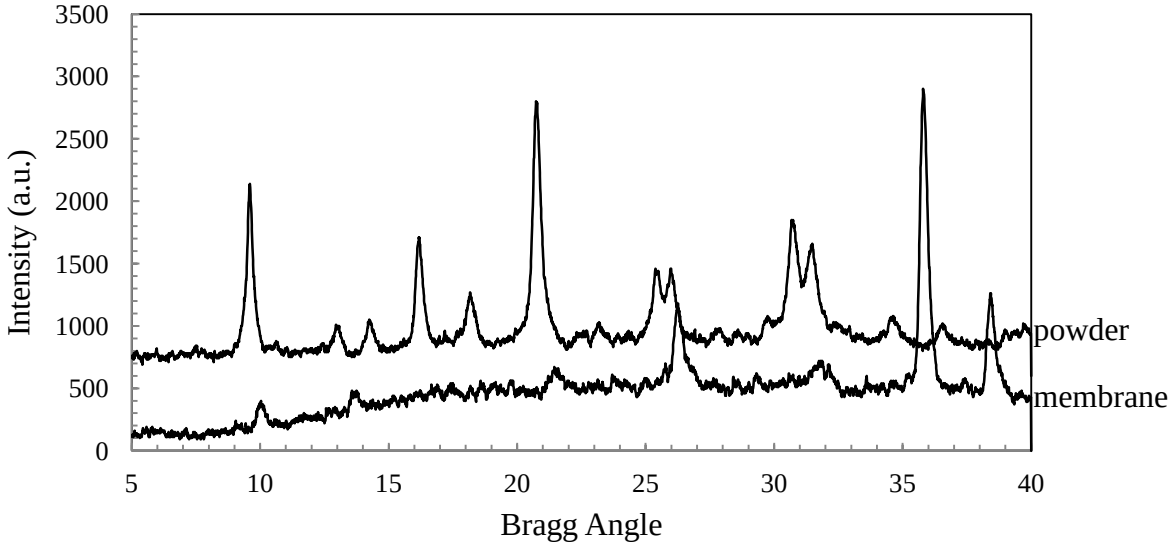

Figure 4.19:XRD patterns of SAPO-34 membrane synthesized in a stagnant mixture at 200°C and corresponding residual powder

SAPO-34 membranes were formed by intergrown cubic crystals having 3-4μm diameter [19]. Additionally smaller crystals (<1 μm) were also located on the surface between the boundary layers of the larger ones, which results in 5-10 μm thick membrane. Li et al. investigated the effect of Si/Al ratio on SAPO-34 membranes by changing the ratio from 0.05 to 0.3 [16]. A 4 layer, 0.15 Si/Al ratio SAPO-34 membrane had a thickness of 5μm formed by intergrown rectangular crystals with a size of 0.1x1 μm. Chew et al. synthesized H-SAPO-34 membranes by microwave heating at 200°C and ion-exchanged these membranes with alkaline earth cations [20]. The thickness of H-SAPO-34 membrane was 3-4μm and average crystal size of the orthorhombic particles was less than 1μm.

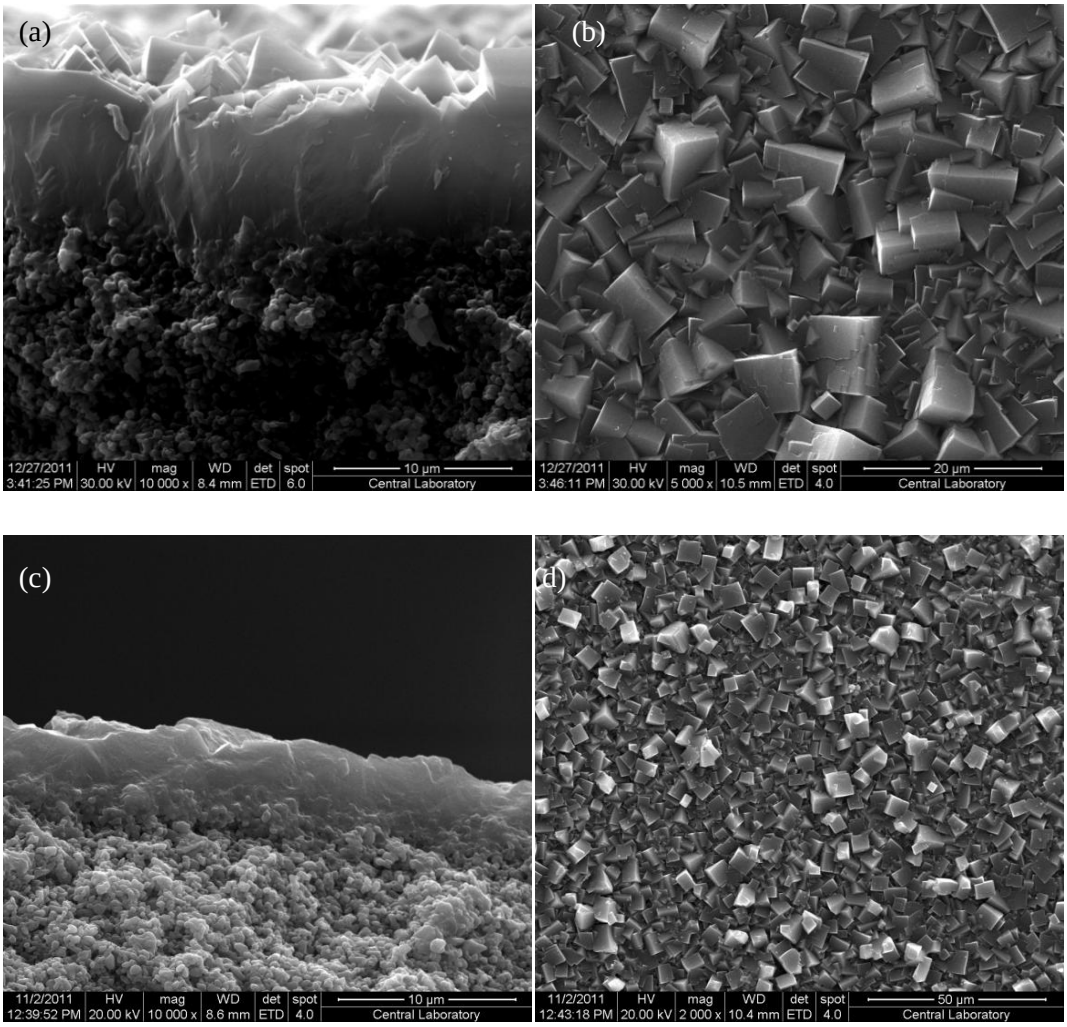

Figure 4.20:SEM micrographs of SAPO-34 membranes synthesized in a stagnant mixture at 200°C (AON-230) (a) cross-section (b) surface views and at 220°C (AON-224) (c) cross-section (d) surface views.

4.5.2 Gas Permeation and Separation of CH_4/CO_2 Mixtures with SAPO-34 Membranes

N_2 permeance before heat treatment shows that the membrane synthesized with a gel composition of D in stagnant mixture at 160°C (AON-46) yielded a continuous film without any non-zeolitic pores larger than N_2 molecule size (Table C.2). Ideal selectivities of CO_2/CH_4 gas pair increased from 15 to 40 upon increasing the number of applied SAPO-34 layers. N_2 permeances through the membranes

synthesized with a same gel composition in a flow system are in the order of approximately 10^{-7} mol/m^2sPa indicating the presence of non-zeolitic pores before the calcination. On the other hand, AON-96 membrane had no N_2 flow before the calcination but the ideal selectivity of CO_2/CH_4 gas pair was found as 1.85 upon heat treatment at 400°C. This ideal selectivity is very close to the Knudsen selectivity for CH_4/CO_2, which 1.7, suggesting the formation of cracks/defects in the mesopore size range in the course of heat treatment. The significant amount of amorphous structure might cause the decrease in membrane performance.

SAPO-34 membranes synthesized using multiple structure-directing agents had CO_2/CH_4 separation factors of in the range of 60-227 depending on the applied pressure difference and the utilized support type [12-15]. The ideal selectivities of 2-layer SAPO-34 membrane synthesized with a gel composition of E in stagnant medium were 227, and >1000 at 220 and 200^oC, which are comparable to the separation factors of SAPO-34 membrane reported in the literature. Figure 4.21 represents the permeability-selectivity relationship for the separation of CO_2/CH_4 mixture [102]. The accurate thicknesses of the SAPO-34 membranes cannot be measured due to the penetration into the support pores. Therefore, the permeabilities were calculated assuming apparent membrane thicknesses of 5 μm and 7 μm for the one-layer and the two-layer membranes, respectively (Figure 4.18 and Figure 4.20). The selectivities and permeabilities of SAPO-34 membranes synthesized in a stagnant medium were significantly higher than those through membranes synthesized in a recirculated flow medium as shown in Figure 4.21. The presence of amorphous structure and the additional secondary phases (impurities) for the membranes synthesized in flow mixture may reduce their performance in comparison to their batch counterparts.

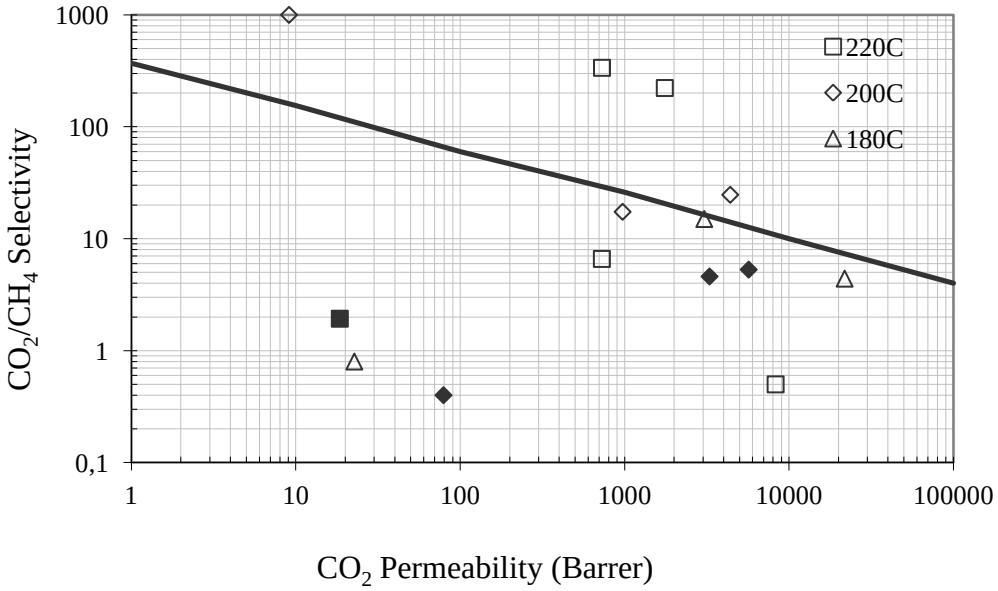

Figure 4.21:Comparison of SAPO-34 membranes in Robeson plot for CO_2/CH_4 gas pair. Membranes were synthesized with a gel composition of B2 in a stagnant and recirculated mixture in the temperature range of 180-220°C (empty symbols:stagnant mixture: solid symbols: recirculated flow mixture

Recirculation of the synthesis solution during the membrane synthesis provides a synthesis media with uniform composition. In our system, synthesis solution is recirculated by means of a centrifugal pump and the synthesis mixture is also mixed by a magnetic stirrer in the autoclave to prevent any precipitation. To ensure the flow and homogeneous media, direction of flow was directed to opposite to gravity. One of the important issues about the flow system is the rate of flow of the synthesis solution through the support. Very low flow rate may result in batch synthesis media and at very high flow rates because of high shear rates sweeping may arise and membrane formation may not come true. Reynolds number in the support was calculated by assuming that the viscosity of the synthesis solution is equal to the viscosity of pure water at 100°C and found as $6x10^{-4}$ where the linear velocity is 2.38cm/s. Second concern about the system is the durability of the system at high temperatures which causes high autogeneous pressure. Since the pressure of the system reaches 28bars, the elements of the system needed to be able to handle that

much pressure. Unlike the batch synthesis autoclaves, the autoclave in the flow system neither coated with PTFE nor has PTFE insert in it. Therefore, during the synthesis, metal ions may interfere in the reaction media and may inhibit the formation of crystals or membrane layers or may favor the formation of unwanted phases as in the case of SAPO-34 synthesis.

CHAPTER 5

CONCLUSIONS

The following conclusions were gathered from this study;

1. Supports were covered with closely packed seed layer by the technique used in this study. According to wet rubbing method, support surfaces were wetted by 50/50(v/v) ethylene glycol-ethanol mixture prior to conventional rubbing.

2. MFI and SAPO-34 membranes were synthesized in recirculated flow system at high temperature and pressure for the first time in the literature. Synthesis temperature was increased up to 180°C and 220°C for MFI and SAPO-34 membranes, respectively.

3. MFI membranes obtained in this study have showed comparable n-C_4H_{10}/CH_4 separation factor with the ones in literature. The highest separation factor of n-C_4H_{10}/CH_4 was 40, which is a sign of high quality membrane.

4. Highest ideal selectivity of CH_4/n-C_4H_{10} was around 35 for MFI membranes. MFI membranes were selective to CH_4 with respect to single gas permeation but selective to n-C_4H_{10} with respect to mixture separation. This is due to pore plugging of n-C_4H_{10} and preventing the pass of CH_4, which shows that MFI membranes contain few cracks and pin holes.

CHAPTER 6

RECOMMENDATIONS

1. High quality MFI membranes were obtained by the synthesis method used in this study. It is necessary to do studies on the reproducibility of membrane synthesis in recirculated flow system at high temperature and pressure.

2. The synthesis method used in this study is promising for obtaining uniform membranes having bigger surface area. It is important to use 25-50cm long supports made of alumina, stainless steel and mullite.

3. SAPO-34 membranes were synthesized successfully in conventional batch autoclaves with PTFE inserts. The flow synthesis setup autoclave and the pump were made of stainless steel. Inside surfaces of the autoclave and the pump should be covered with PTFE line.

REFERENCES

[1] J. Hedlund , J. Sterte , M. Anthonis , Anton-Jan Bons ,B. Carstensen , N. Corcoran , D. Cox , H. Deckman,W. De Gijnst , Peter-Paul de Moor , F. Lai , J. McHenry , W. Mortier , J. Reinoso , J. Peters , "High-flux MFI membranes", Micropor. Mesopor. Mater. 52 (2002) 179-189.

[2] Çulfaz, P. Z., Çulfaz, A., Kalıpçılar, H., "Preparation of MFI type zeolite membranes in a flow system with circulation of the synthesis solution", Micropor. Mesopor. Mater. 92 (2006) 134-144.

[3] Hedlund,J., Noack,M., Kölsch,P., Creaser,D., Caro,J., Sterte,J., "ZSM-5 membranes synthesized without organic templates using a seeding technique", J. Membr. Sci. 159 (1999) 263-273.

[4] Noack, M., Kölsch, P., Schafer, R., Toussaint, P., Seiber, I., Caro, J., "Preparation of MFI membranes of enlarged area with high reproducibility", Micropor. Mesopor. Mater. 49 (2002) 25-37.

[5] Wohlrab,S., Meyer,T., Stöhr,M., Hecker,C., Lubenau,U., Oßmann,A., "On the performance of customized MFI membranes for the separation of n-butane from methane", J. Membr. Sci. 369 (2011) 96-104.

[6] Xomeritakis, G., Gouzinis, A., Nair, S., Okubo, T., He, M., Overney, R. M., Tsapatsis, M., "Growth, microstructure, and permeation properties of supported zeolite (MFI) films and membranes prepared by secondary growth", Chemical Engineering Science 54 (1999) 3521-3531.

[7] Geus, E.R., Bakker, W.J.W., Moulijn, J.A., Bekkum, H. Van, "High-temperature stainless steel supported zeolite (MFI) membranes: preparation, module construction, and permeation experiments", Micropor. Mater. 1 (1993) 131-147.

[8] Arruebo, M., Coronas, J., Menendez, M., Santamaria, J., “Separation of hydrocarbons from natural gas using silicalite membranes”, Sep. Purif. Technol. 25 (2001) 275-286.

[9] Vroon, Z.A.E.P., Keizer, K., Burggraaf, A.J., Verweij, H., “Preparation and characterization of thin zeolite MFI membranes on porous supports”, J. Membr. Sci. 144 (1998) 65-76.

[10] Xomeritakis,G., Nair,S., Tsapatsis,M., “Transport properties of alumina-supported MFI membranes made by secondary (seeded) growth”, Micropor. Mesopor. Mater. 38 (2000) 61-73.

[11] Kwan,S.M., Leung,A.Y.L., Yeung,K.L., “Gas permeation and separation in ZSM-5 micromembranes”, Sep. Purif. Technol. 73 (2010) 44-50.

[12] Venna, S.R., Carreon M.A., “Amino-Functionalized SAPO-34 Membranes for CO_2/CH_4 and CO_2/N_2 Separation”, Langmuir 27 (2011) 2888-2894.

[13] Li, S., Carreon,M.A., Zhang,Y., Funke,H.H., Noble,R.D., Falconer,J.L., “Scale-up of SAPO-34 membranes for CO_2/CH_4 separation”, J. Membr. Sci. 352 (2010) 7-13.

[14] Zhang,Y., Tokay,B., Funke,H.H., Falconer,J.L., Noble,R.D., “Template removal from SAPO-34 crystals and membranes”, J. Membr. Sci. 363 (2010) 29-35.

[15] Carreon,M.A., Li,S., Falconer,J.L., Noble,R.D., “SAPO-34 Seeds and Membranes Prepared Using Multiple Structure Directing Agents”, Adv. Mater. 20 (2008) 729-732.

[16] Li, S., Falconer, J.L., Noble, R.D., “SAPO-34 membranes for CO_2/CH_4 separations: Effect of Si/Al ratio”, Micropor. Mesopor. Mater. 110 (2008) 310-317.

[17] Li, S., Martinek, J.G., Falconer, J.L., Noble, R.D., Gardner, T.Q., "High-Pressure CO_2/CH_4 Separation Using SAPO-34 Membranes", Ind. Eng. Chem. Res. 44 (2005) 3220-3228.

[18] Li, S., Falconer, J.L., Noble, R.D., "SAPO-34 membranes for CO_2/CH_4 separation", J. Membr. Sci. 241 (2004) 121-135.

[19] Poshusta, J.C., Tuan, V.A., Pape, E.A., Noble, R.D., Falconer,J.L., "Separation of Light Gas Mixtures Using SAPO-34 Membranes", AIChE J. 46 (2000) 779-789.

[20] Chew,T.L., Ahmad,A.L., Bhatia,S., "Ba-SAPO-34 membrane synthesized from microwave heating and its performance for CO_2/CH_4 gas separation", Chemical Engineering Journal 171 (2011) 1053-1059.

[21] Pina, M.P., Arruebo, M., Felipe, M., Fleta, F., Bernal, M.P., Coronas, J., Menendez, M., Santamarıa, J., "A semi-continuous method for the synthesis of NaA zeolite membranes on tubular supports", J. Membr. Sci. 244 (2004) 141-150.

[22] Pera-Titus, M., Mallada, R., Llorens, J., Cunill, F., Santamaria, J., "Preparation of inner-side tubular zeolite NaA membranes in a semi-continuous synthesis system", J. Membr. Sci. 278 (2006) 401-409.

[23] Aguado, S., Gascon, J., Jansen, J. C., Kapteijn, F., "Continuous synthesis of NaA Zeolite Membranes", Micropor. Mesopor. Mater. 120 (2009) 170-176.

[24] Çulfaz, Z., "Synthesis of MFI Type Zeolite Membranes in a Continuous System", M.S. Thesis in Chemical Engineering. July 2005, METU: Ankara.

[25] Yamazaki, S., Tsutsumi, K., "Synthesis of A-type zeolite membrane using a plate heater and its formation mechanism", Micropor. Mesopor. Mater. 37 (2000) 67-80.

[26] Pera-Titus , M., Bausach , M., Llorens , J., Cunill, F., "Preparation of inner-side tubular zeolite NaA membranes in a continuous flow system", Sep. Purif. Technol. 59 (2008) 141-150.

[27] Richter, H., Voigt, I., Fischer, G., Puhlfürß, P., "Preparation of zeolite membranes on the inner surface of ceramic tubes and capillaries", Sep. Purif. Technol. 32 (2003) 132-138.

[28] Mulder, M., Basic Principles of Membrane Technology, Second edition, Kluwer Academic Publishers, London, 197.

[29] Koros, W.J., "Evolving Beyond the Thermal Age of Separation Processes: Membranes Can Lead the Way", AIChE Journal 50 (2004) 2326-2334.

[30] Li, S., Alvarado, G., Noble, R. D., Falconer, J. L., "Effects of impurities on CO_2 /CH_4 separations through SAPO-34 membranes", J. Membr. Sci. 251 (2005) 59-66.

[31] Molecular Sieves, Kirk-Othmer Encyclopedia of Chemical Technology,Vol.16, 4^{th} Ed.,443-462.

[32] Akbay,S., "Synthesis of Low Silica/Alumina Zeolite Membranes in a Flow System", M.S. Thesis in Chemical Engineering Department. 2007, METU: Ankara.

[33] Zimmerman,C.M., Singh,A., Koros,W.J., "Tailoring Mixed Matrix Composite Membranes for Gas Separations", J. Membr. Sci. 137 (1997) 145-154.

[34] Pechar,T.W., Tsapatsis,M., Marand,E., Davis,R., "Preparation and Characterization of a Glassy Fluorinated Polyimide Zeolite-Mixed Matrix Membrane", Desalination 146 (2002) 3-9.

[35] Mahajan,R., Koros, W.J., "Factors Controlling Successful Formation of Mixed-Matrix Gas Separation Materials", Ind. Eng. Chem. Res. 39 (2000) 2692-2696.

[36] Caro,J., Noack,M., Kölsch,P., Schafer,R., “Zeolite Membranes- State of Their Development and Perspective”, Micropor. Mesopor. Mater. 38 (2000) 3-24.

[37] Lin,Y.S., “Microporous and Dense Inorganic Membranes: Current Status and Prospective”, Sep. Purif. Technol. 25 (2001) 39-55.

[38] Chiang,A.S.T., Chao,K., “Membranes and Films of Zeolite and Zeolite –like Materials”, Journal of Physics Chemistry of Solids 62 (2001) 1899-1910.

[39] Haiyang,J., Baoquan,Z., Lin, Y. S., Yongdan,L., “Synthesis of zeolite membranes”, Chinese Science Bulletin 49 (2004) 2547-2554.

[40] Motuzas,J., Julbe,A., Noble, R.D., van der Lee, A., Beresnevicius, Z.J., “Rapid synthesis of oriented silicalite-1 membranes by microwave-assisted hydrothermal treatment”, Micropor. Mesopor. Mater 92 (2006) 259-269.

[41] Kanezashi, M., Lin,Y.S., “Gas Permeation and Diffusion Characteristics of MFI-Type Zeolite Membranes at High Temperatures”, J. Phys. Chem. C 113(2009) 3767–3774.

[42] Caro,J., Noack,M., “Zeolite Membranes – Status and Prospective” Advances in Nanoporous Materials, Volume1.

[43] Lai,Z., Tsapatsis,M., “Gas and Organic Vapor Permeation through b-Oriented MFI Membranes”, Ind. Eng. Chem. Res. 43 (2004) 3000-3007.

[44] Tuan,V.A., Noble,R.D., Falconer,J.L., “Boron-Substituted ZSM-5 Membranes: Preparation and Separation Performance” AIChE Journal 46 (2000) 1201-1208.

[45] Voß,H., Diefenbacher,A., Schuch,G., Richter,H., Voigt,I., Noack,M., Caro,J., “Butene isomers separation on titania supported MFI membranes at conditions relevant for practice”, J. Membr. Sci. 329 (2009) 11–17.

[46] Richter,H., Voß,H., Voigt,I., Diefenbacher,A., Schuch,G., Steinbach,F., Caro,J., “High-flux ZSM-5 membranes with an additional non-zeolite pore system by

alcohol addition to the synthesis batch and their evaluation in the 1-butene/i-butene separation", Sep. Purif. Technol. 72 (2010) 388–394.

[47] Noack, M., Kölsch, P., Seefeld, V., Toussaint, P., Georgi, G., Caro, J., "Influence of the Si/Al-ratio on the permeation properties of MFI-membranes" Micropor. Mesopor. Mater. 79 (2005) 329–337.

[48] Gump, C.J., Lin, X., Falconer, J.L., Noble, R.D., "Experimental configuration and adsorption effects on the permeation of C_4 isomers through ZSM-5 zeolite membranes", J. Membr. Sci. 173 (2000) 35-52.

[49] Nair, S., Lai, Z., Xomeritakis, G., Tsapatsis, M., "Separation of close-boiling hydrocarbon mixtures by MFI and FAU membranes made by secondary growth", Micropor. Mesopor. Mater. 48 (2001) 219-228.

[50] Baker,R.W., Lokhandwala,K., "Natural Gas Processing with Membranes: An Overview", Ind. Eng. Chem. Res. 47 (2008) 2109-2121.

[51] Schultz, J. Peinemann, K.-V., "Membranes for Separation of Higher Hydrocarbons from Methane", J. Membr. Sci. 110 (1996) 37-45.

[52] Zhang,X., Wang,T., Liu,H., "Preparation of composite carbon–zeolite membranes using a simple method", Journal of Materials Science 39 (2004) 5603 – 5605.

[53] Oyama, S.T., Stagg-Williams, S.M., "Inorganic, Polymeric and Composite Membranes Structure, Function and Other Correlations", Membrane Science and Technology Series,14 (2011) 2-373.

[54] Dinçer, E., "Effect of seeding on the properties of MFI zeolite MFI membranes", M.S. Thesis in Chemical Engineering. July 2005, METU: Ankara.

[55] Prakash,A.M., SAPO-34, Verified Synthesis of Zeolitic Materials, (2001), 2nd edition.

[56] Venna,S.R., Carreon,M.A., "Synthesis of SAPO-34 Crystals in the Presence of Crystal Growth Inhibitors", Journal of Physical Chemistry 112 (2008) 16261-16265.

[57] Retrieved from http://izasc.ethz.ch/fmi/xsl/IZA-SC/Tilings/CHA.pdf on 05.08.2012.

[58] Lovallo, M. C., Tsapatsis, M., "Preferentially Oriented Submicron Silicalite Membranes", AIChE J. 42 (1996) 3020-3029.

[59] Gouzinis, A., Tsapatsis, M., "On the Preferred Orientation and Microstructural Manipulation of Molecular Sieve Films Prepared by Secondary Growth", Chem. Mater. 10 (1998) 2497-2504.

[60] Kanezashi, M., Lin, Y.S., "Gas Permeation and Diffusion Characteristics of MFI-Type Zeolite Membranes at High Temperatures", J. Phys. Chem. 113(2009) 3767-3774.

[61] Xiao, W., Chen, Z., Zhou,L., Yang, J., Lu, J., Wang, J., "A simple seeding method for MFI zeolite membrane synthesis on macroporous support by microwave heating", Micropor. Mesopor. Mater. 142 (2011) 154-160.

[62] Liu, Y., Yang, Z., Yu, C., Gu, X., Xu, N., "Effect of seeding methods on growth of NaA zeolite membranes", Micropor. Mesopor. Mater. 143 (2011) 348-356.

[63] Funke,H.H., Kovalchick,M.G., Falconer,J.L., Noble,R.D., "Separation of Hydrocarbon Isomer Vapors with Silicalite Zeolite Membranes", Ind. Eng. Chem. Res. 35 (1996) 1575-1582.

[64] Lin,X., Chen,X., Kita,H., Okamoto,K., "Synthesis of Silicalite Tubular Membranes by In Situ Crystallization", AIChE Journal 49 (2003) 237-247.

[65] Shan, L., Shao, J., Wang, Z., Yan, Y., "Preparation of zeolite MFI membranes on alumina hollow fibers with high flux for pervaporation", J. Membr. Sci. 378 (2011) 319-329.

[66] Soydaş, B., Dede, Ö., Çulfaz A., Kalıpçılar, H., "Separation of gas and organic/water mixtures by MFI type zeolite membranes synthesized in a flow system", Micropor. Mesopor. Mater. 127 (2010) 96-103.

[67] Soydaş, B., Çulfaz, A., Kalıpçılar, H., "Effect of Soda Concentration on the Morphology of MFI-Type Zeolite Membranes", Chem. Eng. Comm. 196 (2009) 182-193.

[68] Dinçer, E., Kalıpçılar, H., Çulfaz, A., "Synthesis of ZSM-5-Type Zeolite Membranes on Porous Disks Loaded with Different Amounts of Seed", Ind. Eng. Chem. Res. 47 (2008) 4743-4749.

[69] Burggraaf, A.J., Vroon, Z.A.E.P., Keizer, K., Verweij, H., "Preparation and characterization of thin zeolite MFI membranes on porous supports", J. Membr. Sci. 144 (1998) 65-76.

[70] Poshusta, J.C., Noble, R.D., Falconer, J.L., "Characterization of SAPO-34 membranes by water adsorption" J. Membr. Sci. 186 (2001) 25-40.

[71] Poshusta,J.C., Tuan,V.A., Falconer,J.L., Noble,R.D., "Synthesis and Permeation Properties of SAPO-34 Tubular Membranes", Ind. Eng. Chem. Res. 37 (1998) 3924-3929.

[72] Chew, T.L., Ahmad, A.L., "Rapid synthesis of thin SAPO-34 membranes using microwave heating", J. Porous Mater. 18 (2011) 355-360.

[73] Zhang, Y., Avila,A.M., Tokay,B., Funke,H.H., Falconer,J.L., Noble,R.D., "Blocking defects in SAPO-34 membranes with cyclodextrin", J. Membr. Sci. 358 (2010) 7–12.

[74] Tian,Y., Fan,L., Wang,Z., Qiu,S., Zhu,G., "Synthesis of a SAPO-34 membrane on macroporous supports for high permeance separation of a CO_2/CH_4 mixture", J. Mater. Chem. 19 (2009) 7698–7703.

[75] Carreon,M.A., Li,S., Falconer,J.L., Noble,R.D., "Alumina-Supported SAPO-34 Membranes for CO_2/CH_4 Separation" J. Am. Chem. Soc. 130 (2008) 5412–5413.

[76] Hong,M., Li,S., Funke,H.F., Falconer,J.L., Noble,R.D., "Ion-exchanged SAPO-34 membranes for light gas separations", Micropor. Mesopor. Mater. 106 (2007) 140–146.

[77] Li,S., Falconer,J.L., Noble,R.D., "Improved SAPO-34 Membranes for CO_2/CH_4 Separations", Adv. Mater. 18 (2006) 2601–2603.

[78] Avila, A.M., Funke, H.H., Zhang, Y., Falconer, J.L., Noble, R.D., "Concentration polarization in SAPO-34 membranes at high pressures", J. Membr. Sci. 335 (2009) 32-36.

[79] Dede, Ö., "Pervaporation of organic/water mixtures by MFI type zeolite membranes synthesized in a flow system", M.S. Thesis in Chemical Engineering. August 2007, METU: Ankara.

[80] Soydaş, B., "Characterization of zeolite membranes by gas permeation", Ph.D. Thesis in Chemical Engineering. June 2009, METU: Ankara.

[81] Akbay, S., "Sythesis of low Silica/Alumina Zeolite Membranes in a flow system", M.S. Thesis in Chemical Engineering. September 2007, METU: Ankara.

[82] (Arıcan) Yüksel, B., "Pervaporation of ethanol/water mixtures by zeolite membranes synthesized in batch and flow systems", M.S. Thesis in Chemical Engineering. Janurary 2011, METU: Ankara.

[83] Kalıpçılar, H., Çulfaz, A., "Role of the water content of clear synthesis solutions on the thickness of silicalite layers grown on porous a-alumina supports", Micropor. Mesopor. Mater. 52 (2002) 39-54.

[84] van de Graaf, J.M., van der Bijl, E., Stol, A., Kapteijn, F., Moulijn, J.A., "Effect of Operating Conditions and Membrane Quality on the Separation Performance of Composite Silicalite-1 Membranes", Ind. Eng. Chem. Res. 37 (1998) 4071-4083.

[85] Au, L.T.Y., Yeung, K.L., “An investigation of the relationship between microstructure and permeation properties of ZSM-5 membranes”, J. Membr. Sci. 194 (2001) 33-55.

[86] Nobbmann, U., Morfesis,A., “Light scattering and nanoparticles”, Materials Today 12 (2009) 52-54.

[87] Coronas,J., Falconer, J.L., Noble, R.D., “Characterization and permeation properties of ZSM-5 tubular membranes”, AIChe J., 43 (1997) 1797.

[88] Louis, B., Reuse, P., Kiwi-Minsker, L., Renken,A., “Synthesis of ZSM-5 coatings on stainless steel grids and their catalytic performance for partial oxidation of benzene by N_2O”, Applied Catalysis A: General 210 (2001) 103–109.

[89] van Grieken, R., Sotelo, J.L., Menendez, J.M., Melero, J.A., “Anomalous crystallization mechanism in the synthesis of nanocrystalline ZSM-5”, Micropor. Mesopor. Mater. 39 (2000) 135-147.

[90] Choi, M., Na, K., Kim, J., Sakamoto, Y., Terasaki, O., Ryoo, R., “Stable single-unit-cell nanosheets of zeolite MFI as active and long-lived catalysts”, Nature 461 (2009) 246-250.

[91] Venna, S.R., Carreon, M.A., “Synthesis of SAPO-34 Crystals in the Presence of Crystal Growth Inhibitors”, J. Phys. Chem. B. 112 (2008) 16261-16265.

[92] Kang, M., Lee, C., “Synthesis of Ga-incorporated SAPO-34s _GaAPSO-34/ and their catalytic performance on methanol conversion”, Journal of Molecular Catalysis A: Chemical 150 (1999) 213-222.

[93] Inui, T., Kang, M., “Reliable procedure for the synthesis of Ni-SAPo-34 as highly selective catalyst for methanol to ethylene conversion”, Applied Catalysis A: General 164 (1997) 211-223.

[94] Francis, R.J., O'Hare, D., "The kinetics and mechanisms of the crystallisation of microporous materials", J. Chem. Soc., Dalton Trans. (1998) 3133–3148.

[95] Walton, R.I., "Subcritical solvothermal synthesis of condensed inorganic materials", Chem. Soc. Rev., 31 (2002) 230–238.

[96] Tosun, I., "Thermodynamics of Phase and Reaction Equilibria", Elsevier (2012)

[97] Sandler,S.I., "Chemical, Biochemical, and Engineering Thermodynamics", 4th Ed., John Wiley and Sons, Inc (2006)

[98] Oonkhanond, B., Mullins, M.E., "The preparation and analysis of zeolite ZSM-5 membranes on porous alumina supports", J. Membr. Sci. 194 (2001) 3-13.

[99] Yan, Y., Chaudhuri, S.R., Sarkar, A., "Synthesis of Oriented Zeolite Molecular Sieve Films with Controlled Morphologies", Chem. Mater. 8 (1996) 473-479.

[100] Lai, S.M., Au, L.T.Y., Yeung, K.L., "Influence of the synthesis conditions and growth environment on MFI zeolite film orientation", Micropor. Mesopor. Mater. 54 (2002) 63-77.

[101] Mabande,G.T.P., "Development of Metal-Supported MFI Membranes And Their Applications in Gas/Vapour Separations And Xylene Isomerisation Membrane Reactors" Ph.D. Thesis in Faculty of Engineering Sciences. July 2005, Friedrich-Alexander University of Erlangen-Nuremberg : Erlangen.

[102] Robeson, L.M., "The upper bound revisited", J. Membr. Sci. 320 (2008) 390-400.

[103] Tokay, B., Somer, M., Erdem-Şenatalar, A., Schüth, F., Thompson, R.W., "Nanoparticle silicalite-1 crystallization from clear solutions: Nucleation", Micropor. Mesopor. Mater. 118 (2009) 143-151.

[104] Balbuena, P.B., Gubbins, K.E., "Theoratical interpretation of adsorption behavior of simple fluids in slit pores", Langmuir 9 (1993) 1801-1814.

APPENDIX A

SYNTHESIS METHODS AND SUPPORT MATERIALS OF ZEOLITE MEMBRANES IN LITERATURE

Table A.1: Synthesis methods and support materials of zeolite membranes in literature

s.shape	**s. Material**	**in-situ/ Secondary**	**type/orientation**	**notes**	**author**
disc(h.m.)	α-alumina	secondary	MFI, b-oriented		[43]
tube	SS, α-alumina	in-situ	B-ZSM-5	ion-exchange	[44]
slide	glass	secondary	MFI,c- or h0h-ori.		[59]
disc(h.m.)	α-alumina	secondary	MFI	CVD	[60]
tube	alumina	secondary	silicalite-1		[61]
tube	mullite	secondary	NaA		[62]
tube	α-alumina	secondary	silicalite-1,c- or 101-ori.		[40]
disc,tube	α-alumina	secondary	MFI	polycationic polymer	[4]
tube	γ-alumina	in-situ	silicalite-1		[63]
tube	α-alumina,mullite	in-situ, secondary	silicalite-1		[64]
tube	SS	secondary	silicalite-1		[8]
disc	α-alumina	secondary	ZSM-5	template free	[3]
disc	α-alumina	secondary	ZSM-5	with/Without template	[47]
tube	α-alumina	secondary	MFI		[5]
disc	α-alumina	in-situ	MFI	multiple steps	[9]
disc(h.m.)	α-alumina	secondary	MFI		[10]
wafer	silicon	secondary	ZSM-5,Sil-1	micromembrane	[11]

tube	α-alumina	secondary	NaA	recirculated	[23]
tube	α-alumina	secondary	NaA	semi-continuous	[21]
tube	α-alumina	secondary	NaA	semi-continuous	[22]
tube,capillary	α-alumina	secondary	ZSM-5	continuous flow	[27]
tube	α-alumina	secondary	MFI	recirculated	[2]
square	glass, PTFE	in-situ	A-type	recirculated	[25]
tube	titania	secondary	NaA	continuous flow	[26]
disc	α-alumina	secondary	MFI	masking befoe seeding	[1]
disc(h.m.)	α-alumina	secondary	MFI		[6]
disc(h.m.)	Silicalite/alumina	secondary	MFI,oriented?	supported and unsupported	[58]
hollow-fiber	α-alumina	secondary	MFI		[65]
tube	α-alumina	secondary	MFI	recirculated	[66]
disc(h.m.)	α-alumina	secondary	MFI,c- or h0h-ori.		[67]
disc(h.m.)	α-alumina	secondary	ZSM-5		[68]
disc	α-alumina	in-situ	MFI		[69]
tube	α-alumina	in-situ	SAPO-34		[70]
disc	α-alumina	in-situ	Ba-SAPO-34	Microwave	[20]
tube	SS	in-situ	SAPO-34		[17]
tube	SS	in-situ	SAPO-34		[16]
tube	SS	in-situ	SAPO-34		[30]
tube	SS	secondary	SAPO-34	2SDA	[15]
tube	alumina	secondary	SAPO-34	2SDA	[14]
tube	SS	secondary	SAPO-34	2SDA,scale up	[13]
tube	---------	secondary	Amino-func. SAPO-34		[12]

tube	SS, α-alumina	in-situ	SAPO-34		[18]
tube	α-alumina	in-situ	SAPO-34		[19]
tube	α-alumina	in-situ	SAPO-34		[71]
disc	α-alumina	in-situ	SAPO-34	Microwave	[72]
tube	SS, α-alumina	secondary	SAPO-34	Block defects with CD	[73]
wafer	SS	secondary	SAPO-34	a-oriented	[74]
tube	α-alumina	secondary	SAPO-34	different template	[75]
tube	SS	in-situ	SAPO-34	ion-exchanged	[76]
tube	SS	in-situ	SAPO-34	Si/Al ratio	[77]

Table B.1: SAPO-34 membrane synthesis molar compositions in literature

Synthesis Composition	Reference	Synthesis T/time	Seeded	Notes
$1Al_2O_3:1P_2O_5:0.6SiO_2:1.07TEAOH:56H_2O$	[71]	195/20	-	fill tube
	[19]	185/24	-	fill tube wait refill
	[70]	-	-	fill tube wait refill
	[18]	185/20	-	fill tube wait refill
	[17]	195/20	-	fill autoclave
	[30]	185/20	-	fill tube wait refill or fill autoclave
	[76]	195/20	-	fill autoclave
$1Al_2O_3:1P_2O_5:xSiO_2:1.2TEAOH:55H_2O$	[77]	200/24	+	fill autoclave
				x=0.2,0.3, 0.4, 0.6
	[76]	195/20	-	fill autoclave
				x=0.3
	[16]	200/24	-	fill autoclave
				x=0.1, 0.2,0.3, 0.4, 0.6
	[72]	180-200 /0.5-2	-	fill autoclave,MW
				x=0.3
$1Al_2O_3:1P_2O_5:0.3SiO_2:1.2TEAOH:80H_2O$	[20]	200/2	-	fill autoclave,MW
$1Al_2O_3:1.33P_2O_5:0.16SiO_2:1.17TEAOH:150H_2O$	[74]	170-200 /12-72	+	fill autoclave

$1Al_2O_3:1P_2O_5:0.3SiO_2:1.07TEAOH:xDPA:yH_2O$	[15]	220 /23-24	+	fill autoclave
				x=1.6, y=77
	[75]	220/24	+	fill autoclave
				x=1.6,3.2 y=77
	[78]	220/6	+	fill autoclave
				x=1.6 y=150
	[13]	220 /2-24	+	fill autoclave
				x=1.6 y=77,150
	[73]	220 /4-6	+	fill autoclave
				x=1.6 y=150
	[14]	220/6	+	fill autoclave
				x=1.6 y=150
$1Al_2O_3:1.33P_2O_5:0.16SiO_2:1.TEAOH:1.6DPA:77H_2O$	[12]	220/24	+	fill autoclave

APPENDIX C

SYNTHESIS PARAMETERS OF THE MEMBRANES IN THIS STUDY

Membrane codes and synthesis conditions of both MFI and SAPO-34 membranes are given in Table C.1 and Table C.2.

Table C.1: Synthesis parameters of MFI Membranes

Membrane Code	**Synthesis Composition**	**SynthesisT(°C) /Time(h)**	**Number of Layers**	**Synthesis Process**	**N_2 permeance before calc.**
AON-28	A2	140/24	2	Batch (i)	$<10^{-12}$
AON-29	A2	140/24	2	Batch (o)	$<10^{-12}$, broken in module
AON-51	A2	140/24	4	Flow (o)	$1.22x10^{-10}$, broken for SEM
AON-52	A2	140/24	4	Flow (i)	$<10^{-12}$
AON-69	A1	140/28	1	Flow (i)	pump stop
AON-70	A1	140/28	1	Flow (o)	pump stop
AON-77	A2	140/24	3	Flow (i)	$<10^{-12}$/broken for SEM
AON-78	A2	140/24	3	Flow (o)	$3.57x10^{-11}$
AON-83	A1	140/28	1	Flow (i)	pump stop
AON-84	A1	140/28	1	Flow (o)	pump stop
AON-98	B	150/26	1	Batch	$<10^{-12}$
AON-108	A1	160/24	1/2	Flow (i)	$<10^{-12}$/$<10^{-12}$
AON-110	C	130/27	1	Batch	$<10^{-12}$
AON-113	B	150/---	1	Flow (i)	Stopped after gel like mixture
AON-119	A2	140/24	3	Flow (i)	$<10^{-12}$

Table C.1 (continued)

AON-127	B	150/26	1	Batch	$<10^{-12}$
AON-137	A2	160/--	1	Flow	exploded
AON-141	C	130/27	1	Flow	$<10^{-12}$
AON-147	A2	160/16	2	Flow	$<10^{-12}$
AON-160	C	130/27	1	Flow	-
AON-173	A2	180/13	2--1	Flow-- Flow	$<10^{-12}$ $<10^{-12}$
AON-180	A2	180/13-- 180/13	1--1	Flow-- Flow	$<10^{-12}$ $<10^{-12}$
AON-184	A2	160/16	2	Flow	$4.85x10^{-11}$
AON-196	A2	180/13	1	Flow	$<10^{-12}$
AON-204	A2	160/16	2	Flow	$<10^{-12}$
AON-226	A2	180/13	1	Batch	$<10^{-12}$

Table C.2: Synthesis parameters of SAPO-34 Membranes

Membrane Code	**Synthesis Comp.**	**Synthesis T (^{o}C)/Time (h)**	**Number of layers**	**Synthesis process**	**N_2 permeance before calc.**
AON-96	D	140/48	1	Flow	-
AON-155	D	160/48	2	Flow	$<10^{-7}$
AON-168	D	160/48	2	Flow	$<10^{-7}$
AON-175	D	180/24	3	Flow	$<10^{-7}$
AON-243	E	220/5	1	Flow	
AON-240	E	200/11	2	Flow	
AON-243	E	220/5	2	Flow	

Table C.2 (continued)

AON-245	E	220/5	2	Flow	
AON-250(2)	E	200/12.5	2	Flow	$1.3x10^{-11}$
AON-46	D	140/48	3	Batch	-
AON-166	D	160/48	2	Batch	$<10^{-7}$
AON-198	E	220/5	1	Batch	-
AON-210	E	220/5	2	Batch	
AON-212	E	180/24	1	Batch	
AON-224	E	220/5	1	Batch	
AON-228	E	180/11	2	Batch	$6.1x10^{-10}$
AON-230	E	200/11	2	Batch	
AON-232	E	200/8	2	Batch	
AON-252	E	200/12.5	1	Batch	

APPENDIX D

SAMPLE CALCULATION OF SYNTHESIS RECIPE OF COMPOSITION A1

Sample calculation for 100g of $1SiO_2$:0.2TPAOH:$19.2H_2O$ composition is given below. Tetrapropylammonium hydroxide (40 wt% in water, Merck), Ludox HS-40 (40 wt% in water, Aldrich and distilled water are used for preparation of this batch.

Table D.1: Molecular weights of the reactants

Reactant	**Molecular Weight(g/gmole)**
SiO_2	60.09
TPAOH	203.368
H_2O	18.016

Molar composition of the batch: $1SiO_2$:0.2TPAOH:$19.2H_2O$

Formula weight of the batch:

$$1 \times 60.09 + 0.2 \times 203.368 + 19.2 \times 18.016 = 446.671\ g/gmole$$

Ludox HS-40

$$100g\ batch \times \frac{1\ mol\ batch}{446.671\ g\ batch} \times \frac{1\ mol\ SiO_2}{1\ mol\ batch} \times \frac{60.09g\ SiO_2}{1\ mol\ SiO_2} \times \frac{100g\ Ludox\ HS-40}{40g\ SiO_2} = 33.63g\ Ludox\ HS-40$$

TPAOH(40%)

$$100g\ batch \times \frac{1\ mol\ batch}{446.671\ g\ batch} \times \frac{0.2\ mol\ TPAOH}{1\ mol\ batch} \times \frac{203.369g\ TPAOH}{1\ mol\ TPAOH} \times \frac{100g\ TPAOH(40\%)}{40g\ TPAOH} = 22.77g\ TPAOH(40\%)$$

H_2O

$$100g\ batch \times \frac{1\ mol\ batch}{446.671\ g\ batch} \times \frac{19.2\ mol\ H_2O}{1\ mol\ batch} \times \frac{18.016g\ H_2O}{1\ mol\ H_2O} \times = 77.44gH_2O$$

$$33.63g\ Ludox\ HS-40 \times \frac{60g\ H_2O}{100g\ Ludox\ HS-40} \times$$

$$= 20.18gH_2O\ from\ Ludox\ HS-40$$

$$22.77g\ Ludox\ TPAOH(40\%) \times \frac{60g\ H_2O}{100g\ TPAOH(40\%)} \times$$

$$= 13.66gH_2O\ from\ TPAOH(40\%)$$

$$m_{H_2O_{needed}} = 77.44 - 20.18 - 13.66 = 43.6gH_2O$$

Table D.2: Materials needed for 100g synthesis solutions

Composition	**Chemicals for 100g basis**
Comp A1	33.63g Ludox HS-40, 22.77g TPAOH(40%),43.6g H_2O
Comp A2	34.96g TEOS, 17.15g TPAOH(40%),47.89g H_2O
Comp B	20.97g Ludox AS-30, 7.69g TPABr,0.34g NaOH pellets, 71g H_2O
Comp C	15.9g TEOS, 3.88g TPAOH(40%),0.027g Sodium aluminate, 80.19g H_2O
Comp D	13.45g Aluminum isopropoxide, 11.16 H_3PO_4, 1.239g Ludox HS-40, 20.2518g TEAOH, 4.498g DPA,
Comp E	11.465g Aluminum isopropoxide, 6.342 H_3PO_4, 1.45g Ludox HS-40, 71.375g TEAOH, 56.204g H_2O

APPENDIX E

SAMPLE CALCULATION FOR PERMEANCE AND IDEAL SELECTIVITY

Table E.1: Single gas permeation data for membrane AON-226 at room temperature

Gases	**H_2**	**n-C_4H_{10}**
Volume Change (ml)	90	1
Time interval (s)	7.04	22.72
Effective membrane area (m^2)	$5.5x10^{-4}$	$5.5x10^{-4}$
Pressure Difference (Pa)	$1.03x10^{+5}$	$0.97\ x10^{+5}$

Volumetric flow rate of H_2

$$\frac{\Delta V}{\Delta t} = \frac{90ml}{7.04s} \times \frac{1\ cm^3}{1\ ml} \times \frac{10^{-6}\ m^3}{1\ cm^3} = 1.28x10^{-5}\ m^3/s$$

Molar flow rate of H_2 by assuming to be ideal

$$\frac{p}{RT}\frac{\Delta V}{\Delta t} = \frac{0.91x10^{+5}Pa}{8.413\ m^3Pa/molK \times 291.15K} \times 1.28x10^{-5}\ m^3/s = 4.81x10^{-4}\ mol/s$$

H_2 permeance is:

$$P_{H_2} = \frac{4.81x10^{-4}\ mol/s \times \frac{1}{5.5x10^{-4}m^2}}{1.03x10^{+5}Pa} = 8.49x10^{-6}\frac{mol}{m^2sPa}$$

Similarly n-C_4H_{10} permeance is:

$$P_{n-C_4H_{10}} = 2.92x10^{-8}\frac{mol}{m^2sPa}$$

Ideal selectivity of H_2/n-C_4H_{10}

$$\alpha_{H_2/n-C_4H_{10}} = \frac{P_{H_2}}{P_{n-C_4H_{10}}} = \frac{8.49x10^{-6}}{2.92x10^{-8}} = 290.8$$

APPENDIX F

CALIBRATION OF MASS FLOW CONTROLLERS

In this study, binary mixtures of CH_4/n-C_4H_{10} and CH_4/CO_2 were prepared by adjusting the mass flow controllers. Three different mass flow controllers were used for CH_4, n-C_4H_{10}, CO_2. The calibration curves of these gases are given in Figure F.1, F.2, F.3.

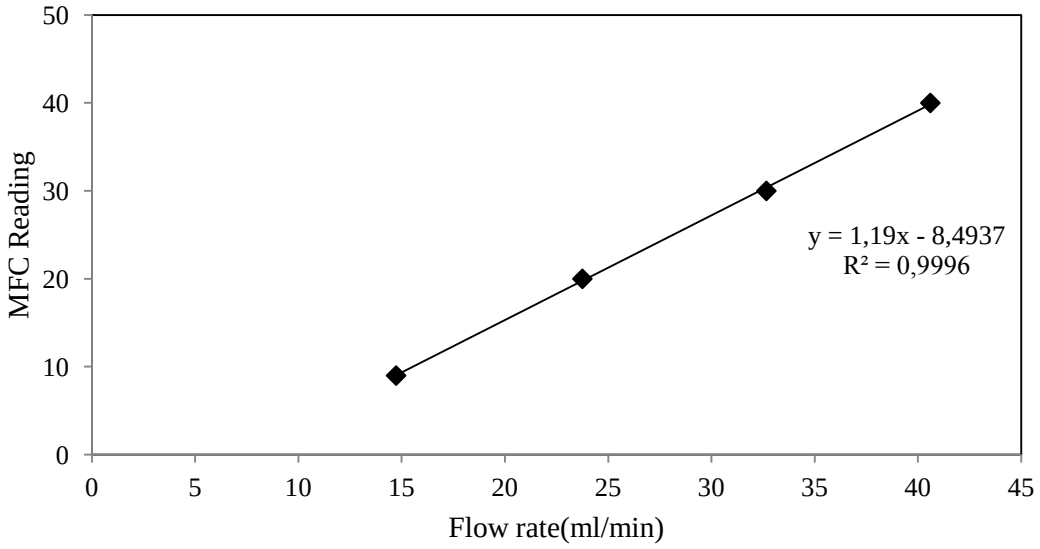

Figure F.1: Calibration of the mass flow controller for CH_4

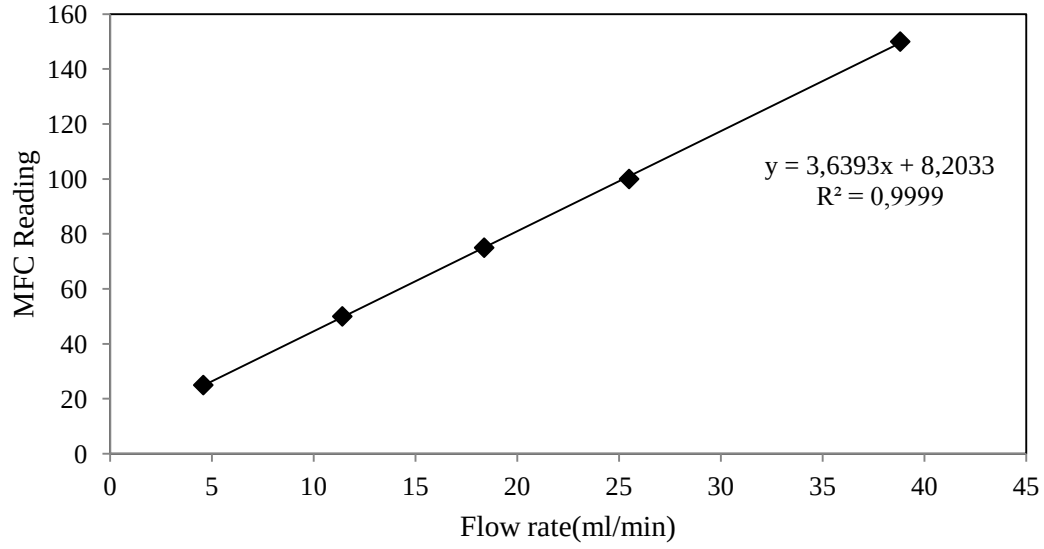

Figure F.2: Calibration of the mass flow controller for n-C_4H_{10}

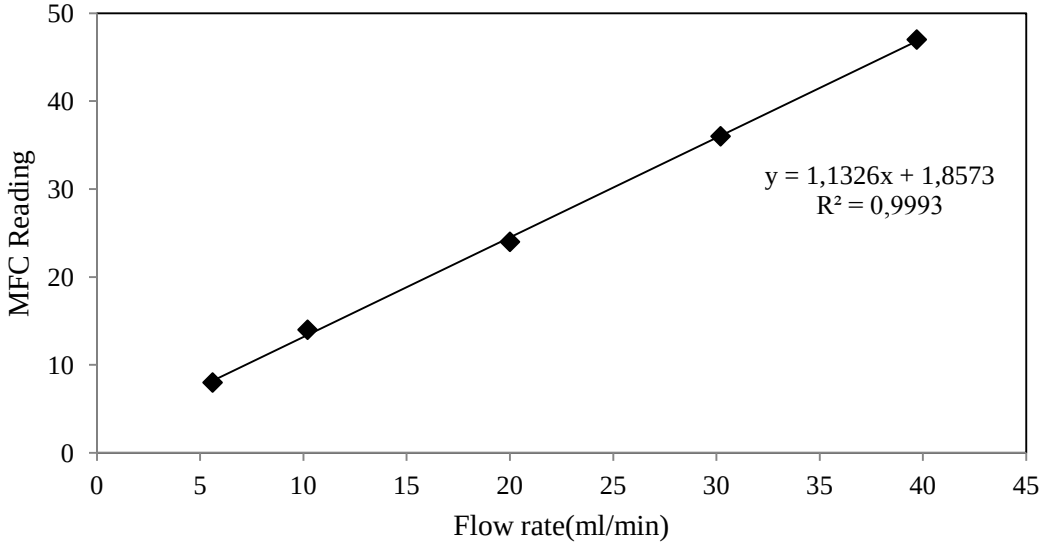

Figure F.3: Calibration of the mass flow controller for CO_2

APPENDIX G

CALIBRATION OF GAS CHROMATOGRAPH

In the separation experiments of binary mixtures, gas chromatograph calibrations for CH_4, n-C_4H_{10}, CO_2 gases were done. The calibration curves were obtained by relating the peak areas at different partial pressures of each gas under fixed operating conditions of GC. The fractions of each gas in feed, permeate and retentate were obtained by these calibration curves. (Figure G.1, G.2, G.3.)

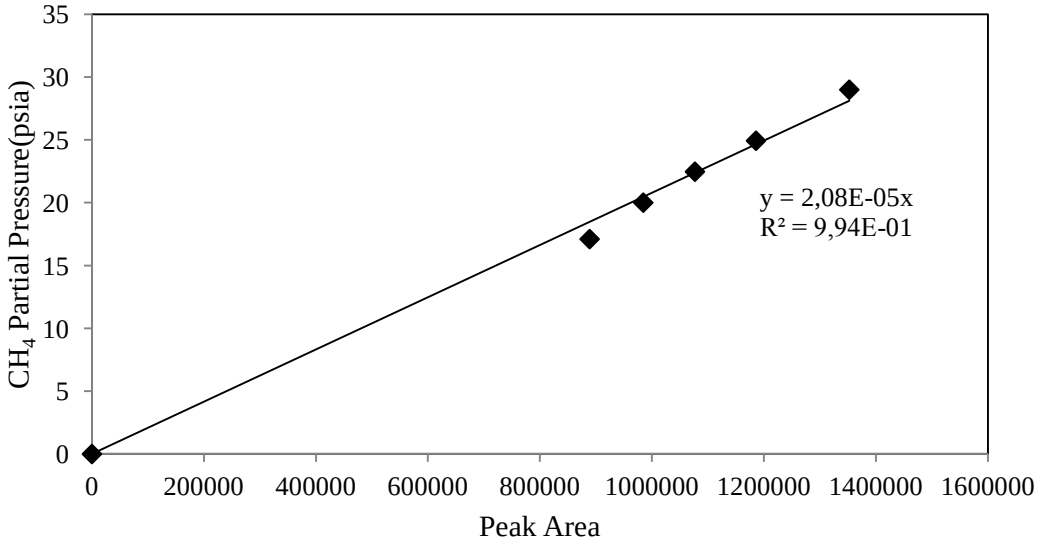

Figure G.1: GC Calibration for CH_4

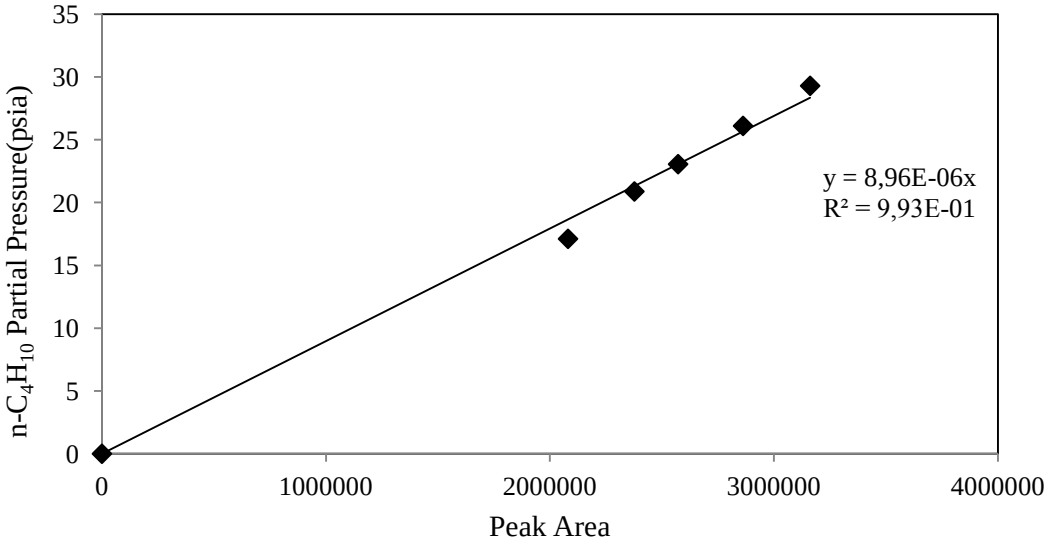

Figure G.2: GC Calibration for n-C_4H_{10}

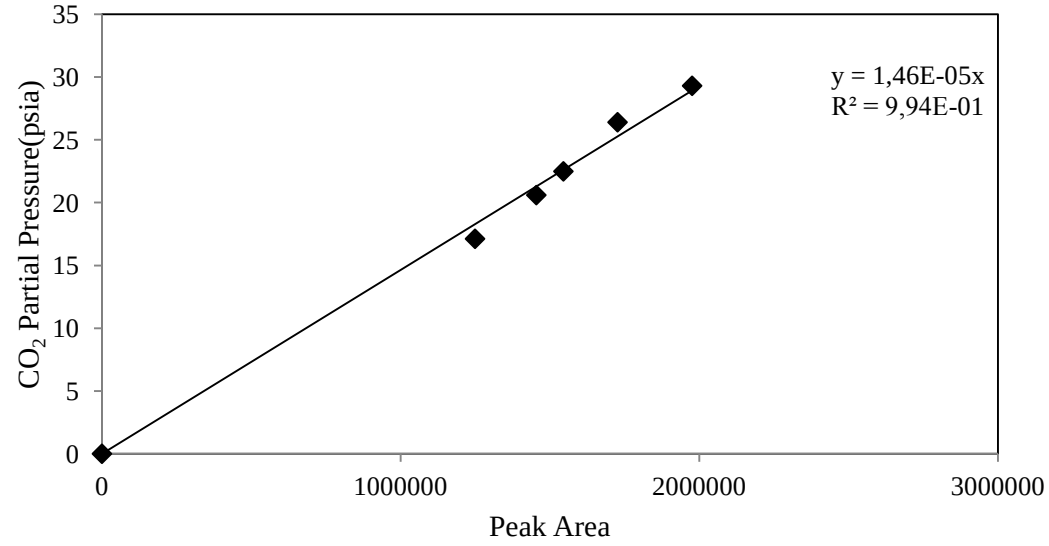

Figure G.3: GC Calibration for CO_2

APPENDIX H

SAMPLE GC CHROMATOGRAM AND SAMPLE CALCULATION OF MOLAR FRACTIONS

Compositions of feed, permeate and retentate were calculated by the GC analysis results and the calibration curves of the gases. Sample GC analysis outputs of both permeate and retentate is given in Figure H.1. Retentate analysis was done in the 5 minutes of the analysis and permeate was analyzed in the remaining 5 minutes with Belma multi method. For both analyses, the first peak represents the CH_4 (retention times: 0.297min and 5.290min) and the second ones stand for n-C_4H_{10} (retention times: 2.761 min and 7.547 min).

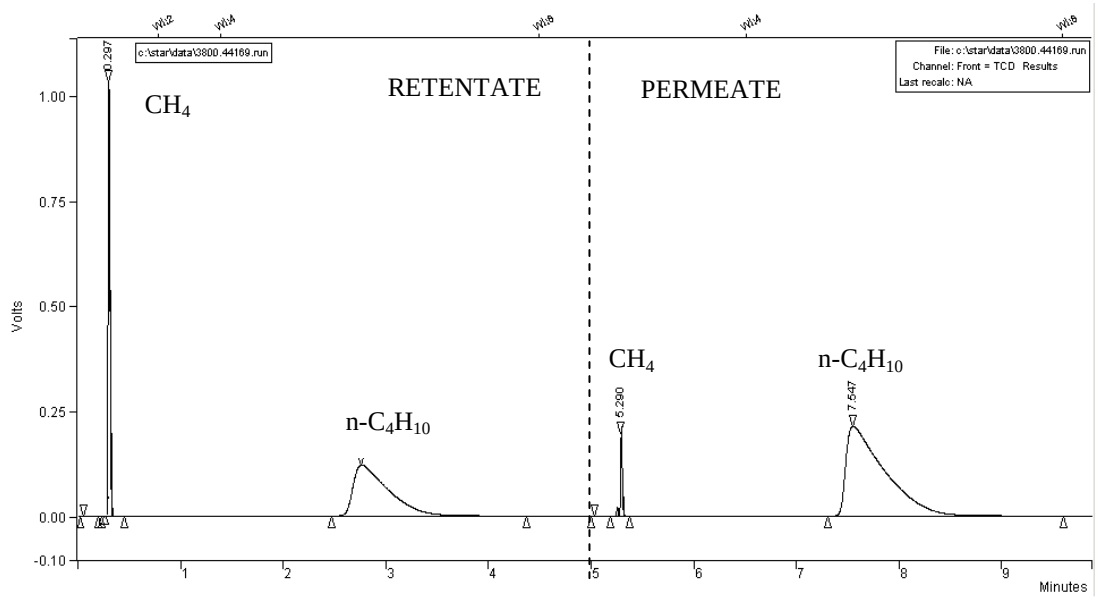

Figure H.1: GC output of membrane AON-173 (experiment was done at 24°C)

Permeate and retentate compositions were calculated as follows:

Permeate composition of CH_4:

$$y_{CH_4} = \frac{(Area\ of\ CH_4) \times (2.08x10^{-5})}{[(Area\ of\ CH_4) \times (2.08x10^{-5}) + (Area\ of\ n-C_4H_{10}) \times (8.96x10^{-6})]}$$

Permeate composition of n-C_4H_{10}:

$$y_{n-C_4H_{10}} = \frac{(Area\ of\ n-C_4H_{10}) \times (8.96x10^{-6})}{[(Area\ of\ CH_4) \times (2.08x10^{-5}) + (Area\ of\ n-C_4H_{10}) \times (8.96x10^{-6})]}$$

Sample calculations of permeate compositions for membrane AON-173 at 24°C are as follows:

$$y_{CH_4} = \frac{(249687) \times (2.08x10^{-5})}{[(249687) \times (2.08x10^{-5}) + (5572523) \times (8.96x10^{-6})]} = 0.094$$

$$y_{n-C_4H_{10}} = \frac{(5572523) \times (8.96x10^{-6})}{[(249687) \times (2.08x10^{-5}) + (5572523) \times (8.96x10^{-6})]} = 0.906$$

Feed and retantate side compositions can be calculated similarly and the results are given in Table H.1.

Table H.1: Feed and retentate compositions

	CH_4 Fraction	**n-C_4H_{10} Fraction**
Feed Side	0.478	0.522
Retentate Side	0.516	0.484

APPENDIX I

SAMPLE CALCULATION OF PERMEANCES AND SEPARATION SELECTIVITY FOR BINARY MIXTURES

Permeance of a component in a binary mixture is calculated as follows:

$$P_A = \frac{J_A}{\Delta P_{transmembrane}}$$

where J_A is the flux of component A and $\Delta P_{transmembrane}$ is the transmembrane pressure difference through the membrane (Pa).

$$J_A = \frac{P_{atm}}{R \times T \times A_{membrane}} \times y_A \times \left(\frac{\Delta V}{\Delta t}\right)$$

Where P_{atm} is the atmospheric pressure (atm), R is the ideal gas constant (L.atm/mol.K),), T is the separation temperature (K), A is the effective permeation area, which is 5.5x10^{-4} m^2, y_A is the mole fraction of component A in the permeate and $\Delta V/\Delta t$ is the total flow rate of the permeate.

$$\Delta P_{transmembrane} = \frac{\left(P_{A,B}^{feed} - P_{A,B}^{permeate}\right) - \left(P_{A,B}^{retentate} - P_{A,B}^{permeate}\right)}{ln\left(\frac{P_{A,B}^{feed} - P_{A,B}^{permeate}}{P_{A,B}^{retentate} - P_{A,B}^{permeate}}\right)}$$

P_A^i : partial pressure of component A in feed, permeate or retentate

Separation selectivity can be calculated by Equation 2.4 after calculation of permeances of the components in the permeate side.

$$Separation\ Selectivity_{A/B} = \frac{P_A}{P_B}$$

Sample calculations for membrane AON-173 at 24°C are as follows:

Table I.1: Mole fractions in the feed, permeate and retentate sides

			Mole fractions		Partial pressures	
Stream	**Flowrate**	**Pressure**	**CH_4**	**n-C_4**	**CH_4**	**n-C_4**
FEED	40,16	2,09	0,478	0,522	0,999	1,091
PERMEATE	3,52	0,9	0,094	0,906	0,085	0,815
RETENTATE	36,64	2,09	0,516	0,484	1,078	1,012

n-C_4H_{10} flux in the permeate:

$$J_{n-C_4H_{10}} = \frac{0.9\ atm}{(0.082L.atm/mol.K) \times (297K) \times (5.5x10^{-4}m^2)} \times 0.906 \times \left(3.52\frac{ml}{min}\right) \times \left(\frac{1L}{1000ml}\right) \times \left(\frac{1min}{60s}\right) = 3.57x10^{-3}mol/m^2s$$

Similarly, CH_4 flux in the permeate:

$$J_{CH_4} = \frac{0.9\ atm}{(0.082L.atm/mol.K) \times (297K) \times (5.5x10^{-4}m^2)} \times 0.094 \times \left(3.52\frac{ml}{min}\right) \times \left(\frac{1L}{1000ml}\right) \times \left(\frac{1min}{60s}\right) = 3.71x10^{-4}mol/m^2s$$

Transmembrane pressure difference of n-C_4H_{10}:

$$\Delta P_{transmembrane,n-C_4H_{10}} = \frac{(1.091 - 0.815) - (1.012 - 0.815)}{ln\left(\frac{1.091 - 0.815}{1.012 - 0.815}\right)} = 0.234atm \times \frac{1Pa}{0.9869x10^{-5}} = 23673\ Pa$$

Transmembrane pressure difference of CH_4:

$$\Delta P_{transmembrane,CH_4} = \frac{(0.999 - 0.085) - (1.078 - 0.085)}{ln\left(\frac{0.999 - 0.085}{1.078 - 0.085}\right)} = 0.954atm \times \frac{1Pa}{0.9869x10^{-5}} = 96624\ Pa$$

Permeances of n-C_4H_{10} and CH_4:

$$P_{n-C_4H_{10}} = \frac{3.57x10^{-3}mol/m^2s}{23673\ Pa} = 1.51x10^{-7}\frac{mol}{m^2sPa}$$

$$P_{CH_4} = \frac{3.71x10^{-4} mol/m^2 s}{96624\ Pa} = 3.83x10^{-9} \frac{mol}{m^2 sPa}$$

Separation selectivity of CH_4/n-C_4H_{10}

$$Separation\ Selectivity = \alpha_{CH_4/n-C_4H_{10}} = \frac{P_{CH_4}}{P_{n-C_4H_{10}}} = \frac{1.51x10^{-7}}{3.83x10^{-9}} = 39.3$$

APPENDIX J

IDEAL SELECTIVITIES OF MFI MEMBRANES

Table J.1: Single gas permeances of the MFI membranes

	Permeance x 10^8 (mol/m^2sPa)				
Gas	**AON-28**	**AON-226**	**AON-52**	**AON-147**	**AON-173**
H_2	90,3	951	4,21	667	573
CO_2	137	1160	16,6	849	811
N_2	55,9	486	26,4	447	384
CH_4	114	42,1	6,54	17,9	276
C_2H_6	84,7	371	17,9	723	465
C_3H_8	30,9	106	3,54	170	48,7
n-C_4H_{10}	7,43	29,2	0,632	84,5	11,4
i-C_4H_{10}	2,82	2,92	0,0975	10,7	0,024

Table J.2: Ideal selectivities of MFI membranes synthesized in this study

Ideal Selectivities		**CH_4 /n-C_4**	**n-C_4 /i-C_4**	**H_2 /i-C_4**	**CO_2 /CH_4**	**CO_2 /i-C_4**
B-140	AON-28	15	3	32	1	49
B-180	AON-226	1	10	326	28	397
F-140	AON-52	10	6	43	3	170
F-160	AON-147	0.2	8	62	47	79
F-180	AON-173	24	475	23875	3	33792

Table J.3: Experimental Data of Figure 4.15

Membrane Code	**Permeance x 10^8 (mol/m^2sPa)**		**Ideal Selectivity**
	CH_4	**n-C_4H_{10}**	
AON-28	114	7,43	15,61
AON-51	165	41	4,07
AON-52	6,54	0,632	10,35
AON-119	69,9	19,6	3,57
AON-147	757	104	7,28
AON-173	24,1	24,4	0,99

Table J.3 (continued)

AON-180	8,63	25,8	0,33
AON-184	20,1	23,5	0,86
AON-180(2)	23,9	8,54	2,8
AON-196	27,4	17	1,62
AON-204	14,8	5,09	2,77
AON-226	42,1	29,2	1,44

Table J.4: Experimental Data of Figure 4.16

Membrane Code		**Permeance x 10^8 (mol/m^2sPa)**		**Separation Factor**
	T (°C)	**CH_4**	**n-C_4H_{10}**	
AON-147	25	1,97	86	43,6
	50	4,47	75,3	16,9
AON-52	25	0,586	2,06	3,5
AON-119	25	2,31	13,5	5,9
AON-110	25	2,42	8,49	3,5
AON-173	25	0,361	14,2	39,4
	50	1,03	31,1	30,4
AON-180(1)	25	0,529	14,4	27,3
AON-184(1)	25	1,01	22,3	22
AON-180(2)	25	0,466	5,86	12,6
AON-196	25	1,05	13,6	13
AON-204	25	3,45	12,2	3,53
AON-147	100	15,2	157	10,3
AON-173	100	9,72	56	5,8
	150	59,6	121	2
AON-180(1)	100	8,43	104	12,4
	150	49,4	132	2,7
AON-184(1)	100	7,25	83,4	11,5
	150	38,5	107	2,8
AON-180(2)	100	4,86	72,5	14,9
	150	35,1	111	3,2
AON-196	100	9,26	95,6	10,4

APPENDIX K

XRD PATTERNS OF SOME MEMBRANES AND THE RESIDUAL POWDERS OBTAINED DURING THEIR SYNTHESIS

A few membranes synthesized with composition A1 and A2 were given in this part. Synthesis properties of these membranes are given in Table K.1 and XRD patterns are given in Figure K.1, Figure K.2, Figure K.3 and Figure K.4

Table K.1: Synthesis properties of the selected membranes

Membrane Code	**Synthesis Composition**	**SynthesisT(°C) /Time(h)**	**Number of Layers**	**N2 permeance before calc.**
AON-69	A1	140/28	....	....
AON-51	A2	140/24	4	...
AON-77	A2	140/24	3	....
AON-180	A2	180/13--180/13	1--1	$<10^{-12}/<10^{-12}$

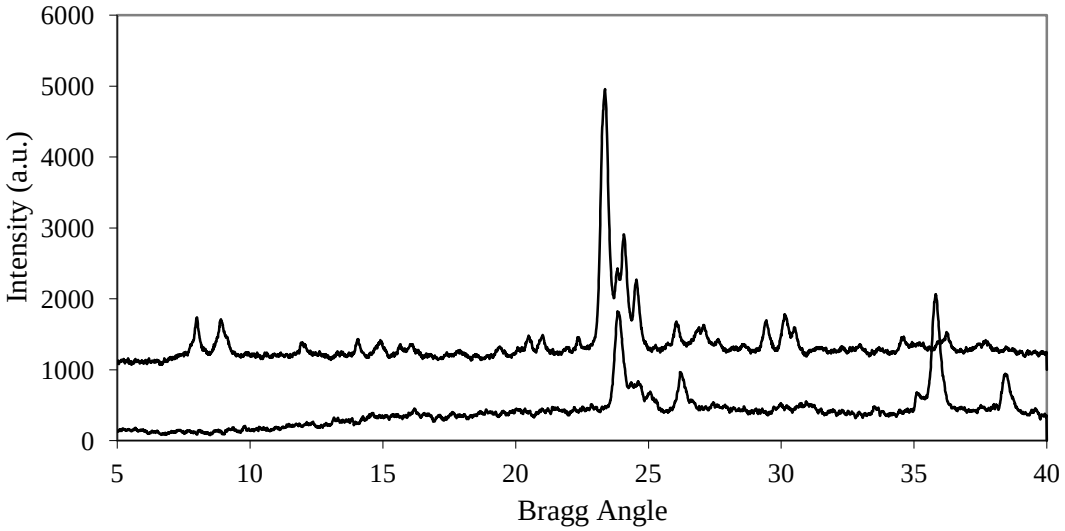

Figure K.1: XRD pattern of membrane AON-69 and the residual powder

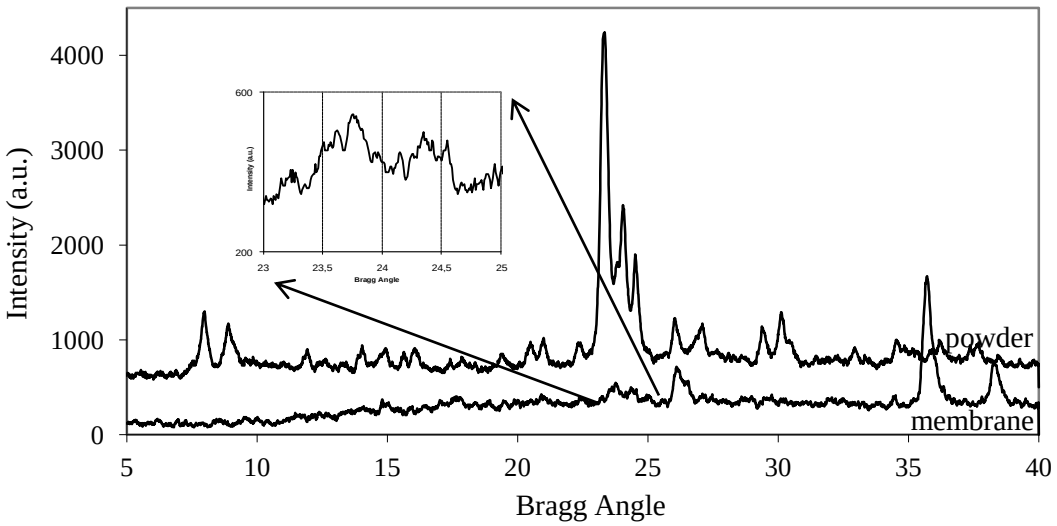

Figure K.2: XRD pattern of membrane AON-51 and the residual powder

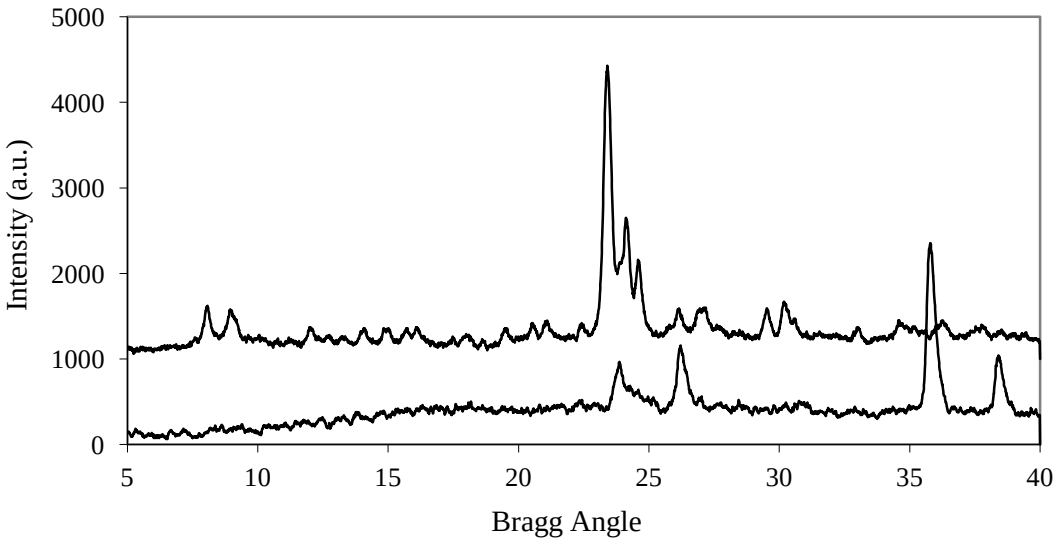

Figure K.3: XRD pattern of membrane AON-77 and the residual powder

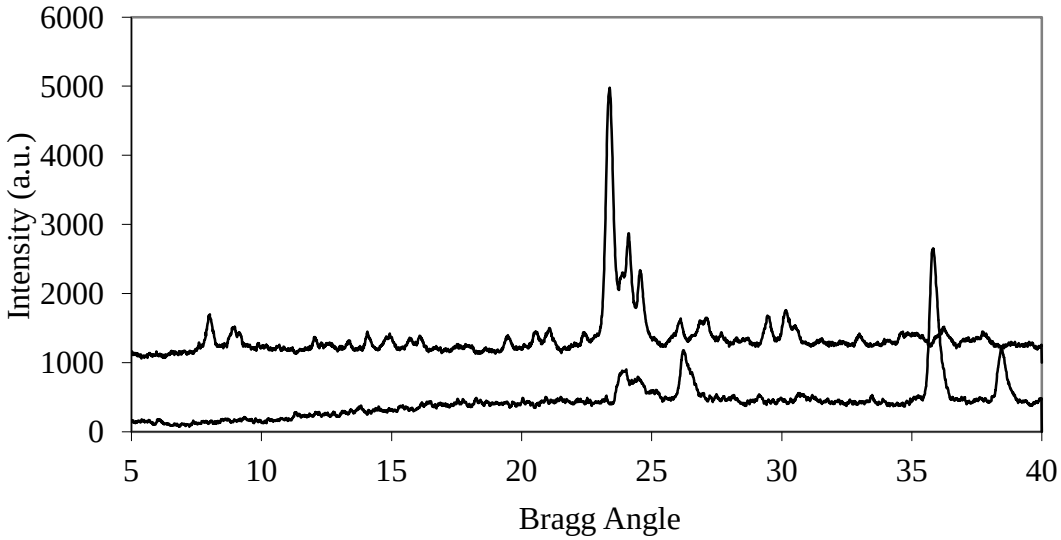

Figure K.4: XRD pattern of membrane AON-180 and the residual powder

APPENDIX L

N_2 ADSORPTION ISOTHERMS OF THE RESIDUAL POWDER OBTAINED IN MEMBRANE SYNTHESIS AT 140, 160, 180°C WITH COMPOSITION A2

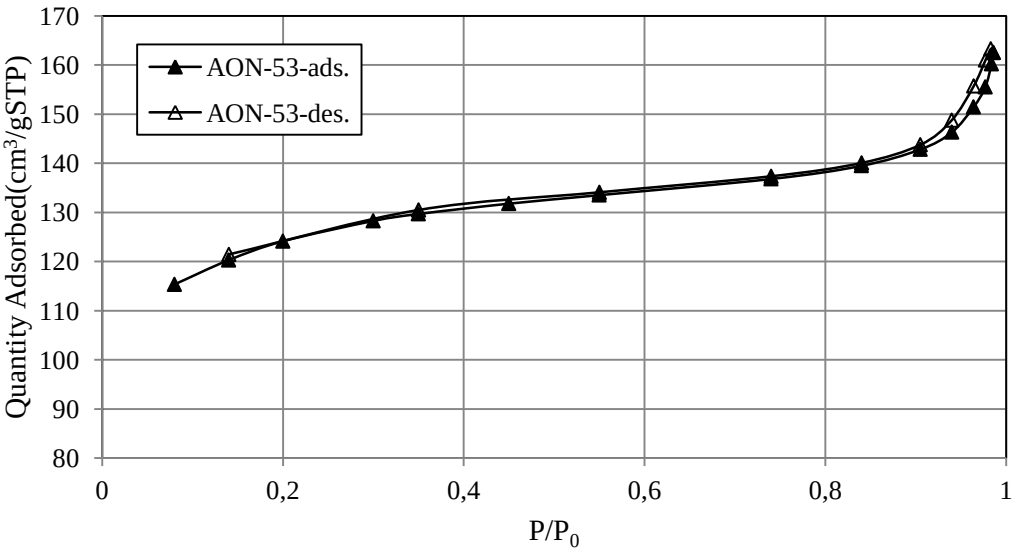

Figure L.1: N_2 adsorption/desorption isotherm of residual powder synthesized at 140°C

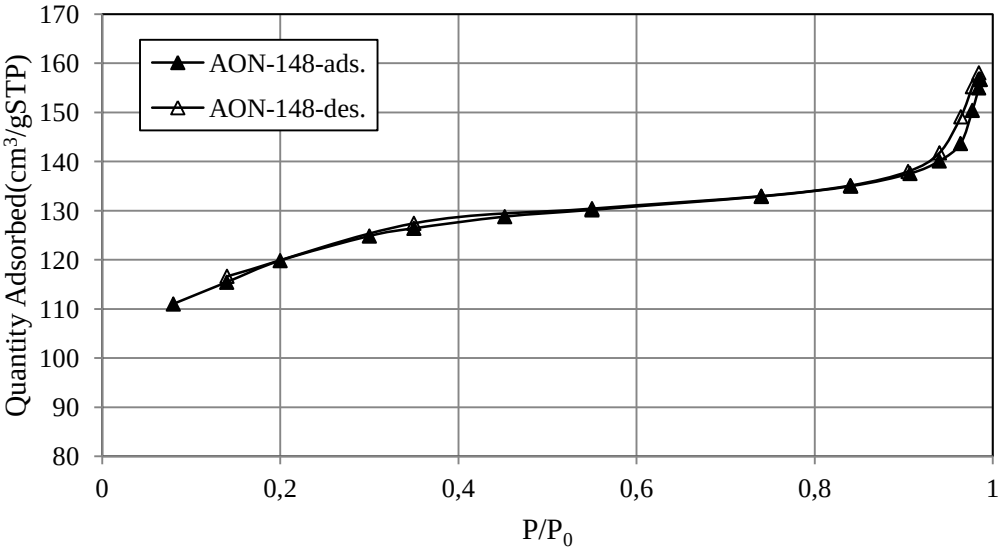

Figure L.2: N_2 adsorption/desorption isotherm of residual powder synthesized at 160°C

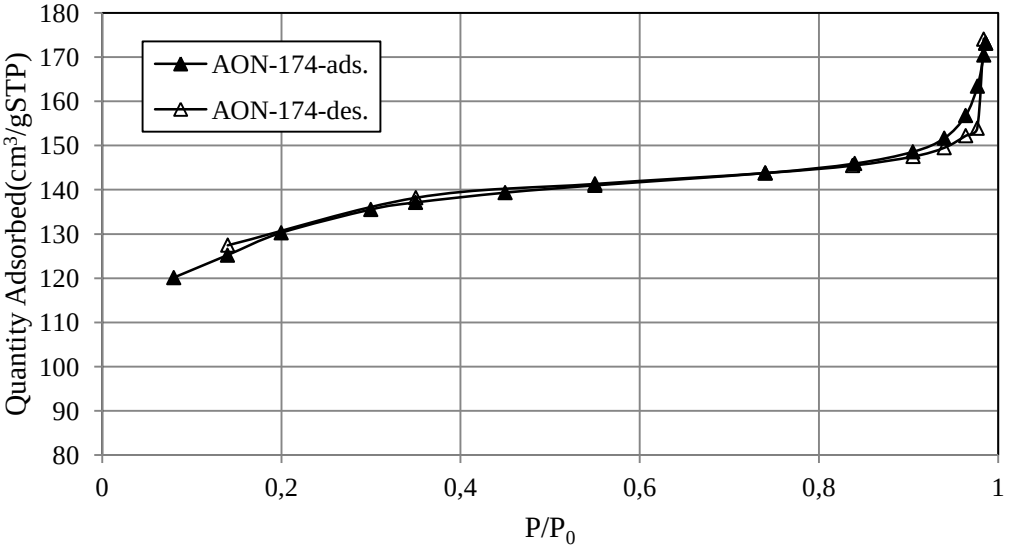

Figure L.3: N_2 adsorption/desorption isotherm of residual powder synthesized at 180°C

APPENDIX M

SEM IMAGES OF SOME MEMBRANES

Cross-section and surface views of AON-69 and AON-77 were given in Figure M.1 and Figure M.2. These membranes were synthesized with composition A1 and A2, respectively.

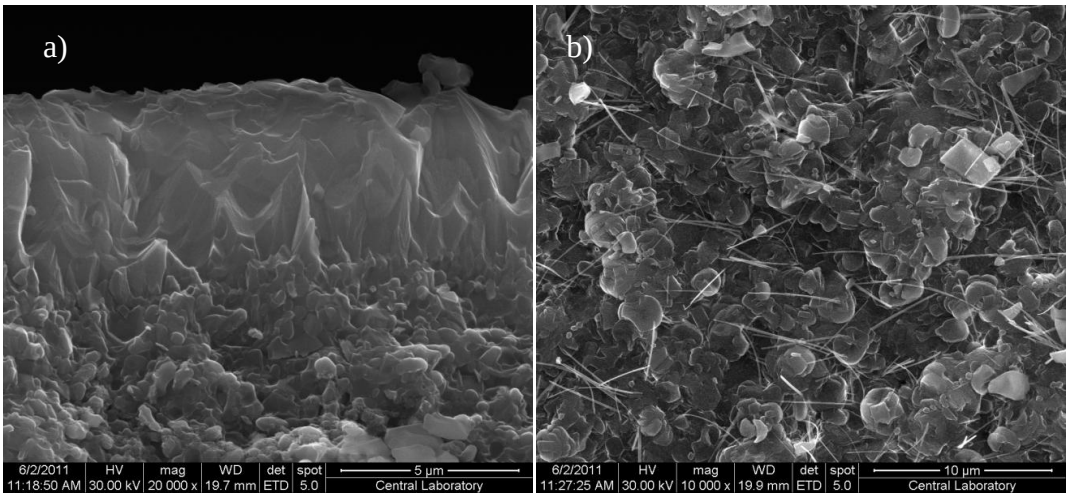

Figure M.1: SEM images of the membrane AON-69 a) cross-section b) surface

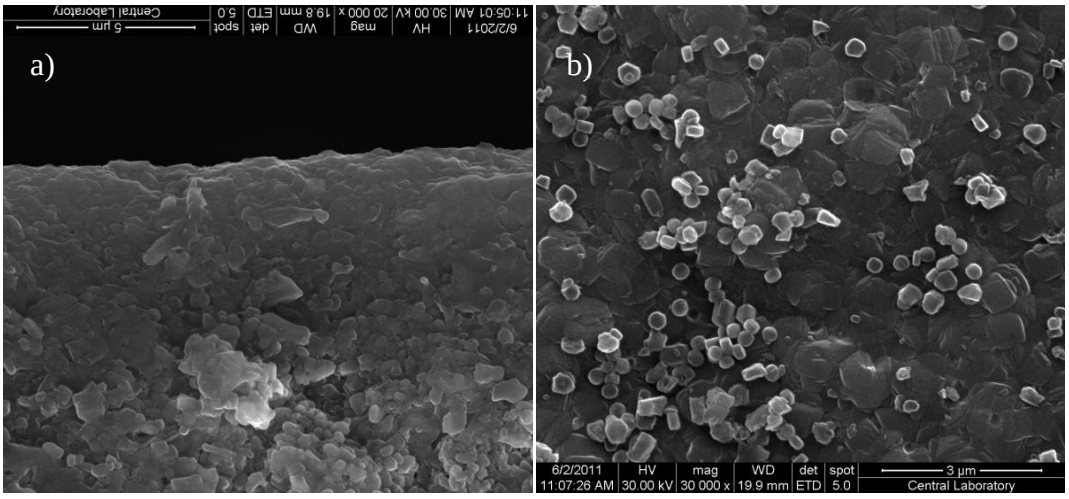

Figure M.2: SEM images of the membrane AON-77 a) cross-section b) surface

APPENDIX N

POWDER MFI SYNTHESIS AND CHARACTERIZATION

The main aim of this section is to choose the most suitable molar composition for MFI membrane synthesis. As mentioned in experimental part, there are four molar compositions for MFI synthesis used in this study. Composition B was not suitable for powder characterization since it can only be used for membrane synthesis and as a result of membrane synthesis, no residual powder was obtained. Composition A1 and A2 were investigated in detail prior to membrane synthesis.

The major difference between the composition A1 and A2 is the type of silica source. The synthesis mixture from composition A1 was prepared by using Ludox, which is a oligomeric silica. The synthesis mixture from composition A2 was prepared by using TEOS, which is a monomeric silica and yields ethanol upon hydrolysis. Thus the solvent of the synthesis mixture will be a solution of ethanol and water with such a composition that, it has higher vapor pressure than pure water at the same temperature. As the synthesis in the flow system is desired to be carried out at low pressures, synthesis mixtures prepared with Ludox can be more preferable than TEOS. This section compares the properties of MFI crystals produced from compositions A1 and A2.

The XRD pattern of the powders obtained in batch and flow synthesis system at 140°C for 28h from composition A1 are given in Figure N.1. Both syntheses resulted in highly crystalline MFI powder with relative crystallinities of 97% and 96% for batch and flow synthesis, respectively.

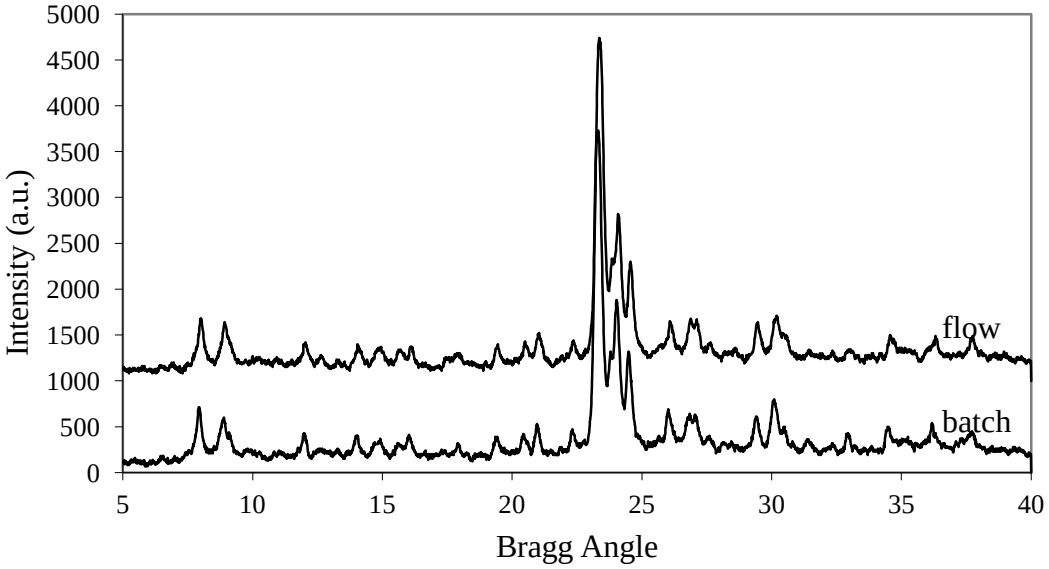

Figure N.1: XRD pattern of composition A1 in batch and flow system at 140°C for 28h

SEM images of the powders obtained in batch and flow system are given in Figure N.2 (a) batch, b) flow) Both powders do not have uniform particle size, but both have a distribution of the size. According to SEM results, particle size range of the crystals synthesized in the batch system is 0.5-4μm, while it is 0.3-2μm for those synthesized in the flow system.

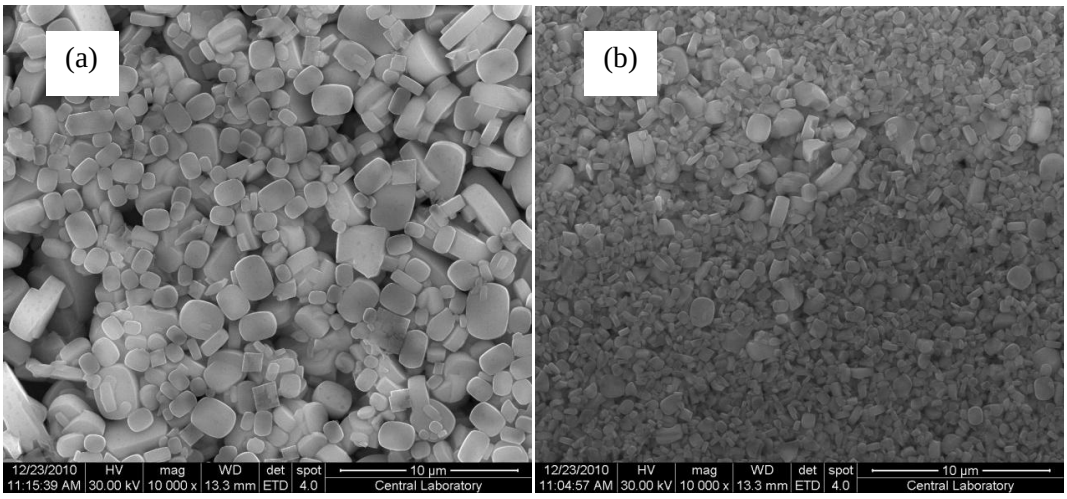

Figure N.2: SEM images of the powders synthesized in a)batch b)flow from composition A1 at 140°C for 28h

Specific surface areas of batch and flow MFI powders were determined by N_2 adsorption/desorption. BET specific surface areas and pore volumes of batch and flow crystals are almost same and 365m^2/g and approximately 0.200cm^3/g, respectively.

Table N.1: Some properties of MFI powders synthesized in batch and flow system with composition A1

Synthesis Mode	**BET (m^2/g)**	**Pore Volume (cm^3/g)**
Batch	366	0.199
Flow	365	0.211

Tetraethyl orthosilicate was used as silica source for synthesis with composition A2. Synthesis duration of composition A2 was investigated in the range of 16-40h. The relative crystallinities of the samples were not change much (around 90%) after synthesis time of 19h. Using tetraethyl orthosilicate instead of Ludox HS-40 decreased the time necessary for the synthesis.

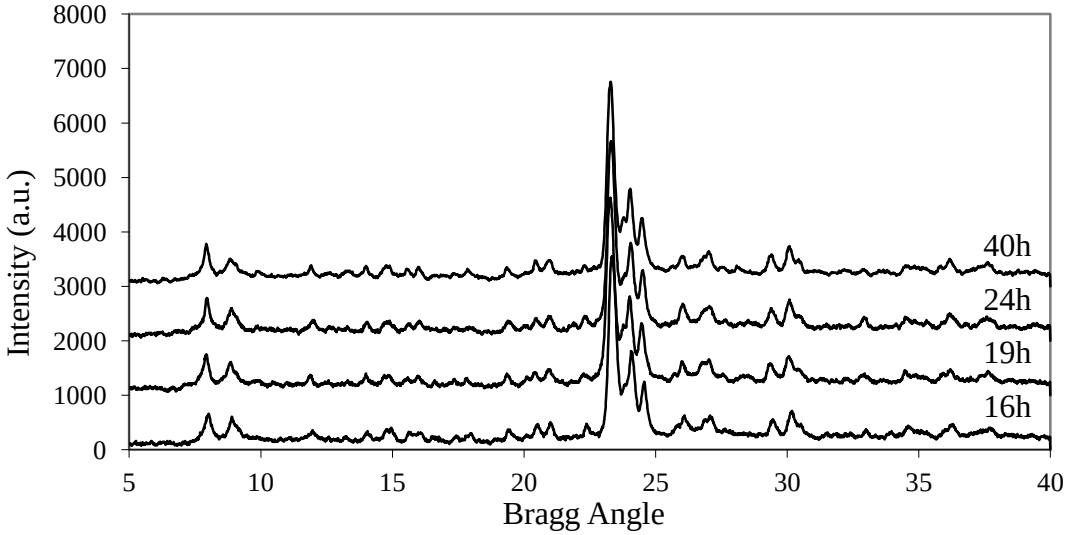

Figure N.3: XRD patterns of the powders synthesized from composition A2 in batch system at 140°C for different durations

Particle size distributions of the crystals synthesized at 140°C are given in Figure N.4. Average particle size of the monodispersed crystals are between 140nm and 220nm for synthesis period of 16 to 40h.

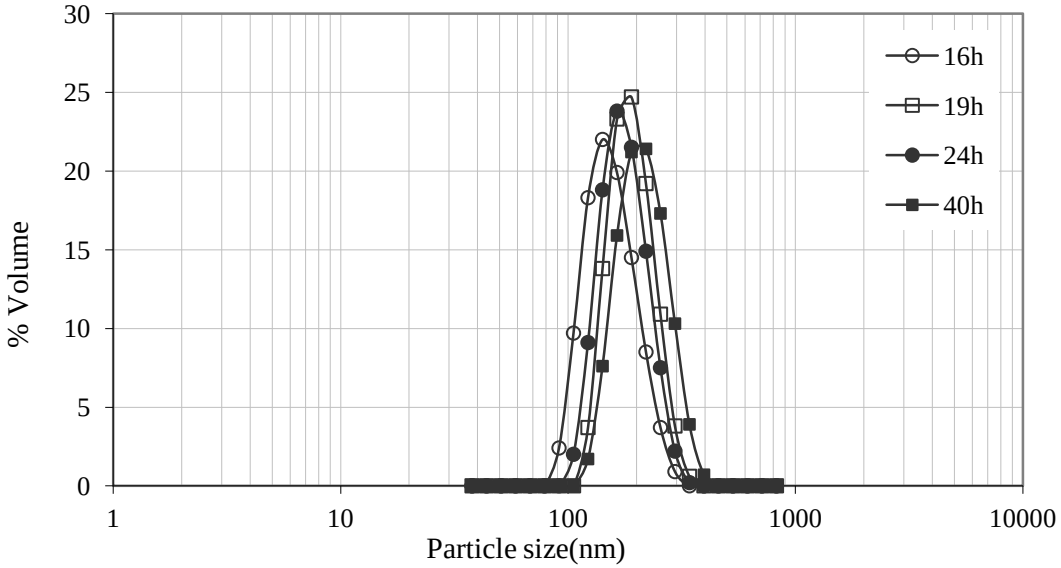

Figure N.4: Change in particle size distributions of the powders synthesized in batch system at 140°C with respect to synthesis time

FT-IR spectra of the powders synthesized with composition A1 (28h) and A2 (24h) at 140°C are given in Figure N.5. Asymmetric Si-O-Si stretching bands of MFI structure (1220cm^{-1}) are present in both spectra but % transmittance of this band is greater for composition A2. Silanol bands at 960cm^{-1} are not present in both spectra indication of consumption of silanols forming MFI structure [103]. The bands belonging to organic template cation TPA^{+} at 1400cm^{-1} and 1500^{-1} was observed more significantly for composition A2 than composition A1. FT-IR spectrum of the powder synthesized at 16-24h range with composition A2 at 140°C are shown in Figure N.6. As seen in Figure N.6, there is no big difference in the peak intensities of the bands of these spectrums. The reason of having no alteration in spectrum may be the result of having no change in the structure of MFI after 16 hours.

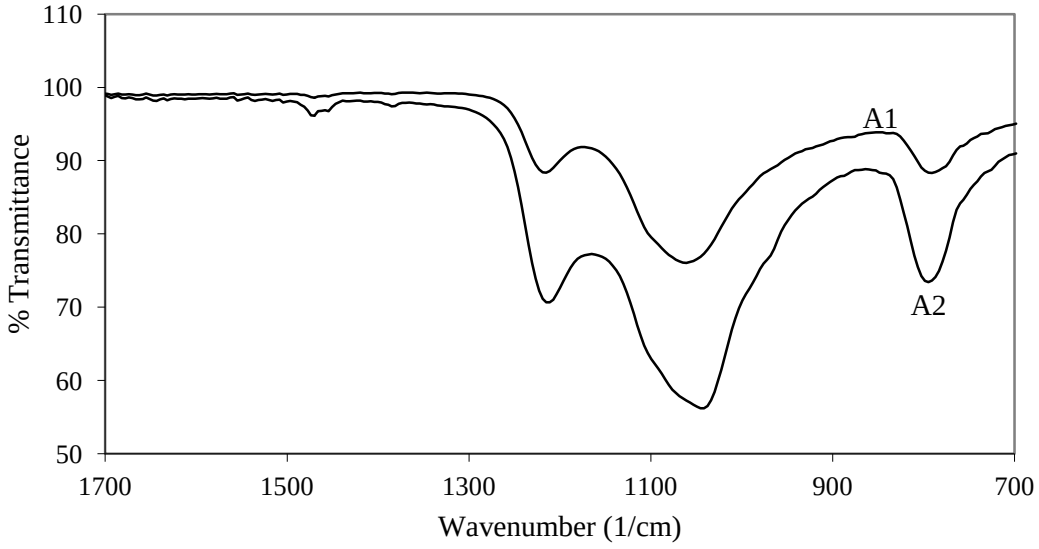

Figure N.5: FT-IR spectra of powders of composition A1 and A2 synthesized in batch systems at 140°C

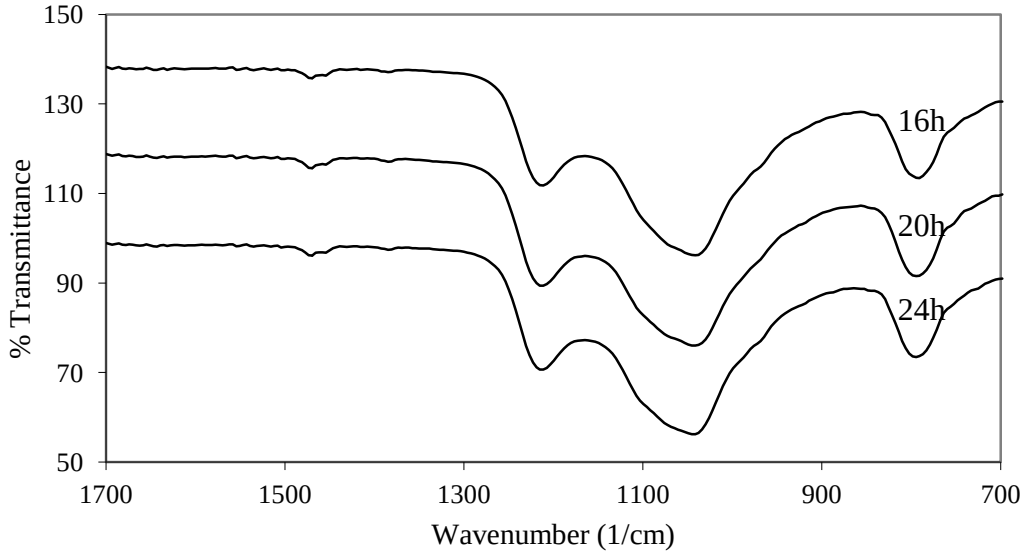

Figure N.6: FT-IR spectra of different samples with composition A2 synthesized in batch system at 140°C

N_2 adsorption isotherms of the powders synthesized with composition A1 and A2 at 140°C are given in Figure N.7. Both powders, which were subjected to heat treatment at 450°C, showed Type I isotherms [104]. Although there is no hysteresis for composition A1, there is hysteresis in the relative pressure range of 0.94-0.98.

These samples have BET surface areas of 366 m^2/gr, 372 m^2/gr for composition A1 and A2 respectively.

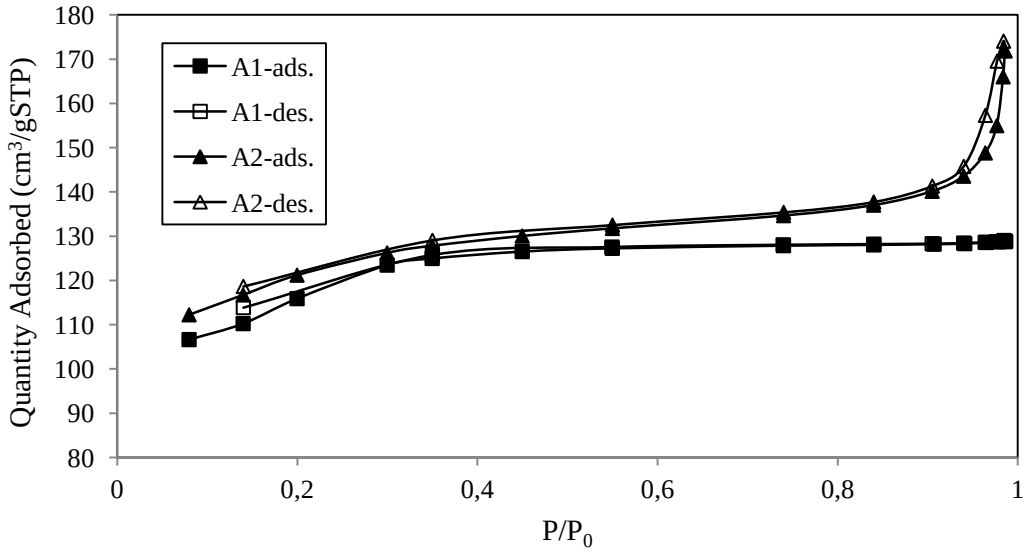

Figure N.7: Change in N_2 isotherms with respect to synthesis composition

Powder synthesis with composition C was carried out at 130°C for 24 hours. XRD pattern of the powder synthesized with composition C is given in Figure N.8 showing high relative crystallinity (85%) of the powder synthesized.

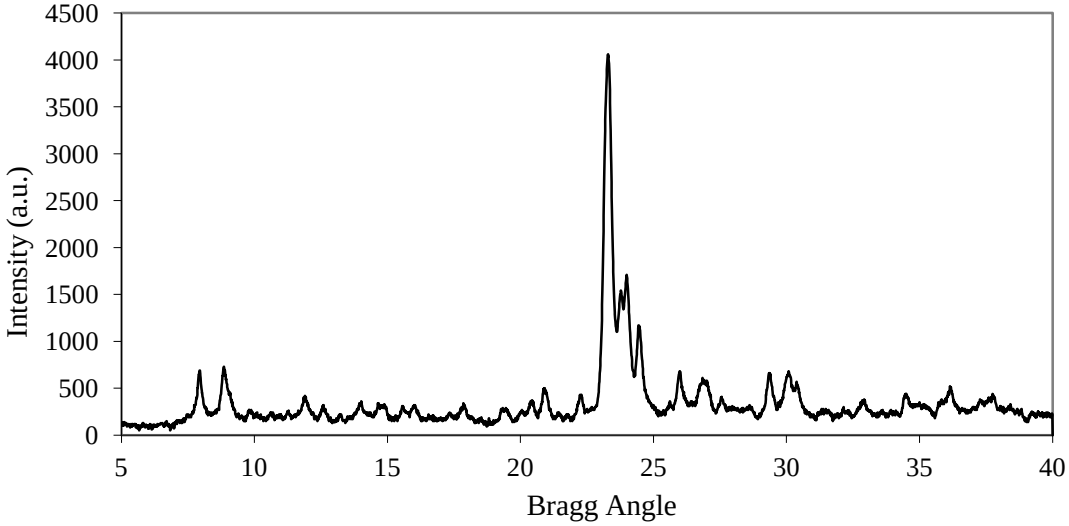

Figure N.8: XRD pattern of powder of Composition C(AON-97) synthesized in batch system at 130°C for 24 hours

APPENDIX O

CHARACTERIZATION OF MFI MEMBRANES SYNTHESIZED IN BATCH SYSTEM WITH COMPOSITION B AND C

Syntheses of membranes in batch system were also carried out with synthesis compositions of B and C at 150°C and 130°C, respectively. Parameters used in membrane synthesis in batch were given in Table O.1. Only composition C contains aluminum in the synthesis gel of the MFI membranes. Composition B results in h0h/c-oriented membranes [67], however it was impossible to use that synthesis gel in flow synthesis system since it was turned out a dense gel which does not flow. Therefore, it was used only for synthesis in batch.

Table O.1: Synthesis parameters of batch membranes

Membrane Code	Synthesis Gel Composition	Synthesis Mode	Synthesis Temperature (°C)	Synthesis Period (hour)	Membrane Layer
AON-28	A2	Batch	140	24	2
AON-226	A2	Batch	180	13	1
AON-98	B	Batch	150	28	1
AON-127	B	Batch	150	28	1
AON-110	C	Batch	130	24	1

No residual powder was obtained as a result of the synthesis with composition B. therefore, only membranes synthesized with composition B were characterized by SEM images, XRD pattern of the membrane and single gas permeation through these membranes. Cross-section and surface images of the membrane (AON-98) synthesized with composition B at 150°C for 28 hours were given in Figure O.1. These images showed that there was a crack between the support and the membrane layer which is ~30μm thick. There were pin holes on the membrane, which can be seen on both images. The XRD pattern of this membrane together with the seeded support was given in Figure O.2. The intensities of the characteristic MFI peaks of the membrane were higher than the ones in seeded support. This was the sign of the

development of the seed crystals and new generation crystals forming the membrane layer.

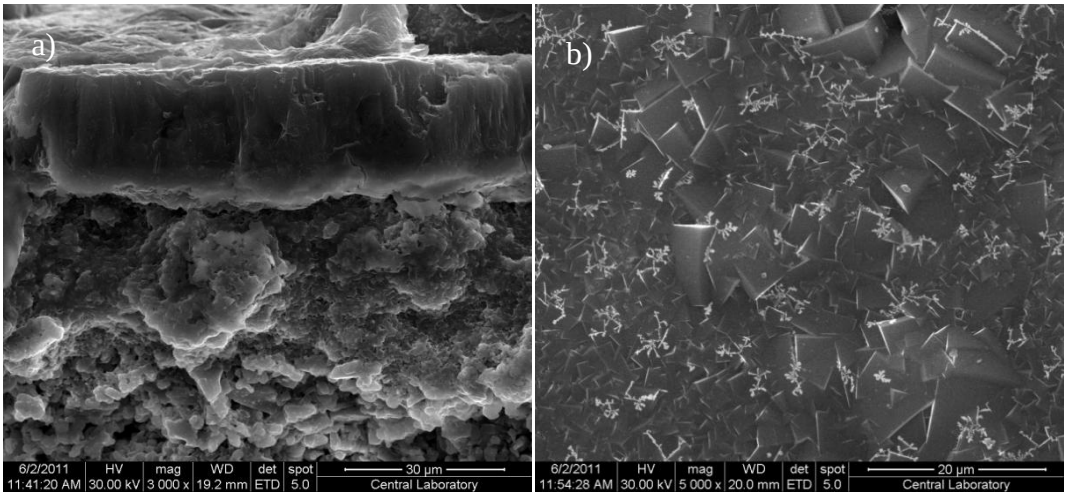

Figure O.1: SEM images of the membrane AON-98 a) cross-section b) surface

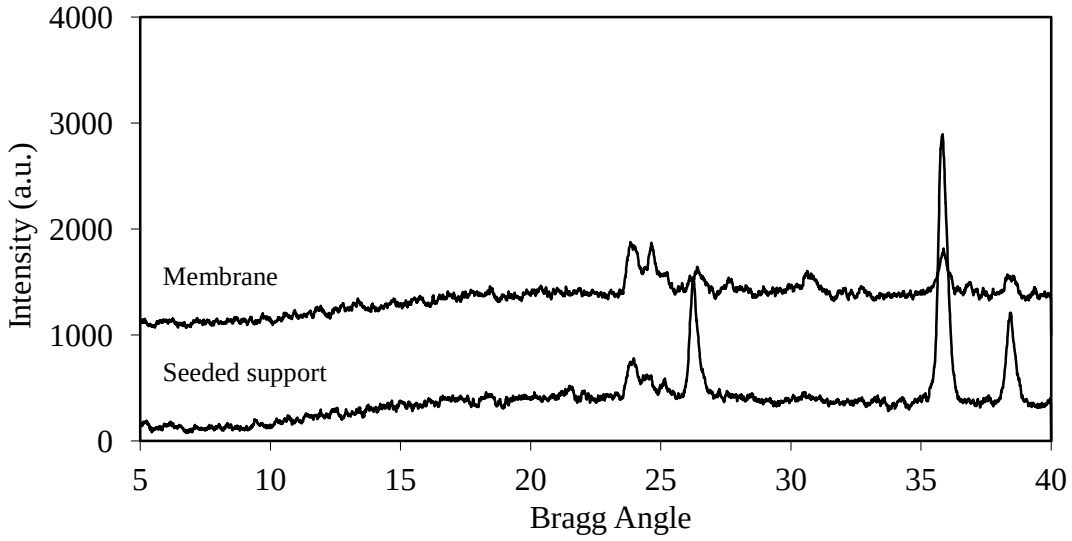

Figure O.2: XRD pattern of seed and membrane AON-98

XRD pattern of the residual powder obtained in the membrane synthesis with composition C was given in Figure O.3. The remaining powder had 100% relative crystallinity.

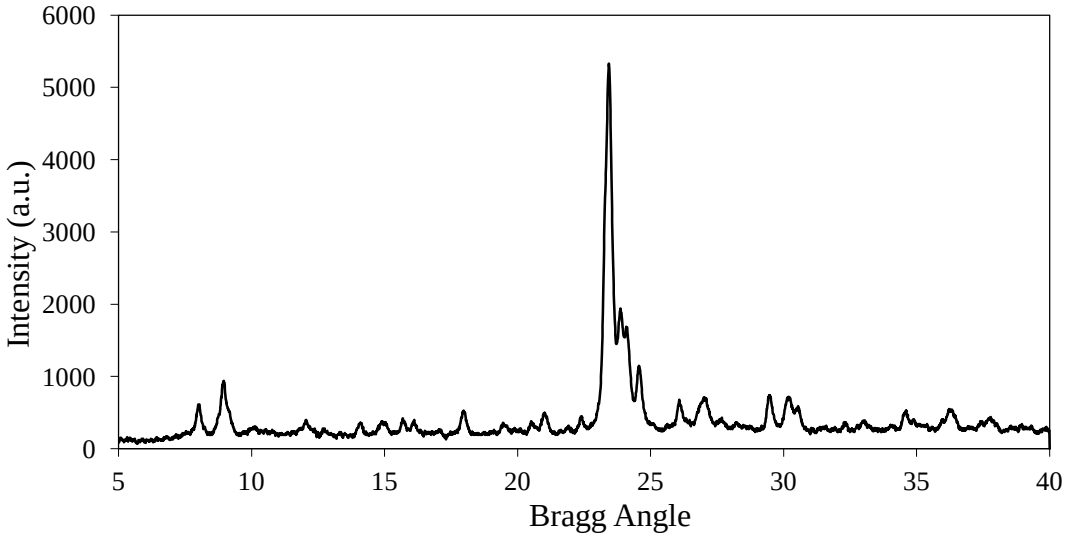

Figure O.3: XRD pattern of the residual powder obtained in the membrane synthesis with composition C(AON-111)

Single gas permeances of N_2, CH_4, n-C_4H_{10} and i-C_4H_{10} and ideal selectivities of N_2/n-C_4H_{10}, CH_4/n-C_4H_{10}, n-C_4H_{10}/ i-C_4H_{10} through membranes AON-98, AON-127 (composition B) and AON-110 (composition C) were given in Table O.2. The highest ideal selectivity of CH_4/n-C_4H_{10} was 759 for AON-98, which was synthesized with a composition resulting in oriented membranes [67].

Table O.2: Permeances and ideal selectivities of the membranes synthesized with composition B and C

Membrane		**Permeance (mol/m^{2}sPa x 10^8)**				**Ideal Selectivity**		
Code	**T(°C)**	**N_2**	**CH_4**	**n-C_4H_{10}**	**i-C_4H_{10}**	**N_2/n-C_4**	**CH_4/n-C_4**	**n-C_4/ i-C_4**
AON-98	25	23.1	38.8	0.0511	0.426	452	759	0.12
	150	17.5	29.9	11.7	-	1.5	2.56	-
AON-127	25	25.5	37.1	1.91	-	0.69	19.42	-
AON-110	25	52	145	4.09	0.852	12.7	35.58	4.8

Composition C was also used for MFI membrane synthesis in the flow system. The XRD pattern of the membrane (AON-141) and the residual powder (AON-142) were given in Figure O.4, which was synthesized at 130°C for 27 hours. Cross-section (a) and surface (b) images of AON-141 were given in Figure O.5. The thickness of the membrane was around 10-13µm and the surface of the membrane was covered with dome-like shapes and these shapes can also be seen on the cross-section view of the membrane. Dome-like defects were also observed by Xomeritakis et al. due to lack of close-packed seed layer under the area of defect causing less-competitive growth resulting in inclined and larger grains [6].

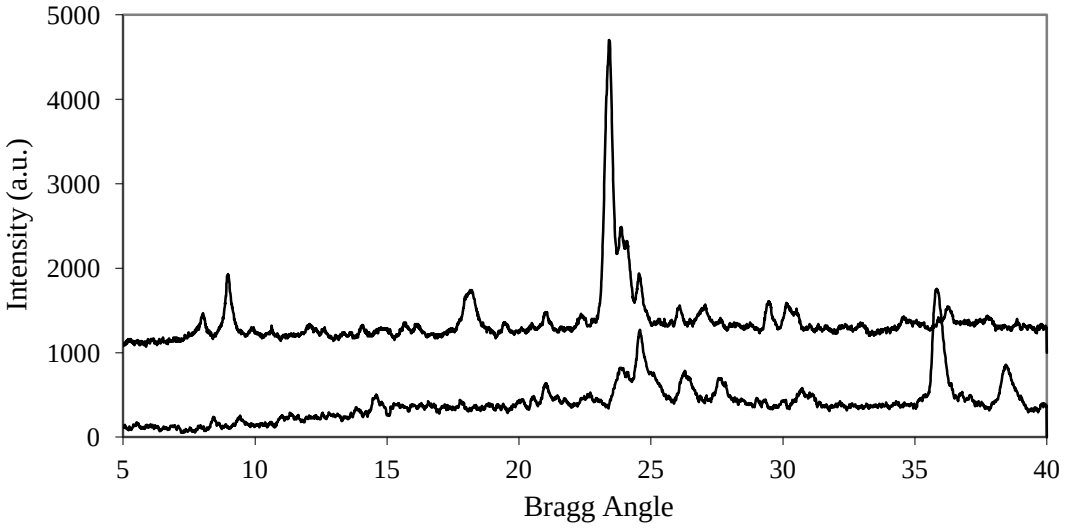

Figure O.4: XRD pattern of membrane AON-141 and the residual powder

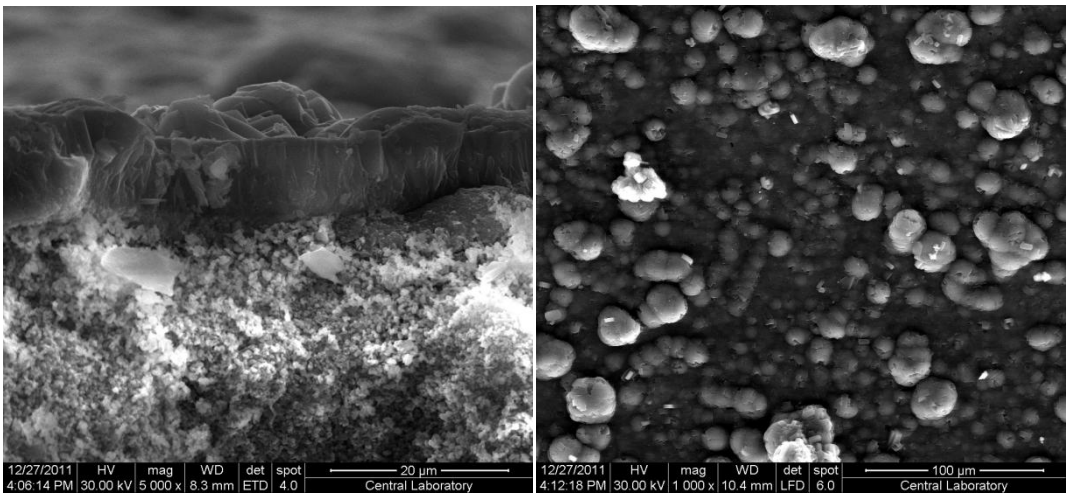

Figure O.5: SEM images of the membrane AON-141 a) cross-section b) surface